2009-01-01

# Exploring Poly(ethylene Glycol) As A Suitable Material For Peripheral Nerve Regeneration Scaffolds Manufactured By Stereolithography

Nubia Zuverza
*University of Texas at El Paso*, nzuverza@miners.utep.edu

# EXPLORING POLY(ETHYLENE GLYCOL) AS A SUITABLE MATERIAL FOR PERIPHERAL NERVE REGENERATION SCAFFOLDS MANUFACTURED BY STEREOLITHOGRAPHY

Nubia Zuverza-Mena

Department of Metallurgical and Materials Engineering

APPROVED:

_____
Ryan B. Wicker, Ph.D., Chair

_____
Lawrence E. Murr, Ph.D.

_____
Brenda Mann, Ph.D.

_____
Patricia D. Witherspoon, Ph.D.
Dean of the Graduate School

**Dedicated to:**

Patricia Mena-Sierra
Luis F. Zuverza-Meza
Jorge L. Zuverza-Mena

*For being my role models*

# EXPLORING POLY(ETHYLENE GLYCOL) AS A SUITABLE MATERIAL FOR PERIPHERAL NERVE REGENERATION SCAFFOLDS MANUFACTURED BY STEREOLITHOGRAPHY

by

Nubia Zuverza-Mena, B.S.

THESIS

Presented to the Faculty of the Graduate School of

The University of Texas at El Paso

in Partial Fulfillment

of the Requirements

for the Degree of

MASTER OF SCIENCE

Department of Metallurgical and Materials Engineering

THE UNIVERSITY OF TEXAS AT EL PASO

August 2009

*Acknowledgments*

There is not enough room and words to thank everyone. However, I would like to mention the sincere gratefulness that I have for my professors and the advisors that I have had.

Thanks to Dr. Ryan Wicker for allowing me into his selective Tissue Engineering research group, for his support, guidance, motivation and wisdom to conduct our investigation. Thanks to Dr. Brenda Mann for her advice and for sharing her knowledge with me. Thank you Dr. Gardea for showing me the path towards my next step by conducting me to the W.M. Keck Center for 3D Innovation. Thank you also Dr. Salvador, David Chavez and Dr. Narayan in the chemistry department; Lani Alcazar, Gladys Almodovar and Dr. Kristine Garza from the biology department for the valuable instruction provided. Moreover, I thank my friends Tania Guardado, Ana Nunez and specially Karina Puebla for their understanding and my apologies to them for the times that we had to cut off the party and come to the lab to attend my experiments. Besides my last mentioned friend who I owe my experience in the scanning electron microscope, other people from the W.M. Keck Center were always very supportive: Liz Pardo, Frank Medina, and Dr. Jae Won Choi. Above all, I am grateful to my brother Jorge L. Zuverza and my dad Luis F. Zuverza who have fully supported me through my whole life, my mom Patricia Mena and Mario Leyva for their company to the lab over the weekends and some nights. Support for this research was provided by the National Science Foundation through Grant No. CBET-0730750. Also, the studies performed at the Biomolecule Analysis Core Facilities were supported by the NIH grant No. 5G12RR008124. This is the perfect opportunity for me to stress the fact that I have been surrounded for the most part by quality human beings and that has been a key fact for me being where I am at today.

## *Executive Summary*

One of the challenges in tissue engineering is to have spatial and temporal control over the biological elements within a scaffold used to guide regeneration including, for example, transected nerves. Some of the physical and chemical characteristics to regulate regeneration include incorporation of bioactive domains and release of chemical signals. This study presents the use of stereolithography (SL) to incorporate localized domains for cell adhesion in addition to include releasable nerve growth factor (NGF) in the process of building poly(ethylene glycol) diacrylate (PEGda) hydrogel scaffolds. The capabilities of SL to build finished parts made out of different materials was shown by building hydrogels composed of inert and biologically dynamic regions. Bioactive areas consisted of the polymer combined with four amino acids: arginine, glycine, aspartic acid and serine (RGDS). The RGDS sequence is recognized by cells as an adhesion signal giving to the PEG substrate the ability to interact biologically. Human dermal fibroblasts (HDFs) were cultured on top of gels to demonstrate bioactivity of the domains by anchoring to PEG-RGDS sites. Evidence of control over cell adhesion sites was provided by HDFs preference to anchor to pre-established domains. Besides providing sites for cell attachment, an ideal nerve guidance conduit (NGC) should be able to release growth factors to promote the axons´ growth. NGF is a neurotrophin known to enhance survival, growth and differentiation of nerve cells. The protein was either encapsulated by adding it to the photocrosslinkable PEGda solution immediately before building the disks or covalently linked (conjugated) to PEGda. The polymer studied varied in concentration of two molecular weights, PEGda 3.4 and 6 kDa. PEG hydrogels released the neurotrphin into RPMI-1640 cell culture medium. An NGF release profile was determined by enzyme-linked immunosorbent assay (ELISA). Results showed an increased release of NGF over time, ultimately reaching a slow

continuous diffusion rate. Protein release rate increased with increasing molecular weight of the matrix´s mesh and diminished with decreased concentration within the same PEG´s chain size. Sample materials from PEG 3.4 kDa showed a gradual initial burst while PEG 6 kDa gels exhibited a marked initial burst release within the first two days of the experiment. The release profile for disks containing the entrapped protein was measured for at least 7 days. Testing of the diffused hydrolyzed protein took place up to 30 days from the 20wt% hydrogels, while the release from PEG 6 kDa was analyzed for 15 days. The total amount of trapped NGF diffused after one week from PEG 20 wt% 3.4 kDa, 30 wt% 3.4 kDa and 10 %(w/v) 6 kDa was 93±1.9, 46±2ng and 292.23±6.5ng, respectively. Gels with the conjugated protein released 254.6±21.1 from 10% (w/v) PEG 6 k Da matrix and 19.2±0.4 from 20 wt% PEG 3.4 kDa gels after 15 days. The hydrogels´ supernatants were added to pheochromocytoma (PC-12) cells to demonstrate NGF bioactivity by observing neurite extension of PC-12 in response to the neurotrophin. Ultimately, SL was shown to be a promising tool for producing bioactive synthetic PEG guides for peripheral nerve regeneration.

*Table of contents*

Page

*List of Figures*

*List of Tables*

*Chapter 1*

## 1.0 Introduction

Different from the central nervous system, the peripheral nervous system has the capacity to repair itself [1]. This is accomplished through mature neurons that cannot reproduce, but have the ability to continue growing their axons [2, 3]. When damage to the nerve communication system occurs, neurotrophic factors that promote axon outgrowth, cell survival, migration and differentiation are released from the distal end to the proximal nerve stump [4]. Suturing nerve end to end will bring back tissue continuity. However, it is not the procedure to follow if nerve elasticity is compromised. A physical guidance is then required for the nerve to find the right way to enervate the correct target [5]. This is a tube like structure scaffold to be implanted at the site of injury to mechanically provide support and guide regeneration. Artificial nerve guidance conduits (NGCs) are being used and investigated for their potential to overcome nerve discontinuity as an alternative to other grafting methods. Nerve guidance conduits are intended to have certain characteristics to maximize the enhancement of nerve regeneration. Unfortunately, the length of 2.5cm is the limit to which successful re-enervation in humans has taken place with the aid of guidance channels [6]. Today, there are commercially available NGCs. Still, they are not optimal models as they can be improved towards the ideal NGC.

One of the main characteristics required in a conduit to approach its optimum function is drug incorporation and release from a predetermined site and at a pre-established rate [7]. Unfortunately, physically entrapped drugs into NGCs are usually diffused from their matrices very rapidly compared to the time that they are required to be present. To effectively promote axon outgrowth and hence, nerve regeneration, drug release rates should be slowed to have them available throughout the healing process [8].

A second important feature of these guidance cylinders is that the material that they are made of should have bioactive sites to sustain cell incorporation [7]. The fact that axons align with respect to support cells makes the addition of these cells into the matrix advantageous because they conduct the physical way of the axon to follow. Moreover, they secrete growth factors such as nerve growth factor (NGF).

The object of this project is to modify a material that can be used in nerve scaffolds that provide chemical and physical guidance for axons to grow along a specific path towards their goal, the distal stump.

A cell anchorage signal was added to specific sites of poly(ethylene glycol) (PEG) the polymer that would make up the conduit hydrogel with the purpose of making it bioactive. The peptide sequence consisted of four amino acids: arginine-glycine-aspartic acid-serine (RGDS). In addition, the release rate of NGF from its PEG matrix was controlled to provide a diminished protein diffusion rate. This was accomplished by modulating the scaffold material concentration, composition, and the neurotrophic factor incorporation technique into the polymer. Poly(ethylene glycol) is known to have chemical and mechanical tunable properties [9]. As a synthetic thermoset, PEG has been studied as a photocrosslinkable material for tissue engineering [10]. Two different studies took place: one to prove modified PEG capable of sustaining cell adhesion and another to demonstrate that the diffusion of NGF from PEG can be diminished. Nerve growth factor inclusion consisted on physically trapping the protein into the scaffold mesh or chemically linking it to PEG before building the scaffolds.

Gelation process consisted of exposing the photocurable solution to ultraviolet (UV) light of 325nm or 365nm wavelength ($\lambda$) depending on the photoinitiator being used. The long wavelength ($\lambda$) source was a UV lamp whereas the short $\lambda$ was produced by a helium-cadmium

(He-Cd) laser on a stereolithography (SL) machine. SL is a rapid prototyping method used in the present work to build hydrogels in a layer by layer fashion. This construction method allows for consistency in repeatable manufactured elements [11]. However, the use of UV light might compromise bioactivity of present biological moieties. To demonstrate that this technology can be employed for tissue engineering purposes, these experiments took place. For the bioactivity experiment, human dermal fibroblasts (HDFs) were seeded on top of gels containing specific sites for cell attachment and were analyzed after at 24 and 48 hours to determine if the HDFs could find bioactive sites for attachment. Regarding the release test, hydrogels were soaked in solution to release NGF contents by diffusion for entrapped NGF or by hydrolysis of the PEG-NGF bond followed by NGF diffusion in the case of covalently bonding the NGF to the polymer.

## 1.1 Tissue Engineering

Tissue engineering (TE) is a relatively new area of research which began in the 1970's and started developing in the 1990's [12]. Literature presents a variety of definitions [2, 12-14]. Ultimately, they all indirectly show TE as an alternative to tissue/organ transplantation. From this perspective, attention is growing towards TE to overcome the barrier of organs shortage for transplantation [15]. All these concepts together are directed towards the improvement of tissue/organ function of many biological systems. Research on TE has been taking place on hard tissue such as bone regeneration [16], cartilage formation [17], and soft tissue, for example muscle structure [18], angiogenesis (vascular tissue generation) [19], lung [20] kidney[21] and nerves [22], among others. Below is a table that was presented by Cortesini [15] listing investigations on tissue and organs *in vivo* and clinical cases regarding tissue engineering. To know more about the following information, please see reference No.15.

**Table 1. 1. Research projects: in vivo animal studies and clinical studies [15]**

| Tissue | In vivo studies | Clinical studies |
|---|---|---|
| Bladder | X | |
| Blood vessels | X | |
| Bone | X | |
| Cartilage for joints | | X |
| Ear | X | |
| Genitals | X | |
| Heart muscle | X | |
| Heart valves | X | |
| Intestine | X | |
| Joints | X | |
| Liver | X | |
| Pancreas | X | |
| Meniscus | X | |
| Peripheral nerves | X | |
| Salivary glands | X | |
| Skin | | X |
| Spinal cord | X | |
| Trachea | X | |
| Ureter | X | |

This thesis work is a contribution to the path of tissue engineering towards improving peripheral nerve repair.

## 1.2 The Nervous System

The central nervous system (CNS) and the peripheral nervous system (PNS) make together the nervous system. The CNS is composed of the brain and spinal cord. Glial cells and neurons are the main cell type components of the nervous system [23]. Neurons carry chemical and electrical signals. They have a cell body and extensions called axons or dendrites. Soma is an alternative name to the cell body, where the cell nucleus is located. Axon hillock is the name given to the area by which the axon is connected to the cell body. Depending on the direction of the signal, it is established which is the pre or postsynaptic cell. The presynaptic cell is the neuron sending information and the postsynaptic neuron is the one receiving the message. The synapse is the gap that where neurons meet and communicate. Figure 1.1 shows the neuron components.

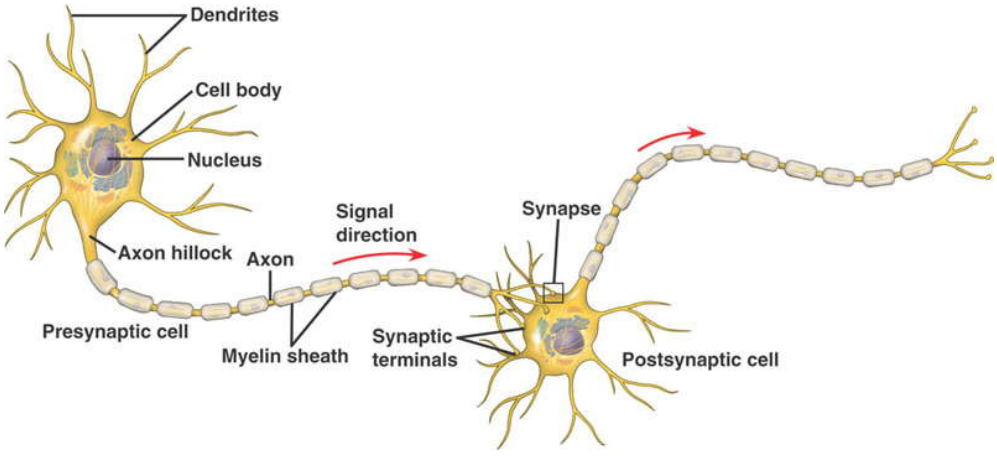


**Figure 1. 1. Neuron components [26]**

When damage to the communication system occurs at the central nervous system, the healing process is far from bonding back the same connections present before damage occurred.

The CNS glial cells consist of astrocytes and oligodendrocytes. At the injury site, CNS glial cells congregate forming a barrier. This obstacle prevents the neuron to connect back to its previous target by forming scar tissue:

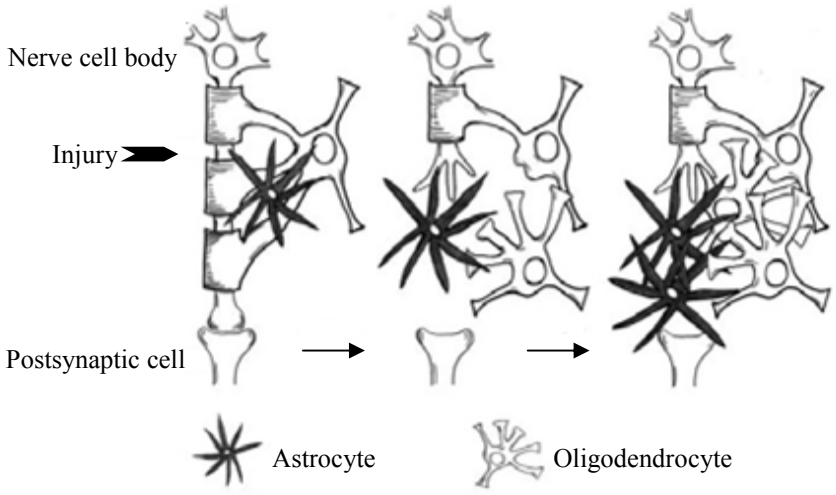


**Figure 1. 2. Regeneration process in the CNS. Modified from [1,3,28]**

However, neurons in the CNS might find a new path for their dendrites to extend and form new neuron to neuron connections.

The CNS is connected to the body through the nerves that make up the PNS. This can be thought as nerves in the PNS being an arrangement of wires sending information to and from the target organ to and from the brain and spinal cord. Information from the spinal cord and brain to the rest of the body is carried by efferent (motor) neurons. Impulses from the organs to the CNS are carried by afferent (sensory) neurons [24]. In the PNS both afferent and efferent neurons are arranged together within a nerve. The following picture shows the cross section of a

neurovascular bundle. It is composed of blood and nerve vessels. It also depicts the basic cell (neuron) of which a nerve is made of:

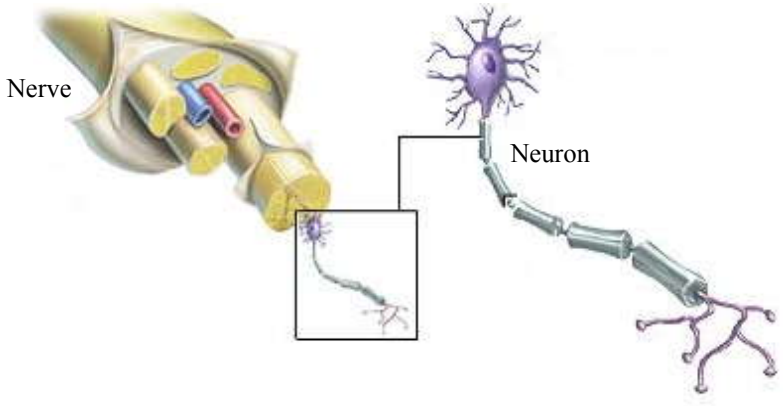


**Figure 1. 3. Anatomy of a nerve [25]**

The longest extension in a neuron is the axon. The axon is located in the PNS and it is surrounded by its supportive Schwann cells which are glial cells. Schwann cells make the myelin sheath that protects, provides support and maintenance for the function of the neuron. Also, the objective of glial cells in the PNS is to transfer the information of an impulse faster.

In the PNS axons surrounded by their respective Schwann cells are arranged longitudinally together in bundles called fascicles. At the same time, organized fascicles are enclosed by connective tissue, the perineurium (peri = around). The outer structure that surrounds all the previous is the epineurium.

Going down the structure scale the synapse is found. It is the region where the presynaptic neurite releases its chemical signals such as neurotrophic factors. Then, these factors reach the postsynaptic cell that has specific receptors for them. The following image (Fig. 1.4) illustrates at various scales the nerve components. At the center two nerve cells interacting are shown. The left side of the image presents the macroscale structures with respect to the neurons.

The right part of the figure depicts the microscale regarding a nerve cell, presenting the synaptic region.

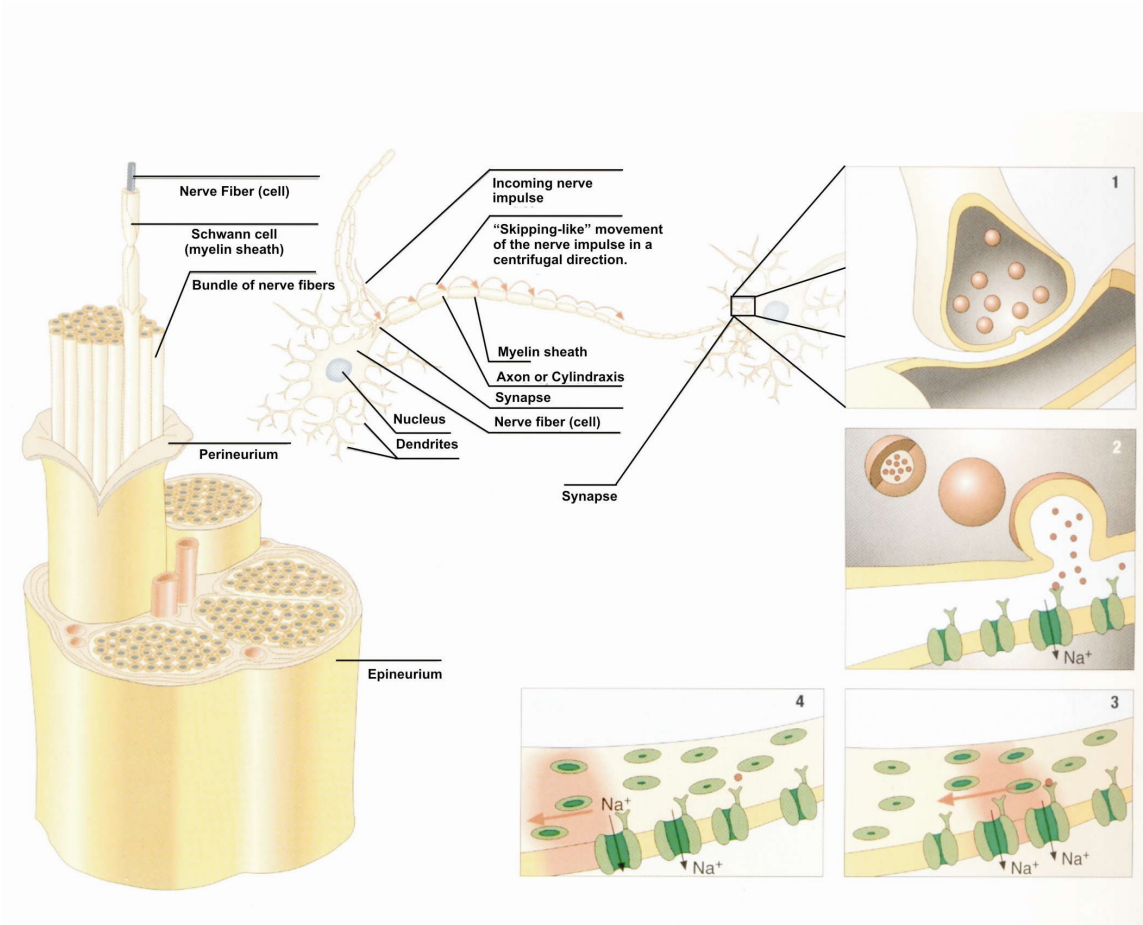


**Figure 1. 4. Macro and micro components of a nerve with respect to a neuron [27]**

Mature nerve cells lack the capacity for replication. Even though mature neurons cannot reproduce, they have the ability to continue growing their axons. Therefore, when damage to the PNS occurs, the proximal end of the nerve has the capacity to regenerate [2]. The axon development takes place from the proximal (nerve end closer to the spine) to the distal end (extreme of the nerve more distant from the spine). This happens because signals from the distal stump are being sent to the proximal to regenerate the nerve.

As mentioned above, as a consequence of an injury, the distal end will react to the damage sending signals –such as neurotrophic factors. Unfortunately, when the axon is completely interrupted and can have no communication with the soma, the distal end is degenerated until the body gets rid of it. This process is called Wallerian degeneration, where macrophages will eat myelin debri. Nevertheless, degeneration might be followed by regeneration. Schwann cells with the aid of macrophages and monocytes will support the axon growth. They will eat debris while protecting and insulating the axon and providing the nutrients necessary for it to grow [1,3,28]. The process is exemplified in Figure 1.5.

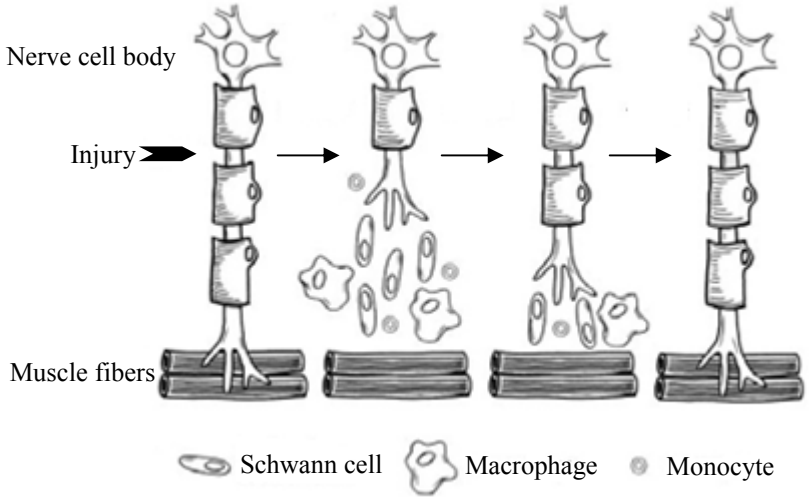


**Figure 1. 5. Degeneration followed by regeneration. Adapted from [1,3,28]**

Nonetheless, the PNS autonomous repair system may sometimes not be enough, but the healing process can be enhanced. To accomplish this, tissue engineering is now a growing area of research with the objective of replacing the function of the damaged tissue and providing a place for the lost tissue to redevelop. Depending on the type of injury nerves can be crushed (partially damaged) or totally disconnected.

### 1.2.1. Injuries

Damage to a nerve can be the result of a medical condition where part of a nerve has to be removed or harm due to trauma. For instance, a neuroma –nerve cancer– may develop in a person. That portion of the damaged nerve has to be taken away leaving a gap of the size of the segment that was removed. When trauma is the cause of the problem, the outcome can be a nerve left compressed or discontinued. Consequently, different gap lengths within different nerve sizes take place, as well as different approaches to repair the injury.

### 1.2.2 Gaps

The size of the gap is said to be large or small in a relative way. The actual length of this space between the nerve stumps is very ambiguous. In literature, it is common to encounter terms of small gaps as "few millimeters" without establishing a defined length. For example, Bozkurt et al. [22] refer to defects of a small number of millimeters as short without an exact definition. Others suggest that 1 cm corresponds to a short nerve defect [6]. Different references define a long space to be considered larger than 2 cm [29], or longer than 0.4 cm [30]. Regardless of the exact definition of a small or long gap, solutions to nerve discontinuity will depend on the actual size of the injury. Usually a nerve gap described as "small" is when suturing the proximal and distal ends can be accomplished without compromising elasticity. Conversely, reference to a nerve discontinuity as "large" is commonly done when a suturing procedure generates tension.

### 1.2.3 Solutions

As stated before, peripheral nerves have the capacity to regenerate by growing their axons. Nevertheless, they need to be guided to enervate the proper objective to be reached. Suturing the nerve ends is the preferred procedure over other alternatives when a gap exists [13, 15]. However, if that procedure is not possible to follow, a graft is required to enhance the healing rate of a long nerve gap [2, 13]. The graft consists of a cylindrical scaffold of open ends to provide communication between the nerve stumps. The ends of the graft are secured to the ends of the nerve providing communication between the two stumps. Autografts are the most widely used guidance conduits. Those are sections of healthy nerves removed from another part of the body from the same patient that will receive it. The drawbacks of these are that there is a limited amount of donor tissue, mismatch between the dimensions of the ends of the nerve and the size of the donor tissue, besides the loss of function from the removed segment. Some other alternatives are the allograft and xenograft. The first comes from another being of the same species and the second is tissue from a different species. They will both be rejected by the receivers' immune system, the reason why immunosuppressant drugs are required. Moreover, other tissues such as veins [31, 32] and muscle [32] had been used to serve as a guide for the nerve to grow over a hollow space that will show the path towards enervating the proper target. It is important to mention that they show a small degree of success. Even autografts, which are preferred over all other alternative guidance conduits because of their lack to generate an immune response, have a high percentage of failure some of them giving rise to the formation of neuroma [29]. Besides the previously mentioned scaffolds, artificial grafts are being investigated for their potential to repair nerve discontinuity. These are conduits that can help to bridge the nerve gap without having to affect a donor site or running out of tissue. Nerve guidance conduits

(NGCs) are intended to have certain characteristics to maximize the enhancement of nerve regeneration. Today, there are commercially available NGCs. Still, they are not optimal models. They are of different materials and different sizes according to the patient's needs. Some of the brand names are NeuraWrap™ and NeuraGen® from Integra™, which are collagen based materials that are biocompatible and bioresorbable [33]. As its name makes reference to, NeuraWrap™ is a protector for the nerve that is not completely transected. It wraps the compressed nerve shielding it from its surroundings. On the other hand, NeuraGen® is a conduit of varying dimensions from 2 cm to 4 cm in length and 1.5 cm to 7 cm inner diameter, segments to join nerve ends. A third commercially available is Neurolac®. This conduit is manufactured by Polyganics B.V. It is a synthetic bioresorbable polyester poly(DL-lactide-ε-caprolactone) [34]. Their final products are lactic acid and ω-hydroxyhexanoic acid, which are resorbed by the body [35].

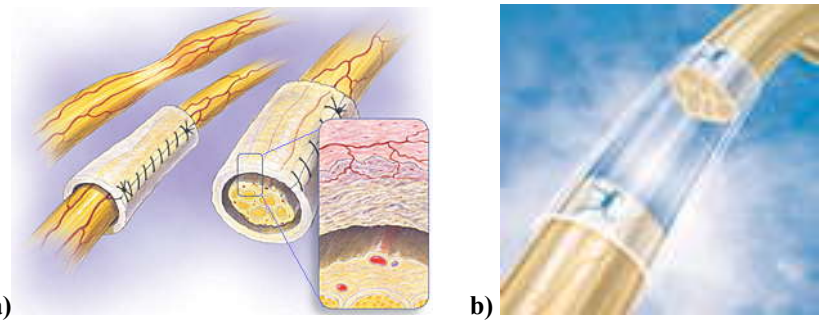


**Figure 1. 6. Commercially available products. a) NeuraWrap™ from Integra™. Modified from [33]. b) Neurolac® from Polyganics BV [36]**

Even though guidance channels help in the healing process better than no surgical intervention, they fail to work better than autografts in rats with nerve gaps greater than 10 mm

[29]. Recently, scientists continue working on finding the optimal conditions and bringing them together in a scaffold to enhance peripheral nerve regeneration.

### 1.3 Conduits and Their Characteristics

Mainly six features (remarked next in bold) had been identified as imperative to achieve the optimum NGC. As of today, there is no conduit that meets all the requirements for the most advantageous NGC.

The material should be **biodegradable**. This is, that the body will be able to get rid of it thorough biological pathways. The advantage of a biodegradable material is that there is no need for revision surgery. Non-biodegradable scaffolds would have to be removed once the nerve has healed. The process involves surgical intervention to be taken out, an undesired practice to follow. **Electrical activity** is another component that should be incorporated in a NGC. Conductivity will stimulate nerve cells to grow. Internal **multilumens** must also be present. As of today, only single lumen conduits are available in the market. An intraluminal channel provides direction and support. Axons tend to grow better here since they have a surface area where to grow longitudinally. An **oriented nerve substratum** will account for cell migration. Best nerve regeneration results had been demonstrated when the previous feature is arranged having a predesigned orientation. Orientation of the extra cellular matrix (ECM) is advantageous for the **incorporation of support cells**. Glia cells then have guidance to achieve certain accommodation where their function can be optimized. NGC materials have to be bioactive to provide a place for cells to adhere. Some materials are naturally bioactive, while others have to be modified to attain cell adhesion. Last, **controlled release of growth factors** is a key in a NGC for enhancing nerve reconstruction. Depending on the type of trauma, the healing time of a nerve might vary dramatically, for instance days or years. It is imperative that the scaffold

remains releasing these cues from start to end of the reconstruction process and at the specific desired site. This leads to the challenge of scaffold building. Its construction should take into consideration the amount of cues to include and their release rate. as well as their location within the scaffold to be further released where needed in the nerve, in addition to preserve bioactivity after signals escape from the matrix.

Next is depicted in Figure 1.7 what illustrates the components that make up the ideal nerve guidance conduit which will ultimately accelerate the regeneration process:

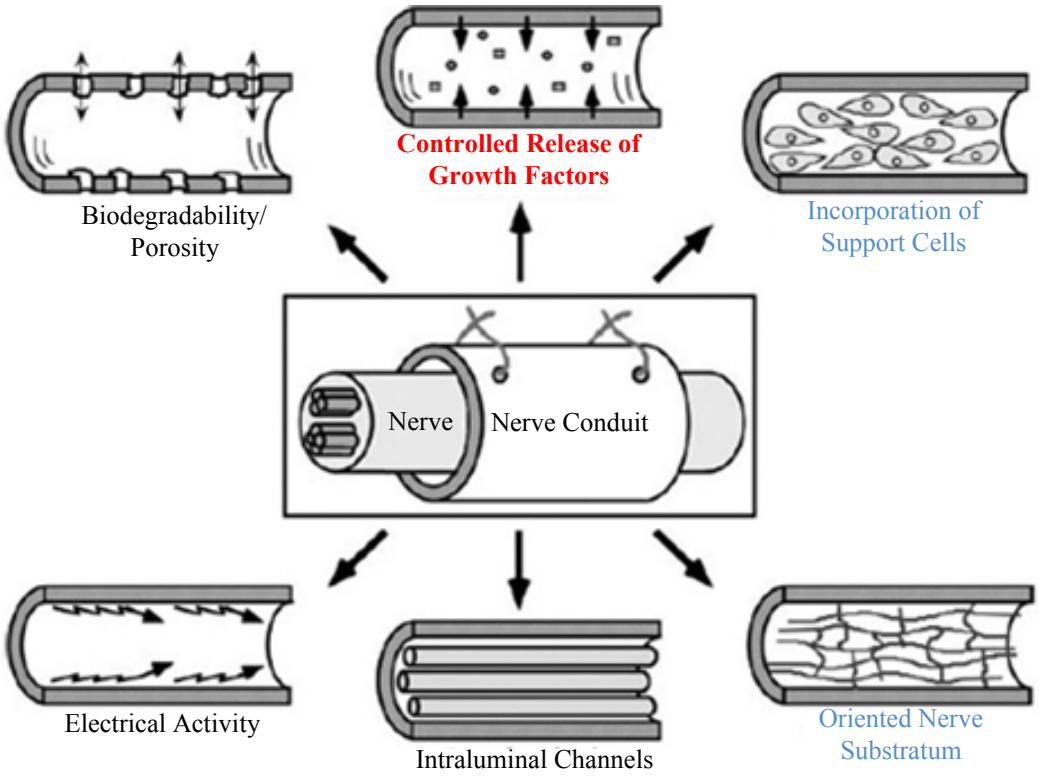


**Figure 1. 7. Model of the ideal nerve conduit features [7]. Modified from [1,3]**

All the previous characteristics should be integrated taking into account the wound healing rate. For example, an ideal scaffold would be worthless if it is absorbed before repair is

accomplished, or if its component characteristics are not there through the entire healing course. Reviews with the most recent advancements regarding tissue engineering and NGC are available [37, 38]

This project presents emphasis on the division of controlled release of growth factors and a means to incorporation of support cells. Bioactivity of growth factors is required to be present for months. However, growth factors are usually diffused from their matrix within few days, promptly losing their effects over the site where they are required. In order to extend their presence within the healing site, different methods to incorporate them into the conduits has been used as well as various materials and techniques which will be reviewed in Chapter 2. Regarding the incorporation of support cells into a NGC, the material of which the conduit is done has to be bioactive. Either natural, synthetic or hybrid materials should be capable of interacting with cells. One of the main concerns at the time of manufacturing NGCs out of any material is if they will preserve activity of their biological domains after the building process.

## 1.4 Engineered NGCs: SL as a Building Method

The way in which nerve scaffolds are fabricated varies from simple to complex techniques. Materials often take the shape of the tool where they are placed such as tubular molds [39, 40]. Unluckily, it is hard to have a precise control over the microstructure. Other systems such as rapid prototyping (RP) are under investigation to accurately deal with characteristics, including, for instance, uncommon scaffold shapes, porosity and biological cues inclusion [41-45]. Rapid prototyping is a set of technologies that produces parts out of powder, liquids or solids [46]. The achievable complex shapes of end products through RP come from the beginning of the process. Taking advantage of the accurate capabilities of software sketches, drawing of the part is created using a computer-aided design (CAD) program. The file design is

then converted to a compatible mode that can be read by a laser manufacturing machine to be constructed in three dimensions [43]. The conversion is about slicing the file design so that the machine builds each slice at a time. It is an additive process in which thin layers are formed at a time and aggregated one on top of the other until completing the desired structure. In a recent past, RP was strictly a tool for the manufacture industry. Before proceeding to build a finished part, a model prototype is commonly manufactured for review before the mass production takes place. Today, rapid prototyping allows for the execution of these preliminary replicas while RP´s previous application was restricted to create design models [47]. Recently, it has been intended to be used with other purposes such as building soft [48] and hard [49] scaffolds as finished parts. Stereolithography (SL) is under the scope as a suitable and proliferating RP technique for the creation of tissue engineering scaffolds [50, 51]. SL takes advantage of the crosslinking ability of some polymeric materials. The apparatus used in this study is equipped with a helium-cadmium (He-Cd) laser that provides the energy to produce free radicals that initiate the curing process, in which a liquid solution turns into a solid. This laser exerts a wavelength ($\lambda$) of 325 nm and has a diameter of ~250 μm at the place where it hits the solution to be gelated, detailed information on this is provided on Section 3.1.1.1. Poly(ethylene glycol) hydrogels built under this process were investigated to determine if they retain bioactivity of their incorporated domains (RGDS) and the released nerve growth factor (NGF).

## 1.5 Chemistry Involved: poly(ethylene glycol)

Poly(ethylene glycol) (PEG) is also known as poly(ethylene oxide) (PEO) depending on its molecular weight (mw). Usually, people refer to this polyester as PEO when its mw is low and PEG when its mw is high. Still, this is ambiguous. For example, in a work by Chen et al. [52], for molecular weights of 400, 1000 and 2000 daltons (Da) is called PEO, while Park et al.

[53] refer as PEG to this polymer of 570 Da. Here it is called by the name of PEG. This extensively used polymer has various applications. Given that natural polymers lack advantageous attributes that the synthetic ones provide such as photocrosslinking, they are often modified with PEG. This modification allows the incorporation of functional groups into natural materials that permit their crosslinking. As a result, physical and chemical properties can be controlled such as porosity, crosslinking degree, elasticity, swelling behavior and the faculty to achieve complex shapes [53]. Benefit is taken from PEG's non-toxic bioinert characteristics as a cover for other materials to improve their biocompatibility [52]. However, this can also be a limitation for PEG itself. For example, plain PEG hydrogels are not biodegradable. Despite the fact that the body cannot get rid of PEG networks, those can be modified with peptides susceptible of enzymatic attack for their degradation [54], chemically changed with linkages which bond or dissociate and are pH dependent [55], or copolymerized with poly(lactic acid-co-glycolic acid) to not only be bioerodible [56, 57] but to give rise to a biodegradable material [58,59]. In addition, PEG's versatility permits the inclusion of molecular moieties such as cell adhesive peptides for the substratum to become selectively bioactive [60, 61]. As a synthetic thermoset, PEG has been studied as a photocrosslinkable material for tissue engineering [10, 62, 63]. To accomplish this, PEG is chemically functionalized. Its original hydroxyl reactive end groups are replaced by different groups. An example is the addition of acrylate end groups, giving place to poly(ethylene glycol) diacrylate (ACRL-PEG-ACRL or PEGda) [62]. Acrylates contain vinyl groups (double bonded carbon atoms) linked to a carbonyl carbon [64]. These functional groups are the ones that allow for the crosslinking process [65]. Afterwards, those molecules at the ends permit the inclusion of chemical and physical cues that can guide the axon`s growing path.

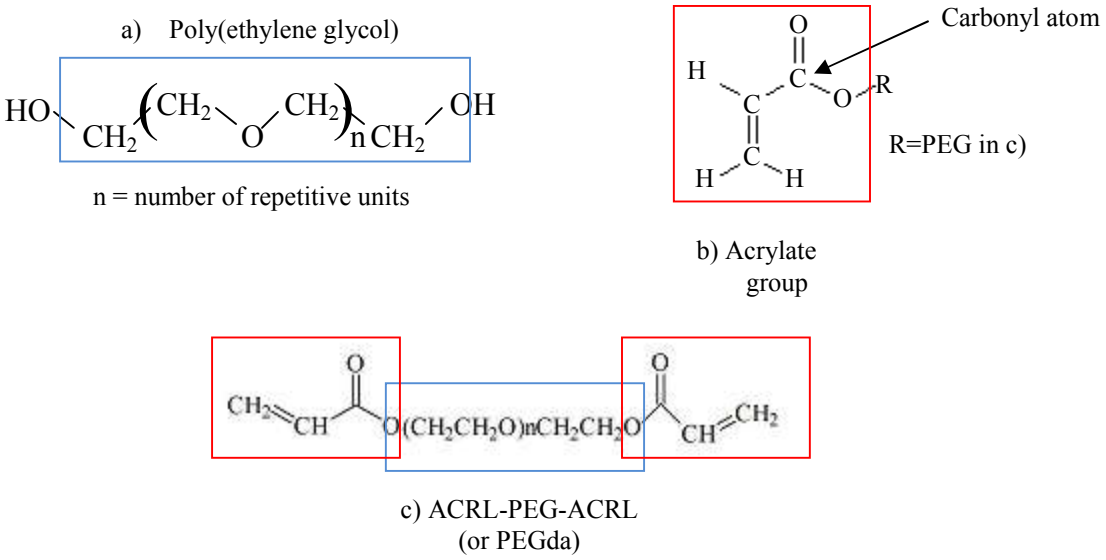


**Figure 1. 8. Chemical structures of a) PEG [52], b) acrylate functional group [64] and c) PEGda [66]**

The crosslinking process takes place via free radical polymerization. It is induced by the ultraviolet (UV) light provided by the SL He-Cd laser or by manually providing UV radiation from a lamp. When the UV light reaches the solution, the photoinitiator reacts (as its name says, it initiates a process when exposed to certain light). The energy provided by the wavelength to which the solution is exposed makes the photoinitiator (PI) generate a free radical which starts a chain polymerization reaction [67]. This free radical is an electron excited from the PI which attacks a double bond at the ends of the PEGda chain, at its acrylate functional group. Then, as the double bond is opened, it is ready to react with another opened end of PEGda, and they might link. When this happens, is when PEGda crosslinks, forming a network. This mesh is the molecular basis under which PEG hydrogel scaffolds are made of in the present work. Another important characteristic of PEG is called PEGylation. This refers to molecules that are covalently linked to the polymer. Here, a sequence of amino acids was linked to specific sites of PEG to turn the polymer bioactive. In addition, given that PEGylation makes this food and drug

administration (FDA) approved polymer a good candidate as a drug carrier [68], NGF was chemically linked to PEG (PEGylated) besides physically trapped to study its diffusion from the polymer.

### 1.5.1 $^{1}$H NMR Spectra

A nuclear magnetic resonance (NMR) spectrum is like a finger print of molecules. Each signal (peak) in the $^{1}$H NMR spectrum is formed from hydrogen atoms present in the molecules of what is being tested and that gives information about the molecule´s chemical organization. NMR emits radial frequency waves. Then, electrons around a hydrogen atom induce an electronic current which provides a local magnetic field. The hydrogen nucleus spins with (aligned) or against (opposed) the magnetic field exerted by the spectrometer. The more hindered a hydrogen atom is, the more energy required to excite it and produce a signal in the NMR spectrum. Signals appear from left (low field) to right (high field) starting with the least hindered protons (deshielded) to the more hindered ones (shielded). For example, hydrogen atoms of tertrametylsilane $(CH_3)_4Si$ are highly shielded. $(CH_3)_4Si$ produces a signal high field, since relatively high energy is required to deshield electrons around its hydrogen atoms and give a peak. To acquire numerical data, the distance in-between signals with respect to $(CH_3)_4Si$ is measured. This is known as the chemical shift (δ). The $\delta_{(CH_3)_4Si} = 0.00$. Chemical shift of a signal = distance of peak from $(CH_3)_4Si$ (in hertz) divided by the spectrometer frequency (in megahertz) and the resulting δ is reported in parts per million (ppm). To quantify the amount of hydrogen atoms that make up a signal, the area under the peak can be measured giving ratios between the different signals. This is known as the "integrated area" and it is used in this work to calculate the number of repetitive units (n) of PEG in the PEGda used for the experiments [69].

Poly(ethylene glycol) diacrylate has four structurally different hydrogen atoms. More clearly, their difference is according to their configuration within the molecule. For example, the four hydrogen atoms of the repetitive monomers account for a single signal (their peaks appear at the same place) in the spectrum since they are chemically equivalent. Hydrogen atoms at the acrylate end groups lead to three more peaks. Even though hydrogen atoms at the outer carbon of the vinyl end group look very similar, they are not superimposable mirror images of each other (not enantiomers), they are diaestereomers of each other. Those hydrogen atoms give rise to different peaks since they are not equivalent. Registered spectra can be found in databases such as SDBS. Following is an NMR found for $C_4H_{10}O_3$ that corresponds to PEG (without the acrylate end groups) [71].

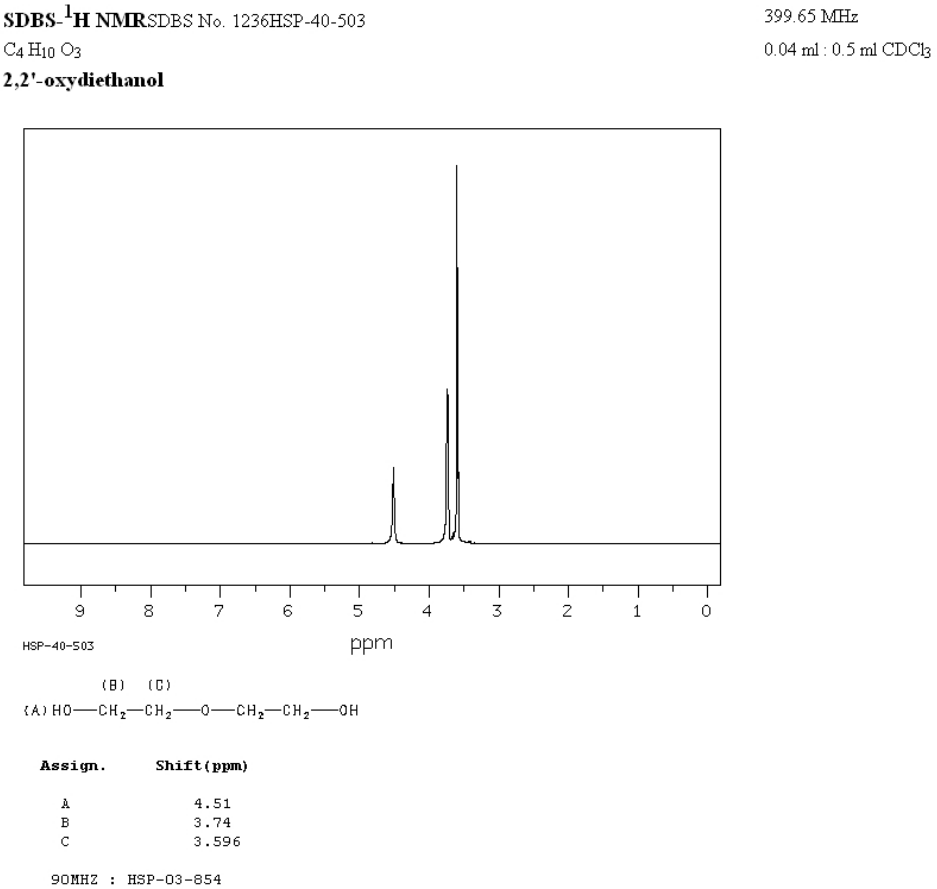


**Figure 1. 9. Proton NMR spectrum of $C_4H_3O_{10}$ provided by SDBS [71]**

## 1.6 Biological Aspect

The material of which nerve scaffolds are made of should be able to support biological activities as mentioned in Section 1.3. However, secondary effects such as immune rejection must be avoided. Due to the fact that PEG causes no response by its host, it makes it a good implantable hydrogel material candidate. PEG can be then combined with chemical moieties that exert specific responses in cells without causing undesired consequences.

### 1.6.1 Arg-Gly-Asp-Ser (RGDS)

Arginine, glycine, aspartic acid and serine (Arg-Gly-Asp-Ser or RGDS) make up a sequence recognized by cells as a signal for attachment. Since PEG is intrinsically non-cell adherent, the RGDS sequence PEGylated to it turned the hydrogel capable of interacting with cells. PEG has previously been linked to this tetrapeptide and hydrogels have been patterned with this material [61]. Incorporation of this oligopeptide contributes to the enhancement of nerve regeneration by providing sites on PEG hydrogels for cell adhesion.

### 1.6.2 Nerve Growth Factor Effect

Nerve growth factor belongs to a family of neurotrophins and it is the best known of them [71]. Its whole complex known as 7S NGF (S being the sedimentation coefficient) is composed of three subunits (α, β and γ). The β-NGF subunit is referred as responsible for the protein activity [72] through the high affinity receptor, tyrosine kynase A (TrkA). However, it has been shown that 7S NGF has different activity than 2.5S NGF *in vitro* [73]. Even though the terms β-NGF and 2.5S NGF are used interchangeably for having identical activities, differences as their preparation have been stated [74]. After its discovery [75] and isolation from the mouse submaxilary glands and snake venom [76], it was known for having specific growth effect on chick embryo nerve cells [77]. It was then known for its potential on regenerating gaps across

nerves [78]. NGF promotes cell growth, survival and differentiation, reason why it is a potential protein to incorporate in nerve guidance conduits to accelerate the nerve regeneration process.

### 1.6.3 Cell Lines

Culturing cells is a process where cells grow and proliferate *in vitro*; this is, in the laboratory. This is advantageous because we can have controlled conditions and specifically see the behavior of these as a consequence of a known change. Depending on the type of study that is being made and what is to be determined is the cell line to be used. In this case, human dermal fibroblasts (HDFs) were used to test the bioactivity of the adhesion ligands on PEG after their presence during the gels manufacture by rapid prototyping. HDFs were chosen for their easiness to culture. HDFs can be cultured over a surface evenly dispersed. They tend to align with each other once they reach a high confluency. HDFs are a finite cell line (derived directly from tissue) and they are better to be used before passage 14. On the other hand, pheochromocytoma (PC-12) cells are an infinite cell line derived from an adrenal gland tumor in a male rat. They tend to grow in colonies forming cell aggregates (or clumps). PC-12s mimic nerve cells. They tend to extend processes when exposed to NGF. For this reason, pheocrhomocytoma cells were chosen to test the bioactivity of NGF after the process of this protein inclusion into the hydrogels and its release from the PEG´s mesh. Different cells require different culture techniques and those are described in Chapter. 3 Materials and Methods, Sections 3.1.1.11.3 and 3.1.2.2.1.

*Chapter 2*

## 2.0 Literature Review

This chapter provides an overview of what other researchers have accomplished regarding the development of conduit scaffolds for peripheral nerve repair. The section describes their methods and how their work contributes towards achieving the ideal nerve guidance conduit (NGC). By ideal, the description according to Hudson et al. [7] as mentioned in Chapter 1 is followed. Specific attention is given to the division of "controlled release of growth factors" since it is the fraction intended to be improved by this thesis work, one of the elemental characteristics required on a NGC.

## 2.1 Biodegradability/Porosity

After reviewing the various aspects of tissue engineering for nerve repair, Huang et al. [3] presented a chitosan and poly($_{D,L}$-lactide-co-glycolide) (PLGA) scaffold as a nerve graft with intraluminal channels. It is a combination of a natural and a synthetic polymer, both biodegradable. Chitosan is a polysaccharide found in many animals (crustaceans´ shell, insects and fungi cell walls) and it is vastly available [79]. PLGA is a copolymer composed of poly(glycolic acid) (PGA) and poly(lactic acid) (PLA). These two polymers by themselves reveal different characteristics in contrast to the exerted properties when they are combined. Together, as PLGA the copolymer provides the mechanical strength and cell adhesion properties that chitosan lacks [80]. Moreover, Huang et al. [3] describe their conduit building technology as an easy and repeatable process. Multichannels are formed within the scaffold. Lyophilization provided the porosity required and nickel-chromium (Ni-Cr) wires were used to form the lumens. These internal channels were consistent in diameter throughout the scaffold, measuring 115 μm wide.

In addition, these researchers gathered and published data provided by different investigators and it is presented next. The following table lists different polymers, copolymers, natural and synthetic materials that have been utilized in the fabrication NGCs. It is shown in which animals were implanted for their study and the gap length of nerve the graft attempted to bridge. All of the following are bioresorbable materials. Table 2.1 is found interesting because it shows not only natural materials, but also synthetic ones that are important for resembling characteristics of the natural ones, such as biodegradation.

**Table 2. 1. Peripheral nerve scaffold clinical studies [3]**

| Material | Animal | Gap length (mm) |
|---|---|---|
| Chitosan | Rat | 15 |
| Collagen | Rat | 30 |
| | Rat | 12 |
| Gelatin | Rat | 10 |
| Polyglycolic acid (PGA) | Monkey | 1-1.5 |
| | Rat | 5 |
| | Human | 5-30 |
| | Rabbit | 30 |
| Polyglactin | Rabbit | 20 |
| Poly(organo)phosphazene | Rat | 10 |
| Glycolide trimethylene carbonate | Rat | 5 |
| Polyurethane | Rat | 8 |
| Methacrylate-based hydrogels | Rat | 10 |
| Poly 3-hydroxybutyrate | Rabbit | 2-4 cm |
| PLGA | Rat | 12 |
| | Rat | 4 |
| Poly(L-lactide-co-caprolactone) | Rat | 10 |
| PGA mesh coated with collagen | Dog | 80 |
| Poly(glycosaminoglycan-co-collagen) | Rat | 15 |
| Poly(L-lactide-co-ε-caprolactone)(inner): a mixture of polyurethane and polylactic acid (outer) | Rat | 7 |

Talking of non natural materials, Bruggeman et al. [81] developed a family of biodegradable poly(polyol sebacate) (PPS) polymers by reacting polyols with sebacic acid. Xylitol, sorbitol, mannitol and maltitol polymers were reacted in different ratios with sebacic

acid, giving rise to poly(xylitol sebacate) (PXS), poly(sorbitol sebacate) (PSS), poly(mannitol sebacate) (PMS) and poly(maltitol sebacate) (PMtS). Ratios between the polyol and sebacic acid were PXS 1:1 and 1:2, PSS 1:1 and 1:2, PMS 1:1 and1:2, and a 1:4 stoichiometry for PMtS.

Physical and mechanical properties of these biodegradable materials were measured such as contact angle, young's modulus, tensile stress, elongation, glass transition temperature, density and molecular weight.

These synthetic polymers were compared to poly(L-lactic-co-glycolic acid) PLGA, a widely known and used copolymer for its biocompatibility and medical applications. Nuclear magnetic resonance (NMR), gel permeation chromatography (GPC) and an Instron® 5542 were required for the prepolymer characterization and fourier transform infrared spectroscopy (FTIR) to evaluate after crosslink. Poly(polyol sebacate) polymers went through *in vivo* and *in vitro* analysis. PPS disks of 10 mm diameter and 1 mm height were implanted in rats to test for biocompatibility and biodegradation. Results showed PPS mass loss in all implanted polymers at different time points. PSS in a 1:1 ratio was completely degraded by the time of twelve weeks. However, cells would not attach to this stage. Images below show the *in vivo* results of histological analysis. Figure 2.1 involves PMS 1:2 implanted after ten days and twelve weeks as compared to PLGA. The column on the left presents pictures of the polymers after 10 days of implantation, whereas the right column shows the panorama after twelve weeks. Muscle is separated from the polymer by the fibrous capsule (C). Label depicts the polymer name and its ratio composition.

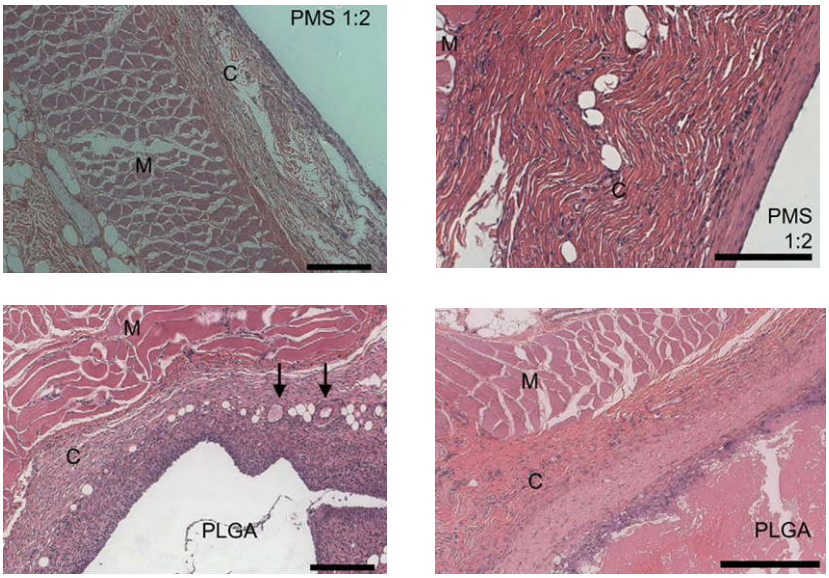


**Figure 2. 1. *In vivo* results. Histological analysis. Degradation comparison between the novel PMS versus PLGA after 10 days (left column) and twelve weeks (right column). Left column scale bar represents 100 µm. Right column scale bar stands for 200 µm. M= muscle, C=fibrous capsule [81]**

For the *in vitro* studies, different primary and cell lines were grown over surfaces of PPS polymers. For instance, BAC cells were cultivated over PLGA and on a PMS surface. In comparison, cells on both surfaces present the same morphology, even though they are unequal in population number. Following is an illustration (Fig. 2.2) of BAC cells cultivated over PLGA (left) and PMS (right).

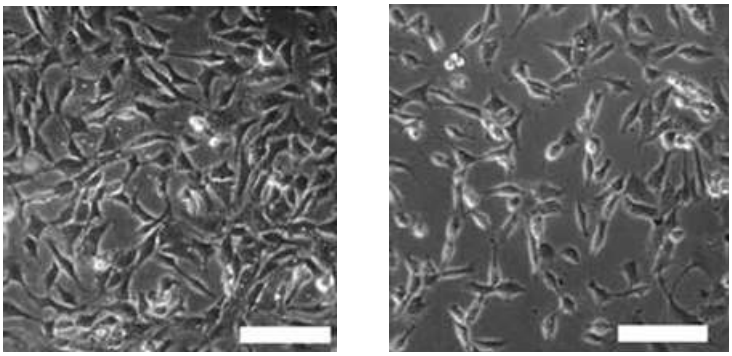

**Figure 2. 2. BAC cells growing over PLGA (left) or PMS (right). Bar = 50µm [81]**

Mano et al. [82] dedicated to analyze biopolymeric materials for hard tissue replacement, bone and cartilage. Only starch and starch based materials were studied here. They studied biocompatible materials to be inside the body for a limited amount of time or to remain there indefinitely. For this objective, they analyzed bioinert non degradable and degradable polymers.

The following image (Figure 2.3) depicts a graph of the mechanical properties of polymeric, biological, ceramic and metallic materials with biomedical applications. The interest in showing this graph is to make the point that if these are mixed, they can give rise to composite materials that provide combined properties according to the needs. These might be of importance if an implant is intended to partially degrade, while part of it might be necessary to stay permanently, for example. Then, a composite material might be chosen based on its components´ properties.

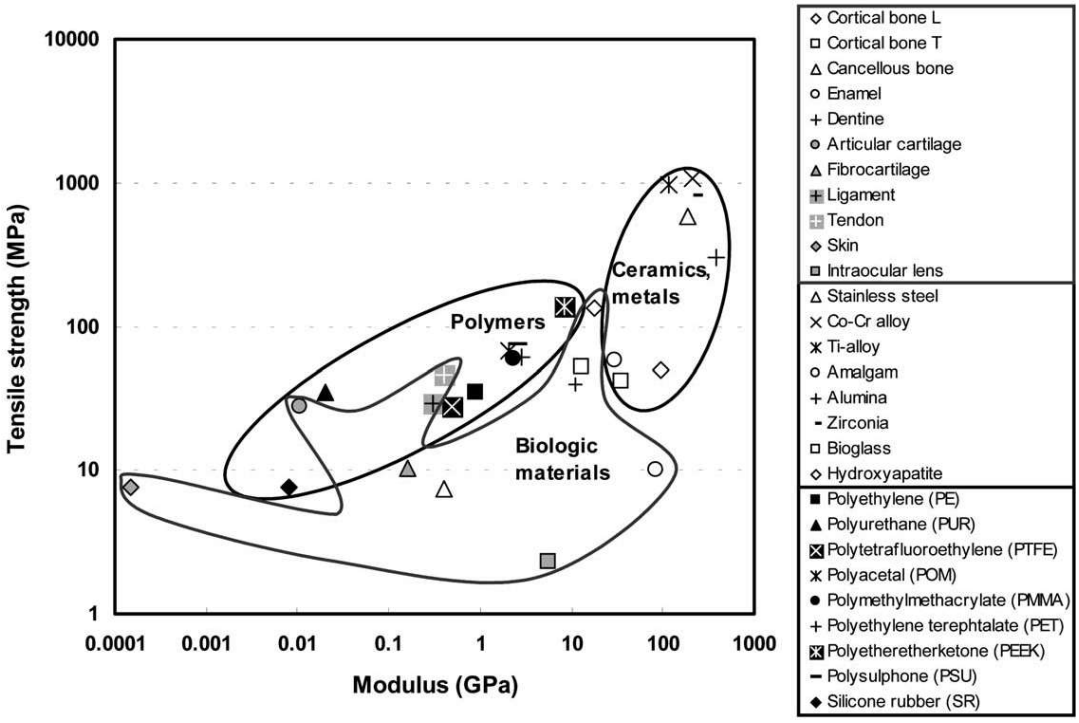


**Figure 2. 3. Mechanical properties of biomaterials [82]**

To have control over the biodegradability rates, materials might be combined to find the best degradation rates [83]. Besides the biodegradability of the material, the method of scaffold construction is important in order to have control over certain features such as the physical structure. Pierucci et al. [84] proposed a solvent evaporation membrane preparation method of known biodegradable polymers. Poly (L-lactic acid) (PLLA) and poly(caprolactone) (PCL) 300 and 100 kDa mw, respectively, were the materials under investigation. Membranes for the conduits were built by this solvent evaporation novelty process and through the extrusion method to compare their efficacy in the regeneration process. Some of the advantages mentioned of using this process were the easiness to manage the conduit when interacting with the nerve regarding suture, resistance and flexibility.

One of the important aspects of biodegradable materials is their porosity. This plays an important role regarding degradation rates and growth factors delivery. Access to nutrients, surface area and redistribution of cells throughout the scaffold are mentioned to be affected by the pores´ size and pores´ distribution. More control over the mentioned features can be achieved if porosity is previously structurally organized. The methods of material fabrication for the scaffold are often responsible for the porosity outcome. Capes et al. [85] proposed the use of sugar spheres of different diameters to generate the desired porosity. A method for calculating numerically how is the surface area of the scaffold affected by the size of the sphere is provided by their study.

In a different investigation, a biodegradable material made of polylactic acid (PLA) and calcium phosphate glass was surface characterized by Chales-Harris et al. [86]. For the scaffold preparation chloroform and dioxane were the two solvents used for solvent casting or phase-separation method. Different results were acquired regarding chemical and physical properties

such as surface morphology, roughness, wettability and the material´s capacity for protein adsorption.

## 2.2 Electrical Activity

A conductive polymer was developed by Schmidt et al. [87]. Oxidized polypyrrole (PP) was the film over which pheochromocytoma (PC-12) cells were grown to test for a response to a 100 mV voltage. PC-12 cells were differentiated with 25 ng/ml nerve growth factor (NGF). Once cells extended neurites, they were exposed to electrical activity. Cells responded to the treatment by elongating their neurites. This paper is a good reference for the present thesis regarding materials and methods. Cells were seeded at 1.33 x $10^4$ cells/$cm^2$. PC-12 cells were maintained with DMEM and 25 ng/mL NGF. Subsequently, 10 – 20 images were taken per well going up to down and left to right. Additionally, it is mentioned that a well measures 1 cm x 1.5 cm from the inside. Figure 2-4 shows the cell response to no electric potential or to 100 mV one day after electrical stimulation through the PP film.

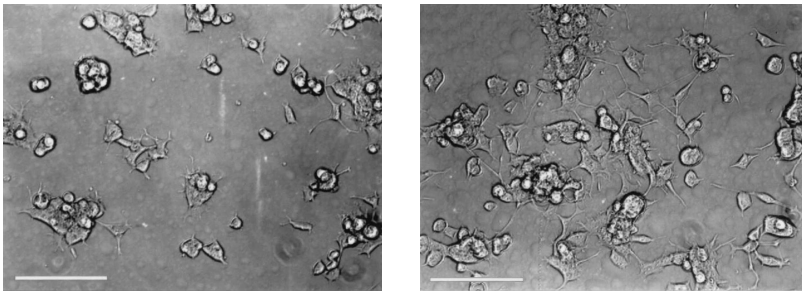

**Figure 2. 4. PC-12 cells unexposed to an electric potential (left) and exposed to 100 mV (right). Bar scale = 100 µm [87]**

*In vivo* studies also took place in this experiment. PP film was implanted in rats as well as a PLGA film for their comparison. After two weeks, PP showed less immunologic response than PLGA, demonstrating its relative bioinactivity.

## 2.3 Multilumen channels

As the result of providing multichannels for neuron like cells to grow, Mahoney et al. [88] were able to influence PC-12 development orientation by providing a physical cue. Different sized polyimide microchannels were built over glass slides and coated with collagen (Fig. 2.5) for further adhesion of pheochromocytoma (PC-12) cells.

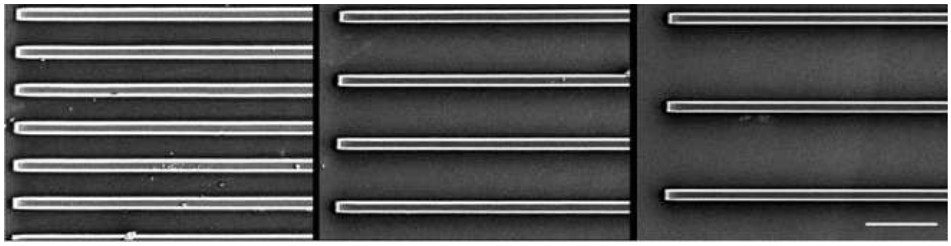

**Figure 2. 5. Scanning electron micrographs of micropatterned channels. From left to right: 20, 40 and 60 µm apart. Scale bar = 50µm [88].**

For the analysis of cell structure within the channels, angles were measured as follows:

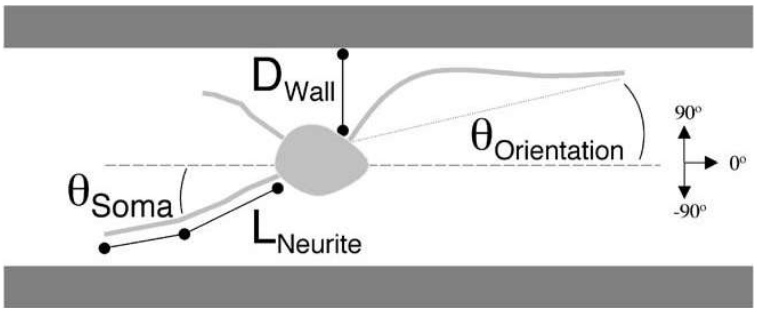


**Figure 2. 6. Growth parameters measured. Different angle orientation concerning cell structure with regards to physical microenvironment [88].**

It was found that cells cultured in microchannels extended less, but longer neurites than without a channel regardless the channel width. Interestingly, it was noticed that neurites directed themselves parallel to the channel wall if these cell processes came into contact with a channel wall (Figure 2.7).

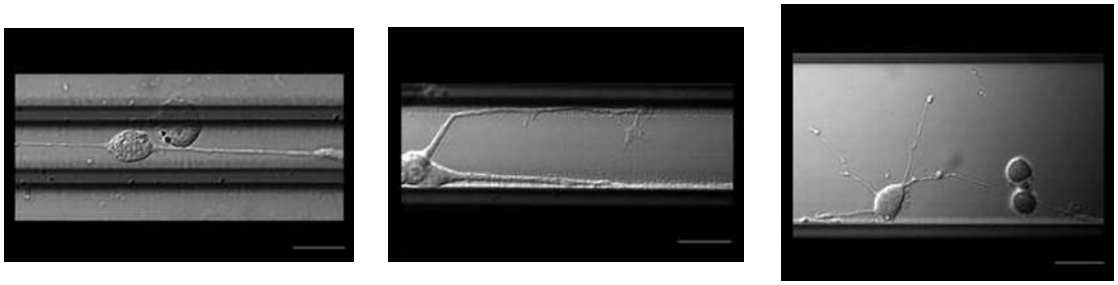

**Figure 2. 7. Neurite development and orientation within different sized channels. From left to right: 20, 40 and 60 microchannel in width. Scale bar represents 20µm [88].**

## 2.4 Oriented Nerve Substratum

Orientation of the extracellular matrix (ECM) is important because it dictates cells a path to follow when growing. Ghasemi-Mobarakeh et al. [89] aligned fibers composed of different ratios of poly(ε-caprolactone) (PCL) and gelatin. Rat nerve stem cells (C17.2 cells) were grown over the aligned matrix to observe their proliferation. Scanning electron micrographs show evidence the alignment of cells with respect to the fibers´ orientation (Fig. 2.8)

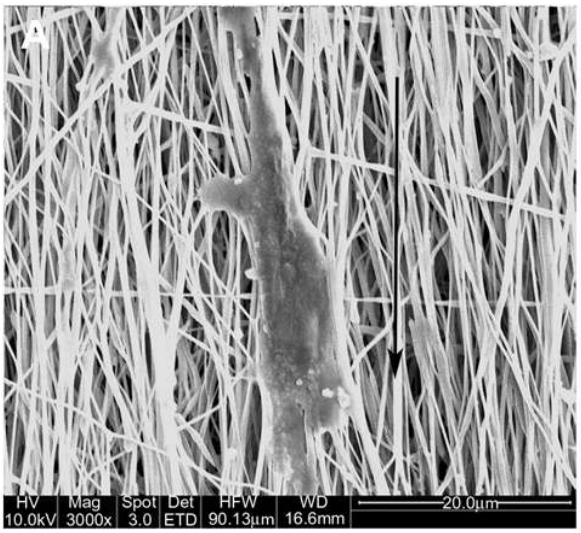


**Figure 2. 8. Nerve cell appearance after cultured in PCL oriented fibers [89].**

Cells will follow not only a physically patterned trail, but also chemical indications of where to adhere that will lead to an oriented cell growth.

Advantage has been taken from the fact that cells will only adhere to places where they find a particular sequence of amino acids. Glycine-Arginine-Glysine-Aspartic acid-Serine (GRGDS), a signal for cell attachment was included in a polymeric mesh. Grafahrend et al. [90] produced blocks composed of a combination of polymers. Poly(ethylene glycol) (PEG) and poly(ε-caprolactone) (PCL) were the basic units composing the block. While PCL is biodegradable and hydrophobic, PEG is the hydrophilic part where the pentapeptide was linked to. Human dermal fibroblasts were used to verify that cell adhesion will be present only where GRGDS was incorporated. The scientific paper names this surfaces as functionalized or non-functionalized depending if they are bioactive or not, respectively. Fluorescent images were taken with a live/dead stain on fibroblasts to analyze cell adhesion. It was shown that cells attached only were to the GRGDS-PEG-PCL surface and not to the PEG-PCL region missing the oligomer.

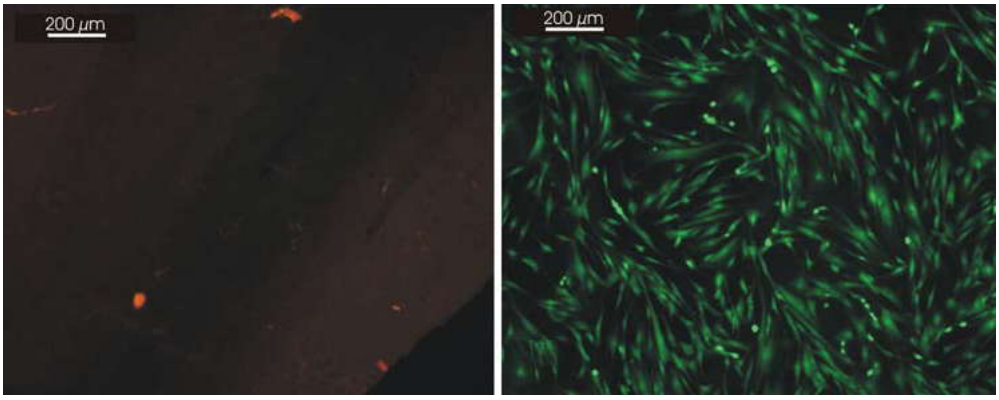


**Figure 2. 9. Live/dead stain on fibroblasts seeded on top of non-functionalized (left) and functionalized (right) PCL-PEG surfaces [90].**

A similar study performed by Hahn et al. [61] permitted the interaction of human dermal fibroblasts (HDFs) with poly(ethylene glycol) (PEG) hydrogels´ regions targeted with a tetrapeptide. The amino acid sequence was RGDS which information is given in Chapter 1, Section 1.6.1. The technology used in this experiment was simple and the instruments included every-day tools: software (Photoshop®) and a laser-jet printer to acquire the masks and desired sketches. PEG hydrogels with the peptides sequence domains were identified by florescent images to make them evident to sight. Moreover, HDFs were seeded on top of the hydrogels containing RGDS domains and attached only to those given adhesion sites (Fig. 2.10).

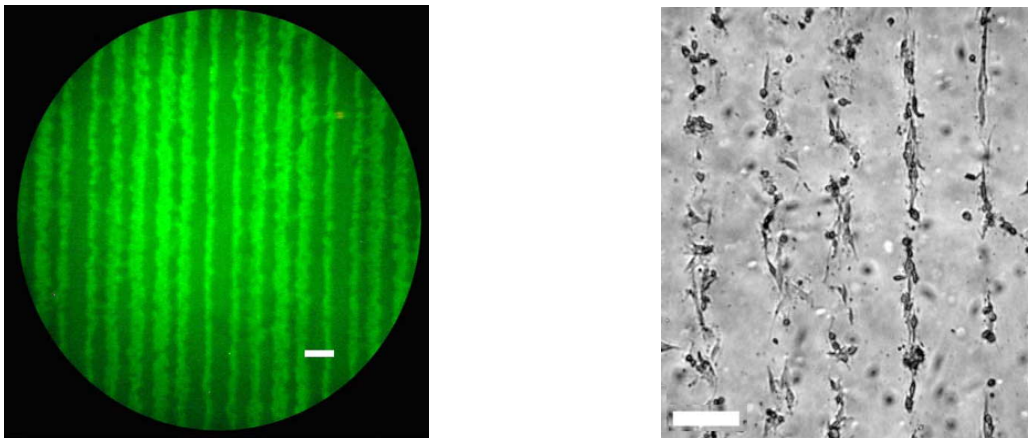

**Figure 2. 10. Left: Fluorescent image of the hydrogel patterned regions containing RGDS. Bar = 250µm [61].**

As stated before, a cell substratum that contains physical orientation and provides chemical guidance is important since a path is predetermined and given to cells for their growth.

## 2.5 Incorporation of Support Cells

The incorporation of Schwann cells (SC) into nerve grafts is a key for reestablishing nerve function. Glial cells provide signals for growth and survival to the regenerating axons such as neurotrophins. Tabesh et al. [91] were given to the task of reviewing materials that could support Schwann cells addition. Interestingly, in this review article it is mentioned that regarding cell inclusion within a scaffold might be better to have cells other than SC, but that behave like them. The reason mentioned is that SC from the patient would have to be harvested from another nerve. This will comprise the donor´s function. To this thesis concern, they reviewed a variety of the most widely used natural and synthetic polymers for nerve scaffold manufacture. Collagen, chitosan, agarose and fibronectin were the natural materials studied. Poly(D,L-lactic acid), poly(lactic-co-glycolic acid), poly-β-hydroxybutyrate, poly-ε-caprolactone, polypyrroles, poly(ethylene glycol), poly(glycerol sebacic acid), and poly(2-hydroxyethyl methacrylate) were the synthetic materials under review. As a result of their study, they proposed a material which composition was a combination of a natural and a synthetic polymer. As an example the combination of poly-ε-caprolactone and collagen was given. Their outcome was based on the polymers´ mechanical and chemical properties that are enhanced when brought together.

Bozkurt et al. [22] isolated Schwann cells from the sciatic nerve of ten Lewis rats and cultivated them. Further on, SCs were seeded into 2D and 3D collagen (type I) scaffolds. Cell migration within 3D cylinders was measured at 3, 7 and 14 days. Graft dimensions were 1 cm long and 2 mm in diameter. Interconnected pores and channels were made by a directional freeze drying technique. SCs aligned themselves throughout the channels of porosity along the collagen nerve graft (Figure 2.11).

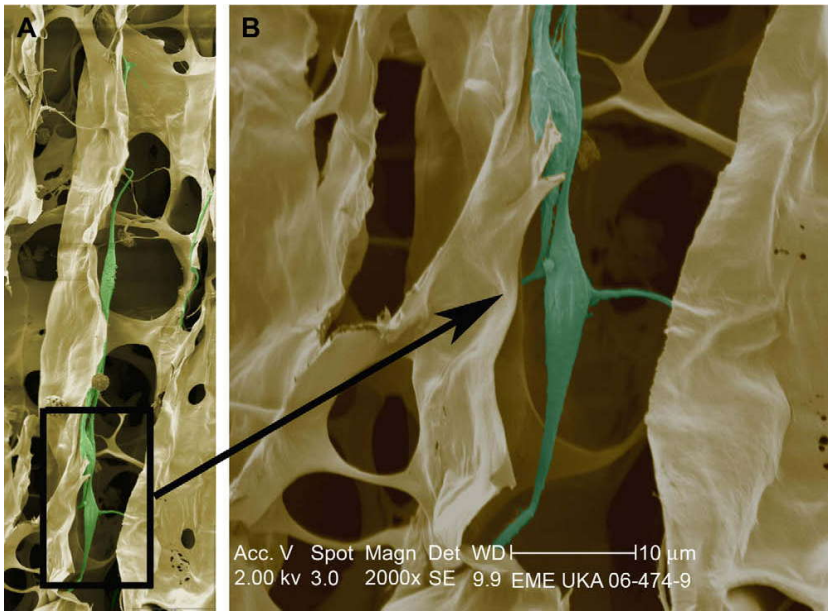


**Figure 2. 11. SEM image of SCs alignment through the porous architecture. Low magnification (A). Higher magnification (B). Green: SC. Ivory: scaffold walls [22].**

Additionally, collagen scaffolds containing SCs were loaded with hemisected dorsal root ganglia (DRG). The purpose was to observe if neurite extension would be guided and supported by SCs. Indeed, the following picture (Fig. 2.12) shows in red an axon behind a Schwann cell.

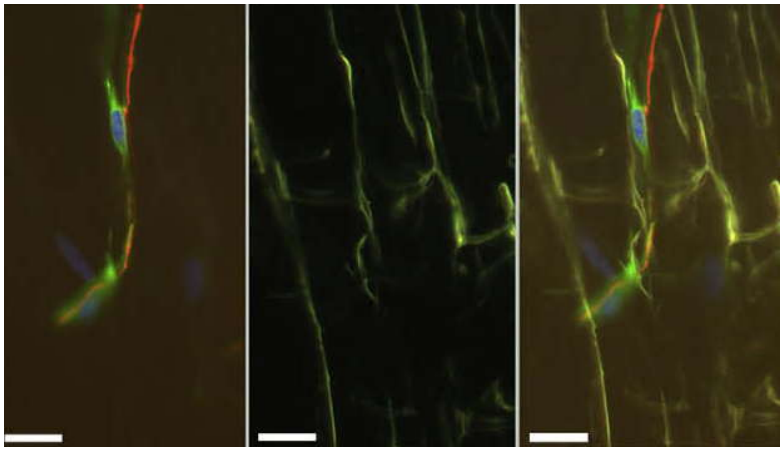

**Figure 2. 12. Fluorescent stains: blue and green for SC, red for axons. Left: SC supporting axons. Middle: Scaffold structure. Right: Overlap of the two previous. Cells aligned within scaffold pores. Scale bar represents 20 µm [22].**

Schwann cells are known to have influence over nerve regeneration by not only physically guiding axon elongation, but providing chemical signals as secreting nerve growth factor [92, 93]. As an NGF source, SCs are good candidates to be incorporated into nerve scaffolds to contribute as an NGF provider to accelerate regeneration. However, large numbers of these cells are required and it is not feasible to have them ready at the time they are needed since they have to be cultured from the host that will receive them to suppress response by the immune system. An alternative being studied is the substitution of SCs for other ones that mimic their function such as transected HEK-293 cells [94]. Cells as the only supply of NGF are not sufficient and this protein source should come from somewhere else such as the scaffold itself. Moreover, its release has to be controlled to ensure activity over the specific desired site.

## 2.6 Controlled Release of Growth Factors

Controlled release of growth factors is object of the present investigation. Even though tubulization helps to avoid diffusion of chemical cues from the site where they are required [95], there is also a need to make drugs available from the various scaffold materials either anchored to the source or entrapped to be released. Our work is based on the following methods and can be compared to them, having in mind that our specific drug and material is nerve growth factor (NGF) within poly(ethylene glycol) (PEG). Detailed reviews describe strategies that have or have not been applied to generate physical and/or chemical gradients. Within those reviews, tables are presented summarizing the work of different researchers. Given data is regarding their methods, incorporated cues, substrates, kind of cells for analytical purposes besides information about polymers and their release capabilities [96, 97]

To have control over the release rate of chemical signals is a challenge. Many methods are under investigation to achieve gradients of different cues. Some experiments have already

gone *in vivo* to test the performance of grafts in regenerating rat sciatic nerve. Even though results were satisfactory, they were not ideal and research has to undergo further [30]. Recently, it has been shown that consciously managing biodegradability rate and porosity of the substrate are suitable ways to have a predetermined influence over drug delivery [98]. In addition, the incorporation of microparticles as drug carriers into scaffolds has shown to be a feasible drug delivery method [99]. For example, Cao and Shoichet [83] investigated the release of a protein from PCL or PCL/PLGA microspheres. Their reason to use a combination of biomaterials was to find the best microspheres´ degradation rate for protein delivery. Ovalbumin (OVA) was used instead of NGF due to their similar molecular weight and thus, comparable release behavior from the matrix. Their analysis was done over 91 days.

NGF release from silk fibroin matrices has been accomplished for 3 weeks [100]. Microspheres made of poly(D,L-lactide-co-glycolide) (PLGA) has also been addressed for encapsulation of NGF. Growth factor diffusion from these particles was observed from different ratios of PLGA components with and without NaCl (salt) to obtain data regarding the best parameters for NGF inclusion and release control. They noticed that salt had an adverse effect on the neurotrophin, although it reduced the unwanted initial high dose release of protein. NGF release was quantified up to 91 days by radioactivity counting. Moreover, NGF that left the samples after one day without salt continued bioactive after the loading and diffusion process as shown by a pheochromocytoma (PC-12) cell bioassay [101]. While these microspheres were porous, other experiments that include the use of non porous (at least non visible) microspheres decreased substantially the leaching of the neurotrophin. This can be considered both positive and negative, as the initial burst release was diminished, but very few of the protein diffused

below the concentration required. And even though small, this system allowed for at least 70 day diffusion time. [8].

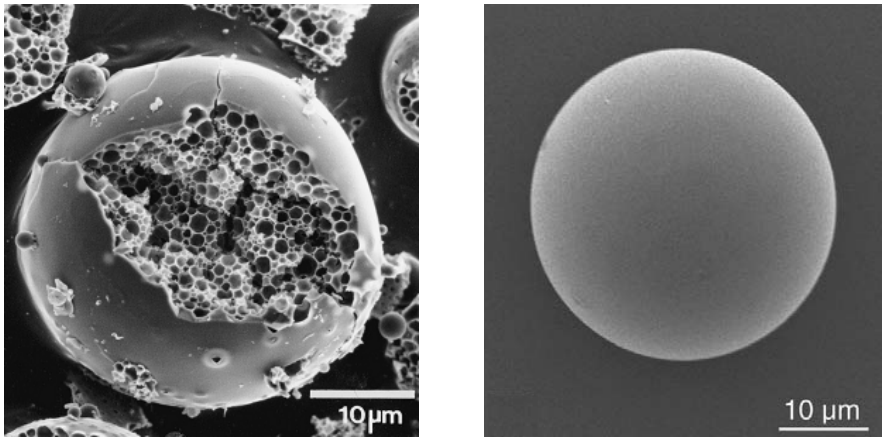


**Figure 2. 13. Microsphere surface comparison between a) visible porous [101] and b) non-porous[8]**

Besides microsphers, other microstructures are promoted as drug carriers, such as microtubules. Agarose hydrogels with lipid microtubules and lipid microtubules themselves have been examined as vehicles for different molecular weight proteins delivery. With the aid of a PC-12 bioassay, results revealed that after the manufacturing process protein bioactivity is preserved. In addition, bovine aortic smooth muscle cells were not affected negatively, showing that the process is cytocompatible. Findings were also that the higher the molecular weight of the protein, the less its release rate [102].

Diffusion rate has also tried to be controlled by relatively weak chemical interactions. Such is the case of affinity based systems for NGF release. In this case, proteins are attracted more or less to certain domains within their matrix, staying with it or leaving it [103,104].

Hydrogel materials do not necessarily contain drugs within a carrier. The scaffold itself can be a source of protein without any additives [105]. The protein is then available free from its source after diffusion or anchored to a surface.

A study by Yu et al. [106] revealed that NGF can be provided immobilized from a natural source. Chitosan (mw. 25,000 g/mol) films were chemically combined with collagen to further enhance cell attachment. Films were then linked to sulfo-SANPAH, a reagent that would make chitosan photocrosslinkable. Then, tetramethylrhodamine cadaverine (Rh) which resembles NGF in this study was bonded to chitosan to further create a gradient over the films. This was accomplished by exposing specific regions to UV light. The light source ($\lambda$ = 364 nm) was coming from a laser adapted to the confocal microscope and the pattern was designed manipulating the microscope´s software. A concentration gradient of a NGF-like reagent was achieved utilizing the accuracy of the confocal microscope. Next, it is structurally shown how Rh was covalently bonded to chitosan. It is clearly seen how an amine group from chitosan is bonded to a carboxyl group in sulfo-SANPAH (Figure 2.14).

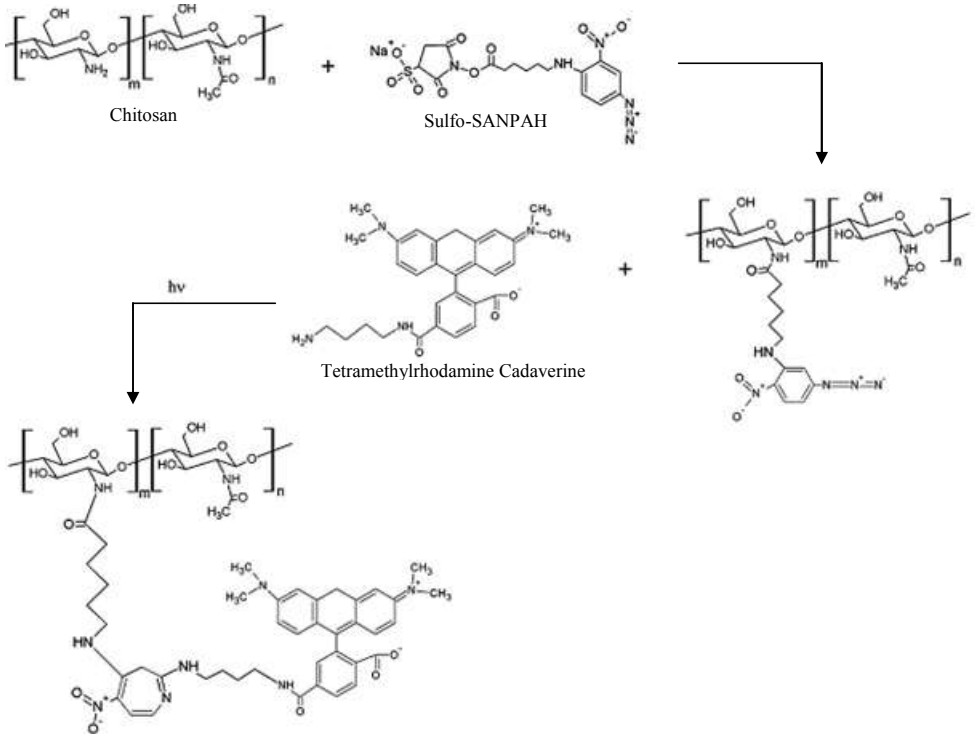


**Figure 2. 14. Chitosan is reacted with Sulfo-SANPAH to produce a photoreactive species. Rh is then added to the photoreactive chitosan and exposed to UV light. As a result, Rh was chemically linked to chitosan [106].**

Because of its primary amine groups, Rh resembles NGF in this experiment. With the previous steps, a concentration gradient of Rh over the chitosan films was achieved. The stage movement was controlled as well as the UV exposure or laser scans. Figure 2.15 shows an increasing concentration of Rh immobilized as the number of scans was increased from left to right.

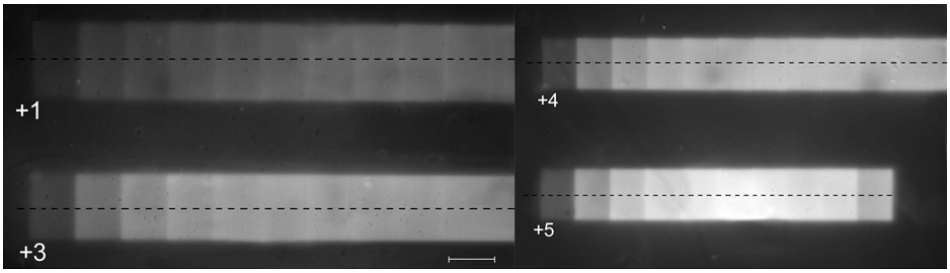


**Figure 2. 15. Tetramethylrhodamine cadaverine immobilized in concentration step gradients on chitosan films. Numbers +1 to +5 indicate the number of scans by the laser over the following pattern. Scale bar = 75 µm [106].**

Moreover, NGF was studied over these films to immobilize it on specific sites and with a specific shape. Also, NGF was conjugated to demonstrate that the same chemistry used to link Rh can be used with this protein.

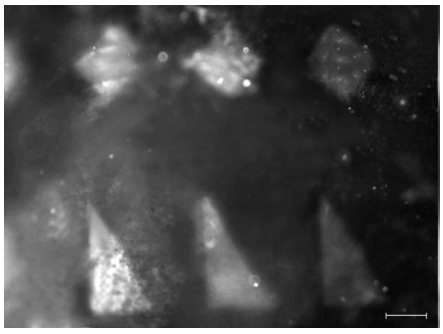

**Figure 2. 16. NGF conjugated to chitosan films by the use of a laser adapted in a confocal microscope. NGF control over different figures, areas and concentration was achieved. Scale bar = 100 µm [106].**

Nerve growth factor was not released into solution once immobilized, but it was made available to superior cervical ganglia (SCG) neurons. Yu et al. [106] were able to show that

NGF was bioactive after the linking process, since SCG neurons extended processes when grown over surfaces containing immobilized NGF.

Similar to the previous mentioned research, Kapur and Shoichet [107] also developed a method to link NGF covalently to a surface and created gradients of this growth factor. Poly(allylamine) (PAA) is the photoreactive material that was placed on top of poly(2-hydroxyethylmethacrylate) (PHEMA) gels, as PAA provides a site for cell attachment and it is the polymer to which NGF was immobilized. In comparison to our work, disks were fabricated and divided into two groups. In contrast to our study, they tested the amount of NGF bound to the surface and its bioactivity. Group 1 was analyzed by a direct enzyme-linked immunosorbent assay (ELISA) and disks from group 2 were plated with PC-12 cells to see if they responded to the growth factor by extending processes. The disks´ dimensions were 0.5 mm in diameter to fit into wells of a 96-well plate and the cell density was $7x10^4$ cells/disk. The information provided in this study demonstrated that NGF can in fact be bonded to PHEMA-PAA gels while maintaining the protein´s bioactivity.

As stated before, biodegradability of materials is one of the properties that permit to control the diffusion of a protein if the degradation rate is managed. Biodegradability can be driven by several factors, such as bonding formation or dissociation according to the environment's pH. PEG has been widely studied as a drug transporter. PEG has been modified with schiff base linkages which make the hydrogel biodegradable. These are bonds that respond to pH changes, leading to release the hydrogel´s contents as it degrades when bonds are broken [55]. To our interest, PEG has been studied for drug release by itself [108]. However, it has also been explored in combination with other materials to take advantage of biodegradability and have better control over drug delivery [57, 109, 110].

*Chapter 3*

## 3.1 Materials and Methods

Turning inert materials bioactive and controlling the release of growth factors has been accomplished using a variety of materials and techniques as mentioned in Chapter 2, Literature Review. In one experiment hydrogel disks were built as a sample of the complete nerve guidance conduit (NGC) material to analyze the neurotrophin release from them. The matrices under investigation here are two molecular weights (mw) of the same polymer: poly(ethylene glycol) diacrylate (PEGda) mw 3.4 kDa amd 6 kDa. The polymeric material of the lower molecular weight (mw) was photocrosslinked in a stereolithography (SL) machine with the aid of Irgacure® 2959 (Ciba®) (I-2959) as the photoinitiator (PI) and the material of higher mw was crosslinked utilizing a UV lamp spot light setup and 2,2-dimethyl-2-phenyl-acetophenone (DMPA) as the PI. Protein incorporation was approached in two ways: physically trapped and chemically conjugated for their comparison. First, the protein solution was combined with the photopolymer solution immediately before the crosslinking process. In this setup the encapsulated neurotrophin (nerve growth factor, NGF) release expectations were that the physically incorporated NGF would come out in a relatively short time frame (faster) compared to the second incorporation method. The other method of inclusion was conjugating (chemically bonding) NGF to PEG in a releasable manner. In this way, PEG and NGF form a covalent hydrolysable bond expected to break under physiological conditions, leaving NGF free to move and diffuse out from its matrix.

To test if SL is a good technique to build bioactive PEG scaffolds, a different experiment took place. Hydrogels of different materials (bioactive and inert PEG) were manufactured with another team member of the tissue engineering research group. The mw of the polymer was 3.4

kDa and solutions contained a 20 wt% PEGda concentration. For all experiments, chemical reagents were supplied from Sigma-Aldrich, St Louis, MO unless otherwise stated. Water supply came from a reverse osmosis ultrapure water system (arium® 611VF, Sartorius).

### 3.1.1 NGF Release from PEG Hydrogels.

Wells of Costar® flat bottom 24-well plates (TC-Treated Microplates, Corning Inc.) were filled with 2mL of RPMI-1640 medium per well and left one day inside the incubator before proceeding with the study. Conditions within the Shel Lab® incubator ($CO_2$ Series Sheldon Mfg. Inc.) were 90% humidity and 5% $CO_2$. In addition, materials to be used such as pipette tips, amber vials and microcentrifuge tubes were sterilized autoclaved (MLS-3750, Sanyo Electric Co., Ltd., Japan) at 121 $^{o}$C for a 20 min cycle. Stock solutions recipes are presented next.

*Phosphate buffered saline (PBS):*

PBS is an isotonic solution and as a buffer it counteracts for changes in pH, making solutions to be stable. Isotonic refers to a solution that has similar electrolytes than those in the physiological environment of cells. Thus, when cells are in contact with this solution, little or no water will come in or out due to difference in ionic concentration, avoiding dehydration of the cell or too much water intake that would make the cell literally to explode.

- 0.256 g Sodium phosphate monobasic monohydrate ($NaH_2PO_4 \cdot H_2O$)
- 1.190 g Sodium phosphate dibasic, anhydrate ($Na_2HPO_4$)
- 8.75 g Sodium chloride (NaCl)
- Volume was filled up to 1 L with ultrapure water
- pH = 7.43 adjusted with 1.0 N HCl or 1.0 N NaOH

*Hydrochloric acid 1.0 N:*

Acid was added to water inside a fume hood. As a safety rule, acid is always added to water. This is an exothermic reaction (heat is produced), but heat is rapidly absorbed by water. If water is added to the acid, an accident can occur.

- Transferred 8.3 mL of 12 N HCl into a 100 mL volumetric flask.
- Filled up with ultrapure water to complete 100mL
- The meniscus was above the flask neck´s mark.

*Sodium hydroxide:*

Sodium hydroxide (NaOH) was opened the minimum possible. For example, while weighing, the NaOH container remained closed to avoid moisture from the environment to come into contact with the sodium hydroxide pearls.

Two different solutions of varying concentrations of NaOH were prepared: 1.0 N and 10 N. If not familiar with the solution to which pH was going to be adjusted, 1.0 N was used to raise pH. For known solutions whose pH is hard to raise (less than 0.01 units per drop of 1.0 N base) the highly concentrated (10 N NaOH) was employed.

1.0 N NaOH solution:

- Weighted 4g (container was opened the minimum possible to avoid moisture into NaOH)
- Transferred to a 100 mL volumetric flask and added ultrapure water up to 100 mL.

10 N NaOH solution:

- Weighted 4g (container was opened the minimum possible to avoid moisture into NaOH)
- Transferred to a 15 mL graduated cylinder flask and added ultrapure water up to 10 mL.

#### 3.1.1.1 PEGda 3.4kDa Photopolymer solutions

Prepolymer solutions were prepared from poly(ethylene glycol) diacrylate 3.4 kDa (Aclylate-PEG-Acrlylate MW 3400, Laysan Bio, Inc., Arab, AL) as previously described [111]. Either 20, or 30 wt % PEGda was mixed with phosphate buffered saline (PBS) and 0.5 wt% of the photoinitiator (PI) Irgacure 2959 (I-2959, Ciba Speciality Chemicals Corp., Tarrytown, NY). One gram (g) and one milliliter (mL) are used interchangeably. A buffer was chosen because resulting experiments would include the use of cells. These cells require an environment similar to that of the body and PBS resembles better physiological conditions than pure water. Moreover, the PI used here has been proven to be cytocompatible [112]. According to the weight percent (wt%,) equation, Table 3.1 shows the proportions that took place depending on the PEGda concentration desired.

$$wt\ \% = \frac{x}{x + y + z} \text{ x } 100\%$$

Where:

$x$ = grams of PEGda,
$y$ = grams of PI and
$z$ = milliliters of solvent (PBS)
$x + y + z = 100\%$

For these specific solutions:
$x + y + z = 2.0$mL
$z$ = 0.5 % fixed PI conc.

Knowing that the concentration of photoinitiator will not change, the volume of solution wanted (mL) and the component percentage desired (g) can be calculated by solving for $x$, $y$ or $z$, as required.

Solving for $x$ to calculate the grams of PEGda needed for a 20 wt% PEGda solution (sol´n):

$$20\ \% = \frac{x}{2.0\text{g}} \text{ x } 100\%$$

$$x = \frac{(20\ \%)\ (2.0\text{g})}{100\ \%}$$

$$x = 0.4 \text{ g PEGda}$$

Solving for $y$ to calculate the grams of PI needed to obtain 0.5 wt% PI of a PEGda sol´n:

$$0.5\% = \frac{y}{2.0\text{g}} \text{ x } 100\%$$

$$y = \frac{(0.5\%)\ (2.0\text{g})}{100\ \%}$$

$$y = 0.01 \text{ g PI}$$

Solving for $z$ to calculate the mL of solvent to obtain 79.5 wt% PBS of a PEGda sol´n:

$$79.5\% = \frac{z}{2.0\text{g}} \text{ x } 100\%$$

$$z = \frac{(79.\ 5\%)\ (2.0\text{g})}{100\ \%}$$

$$z = 1.59 \text{ mL PBS}$$

**Table 3. 1. Amount of reagent required according to its desired concentration**

| | PEGda(g) | PBS(mL) | PI(g) |
|---|---|---|---|
| 20%PEGda<br>79.5% PBS<br>0.5% PI | 0.4 | 1.59 | 0.01 |
| 30%PEGda<br>69.5% PBS<br>0.5% PI | 0.6 | 1.39 | 0.01 |

Poly(ethylene glycol) diacrylate was taken out of the freezer and left on the counter at least one hour to reach room temperature (RT) before being opened. Then, the components were weighed and then mixed in an amber vial as PEGda is sensitive to light and it is desired to avoid

any reactivity that is not controlled. For at least two hours the vial was left in a vortex (Vortex-Genie 2, Scientific Industries, Inc.,) because it is hard to dissolve the photoinitiator even though the provider´s information claims it to be readily soluble in water and PBS is an aqueous solution. The vial was anchored to the vortex´s base with insulating tape strips. Care should be taken as the base of the vortex often detaches and the amber vial can be ejected causing an accident. The photopolymer solution was taken inside the biosafety cabinet (BSC) (Purifier Class II, Labconco Corp., Kansas City, MO) to be syringe filtered. The solution passed through a low protein binding syringe filter (0.22 μm filter, Cole-Parmer, Vernon Hills, IL) and was transferred to a previously autoclaved amber vial.

Note: A little bit more of solution than the actual needed was always prepared. Some is lost in the filtering process and in the pipette tips when transferring solution. In addition, calculations resulting in, for example, 100 % = 2g of solution does not make 2 mL in volume (even though they are equivalent in weight).

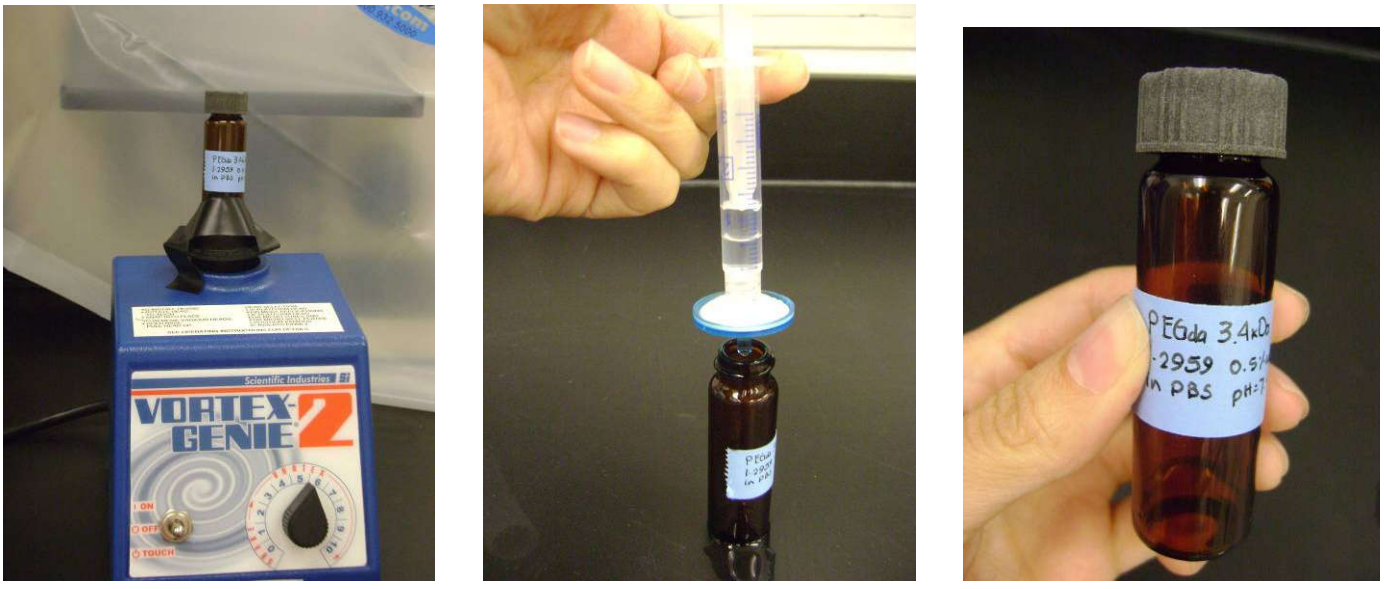


**Figure 3. 1. Final steps to prepare a sterile photopolymer solution**

#### 3.1.1.2 PEGda 6 kDa Photopolymer Solutions

This solution was prepared from 6 kDa PEGda as a 10% weight of solute in volume of solvent (w/v) to compare the release properties of PEG between different molecular weights and concentrations. Following the directions of our PEGda 6 kDa provider and colleague at the University of Utah, Dr. Brenda K. Mann, 6 kDa PEGda hydrogels were crosslinked in a different manner than PEGda 3.4 kDa. The polymer solution was prepared by mixing 1.0 mL PBS and 0.1 g PEGda 6 kDa. Next, the photoinitiator 2,2-dimethyl-2-phenyl-acetophenone (DMPA) was dissolved in 1-vinyl-2-pyrrolidinone (NVP) at 300 mg DMPA per mL NVP. Then, 10 μL of the dissolved PI were added per mL of photopolymer solution and mixed by pipetting up and down. PI solution (DMPA in NVP) was always added to the PEG solution with or without NGF always at last, since this prepolymer solution is good to use only few minutes after combining its reagents, more specifically after adding the PI. After a few minutes of adding DMPA in NVP to the PEGda solution, the vial´s contents exhibit a phase separation that makes an uneven and not homogeneous solution.

One more different step between the 3.4 kDa and the 6 kDa PEGda solutions is that this last one was not filter sterilized. The reason to sterilize is the possible use of the solution or resulting hydrogels with cells, but DMPA in NVP is cytotoxic and thus, there was no concern with sterility if the photoinitiator itself will kill cells. Even then, every step was carefully done in a clean environment where surfaces were wiped with 70% ethanol

Notice that there were discrepancies on how to express the concentration of the solutions and. The agreed terminology is as stated in this thesis: wt% for the previously explained 3.4 kDa PEGda preparation and % (w/v) for the 6 kDa PEG solution preparation procedure. Table 3.2 shows the concentration in terms of grams of PEGda per milliliter of solvent (PBS).

**Table 3. 2. Column on the left describes the concentration of solution either in (w/v) or wt%. Column on the right states the grams of PEGda required per mL of PBS to achieve the desired concentration provided by the left column**

| Concentration | PEGda/PBS |
|---|---|
| 10% (w/v) PEGda 6 kDa | 0.1 g/mL |
| 20 wt% PEGda 3.4 kDa | 0.25 g/mL |
| 30 wt% PEGda 3.4 kDa | 0.43 g/mL |

#### 3.1.1.3 PEGda stock solutions

These were solutions of 3.4 and 6 kDa PEGda that were prepared in siliconized sterile 2mL microcentrifuge tubes (Low Retention, FisherScientific) to take a small part of them to react PEGda in excess with NGF and bond them chemically. Their preparation took place while an NGF aliquot was equilibrating to RT. The solvent was PBS pH =7.6. The solution was syringe filtered before combining it with the neurotrophin.

#### 3.1.1.4 Nerve Growth Factor

Nerve growth factor (mNGF, 2.5S, Promega Corp., Madison, WI) was reconstituted in plain RPMI-1640 with 100 μg of bovine serum albumin (BSA) per mL of medium as a protein stabilizer. In a 15 mL polypropylene (PP) centrifuge tube (CT) 10 mL of plain RPMI-1640 were supplemented with 1 mg of BSA. This PP tube was used to prevent absorption of protein by its container [40]. The solution was taken inside the BSC to be syringe filtered. With a micropipette and sterile pipette tips (Eppendorf Inc., AG, Hamburg, Germany), only 100 μL of the sterilized solution were taken and added to the NGF vial to a final concentration of 1 μg/μL of NGF in medium (original NGF vial contained 100 μg of the protein). The solution was split into siliconized microcentrifuge tubes to minimize NGF adhesion to the walls of its container and leftovers were kept in the original container. The purpose of this was to take NGF as needed

from aliquots and avoid multiple freezing-thawing a single NGF solution. The reason to aliquot is that NGF is susceptible to denature (change in protein structure and thus, lose biological activity) due to constant temperature changes. The splits were in duplicates of 20 and 13 µL since they were further used to add them to 3.4 kDa PEGda or 6 kDa PEGda solutions, respectively, for encapsulation or conjugation. 20 and 13 µL are not random numbers. It was the amount of NGF calculated to entrap or link to PEGda to ultimately produce a photopolymer solution capable of making disks of 500 ng of NGF to release per hydrogel. Aliquots were stored at -20 $^{o}$C in a freezer (Thermo Electron Corp. Asheville, NC) until used. Figure 3.2 illustrates the split.

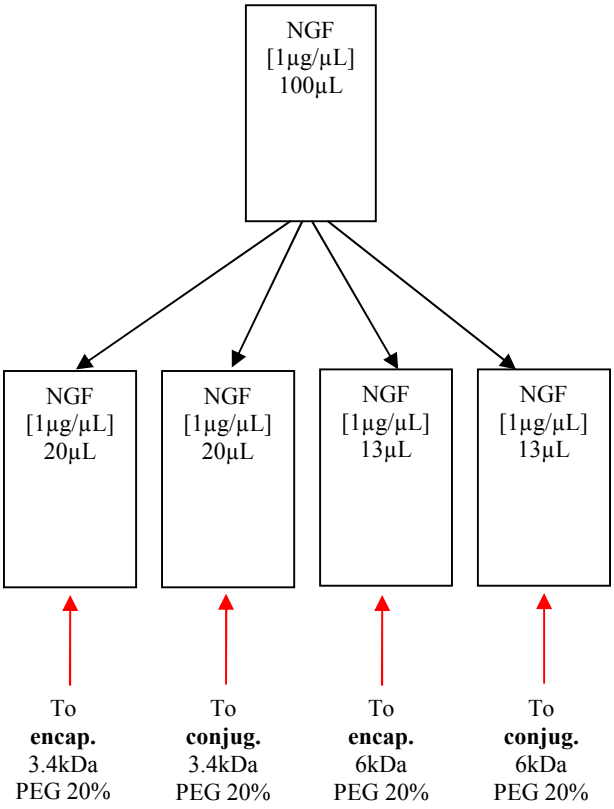


**Figure 3. 2. NGF aliquots and their further use. Rectangles resemble 2 mL microcentrifuge tubes**

Calculations for 3.4 kDa PEG hydrogels indicate that 1mL of photocrosslinkable solution can make up to 80 disks (Appendix 4). Since each disk was intended to contain 500ng, multiplying the number of disks desired times the amount of NGF nanograms (ng) per disk will give the amount of protein required per mL of solution:

(80)(500ng)= 40,000 ng NGF per mL of prepolymer solution.

According to that, previous NGF aliquots contained the exact amount of protein that would be used. This makes more sense and it is explained more in detail in the following section and. The reason to do it like this was to avoid losing NGF while transferring it. Rather than putting in NGF to PEGda, solutions were prepared by adding the reagents into the NGF aliquot vial.

#### 3.1.1.5 Conjugating PEG-NGF

Taking advantage of the PEG´s characteristic ability to link molecules, NGF was PEGylated to 3.4 and 6 kDa PEGda end groups. A Michael-type addition reaction took place. This is, under basic conditions, hydroxyls in solution remove hydrogen from the carboxyl groups located in the amino acids of the NGF protein, giving rise to a nucleophile. This moiety reacts with the carbonyl located at the end groups of PEGda attacking the double bond. As a result, a covalent bond is formed between PEG and NGF and the reaction is reversible as this bond is hydrolysable. The more basic the solution, the more hydroxyl groups present and the faster the reaction. However, it has been reported that NGF denatures under basic conditions [113]. Even though the reaction could have been accelerated, it took place for two hours close to a neutral environment at pH=7.6.

An NGF aliquot was thawed while a PEG stock solution was being prepared. An amount of the PEGda stock solution was taken to the NGF aliquot vial in a 1:5 ratio (NGF:PEG). The purpose of adding 5 times more PEGda than NGF is to increase the possibility that NGF binds to

only one side end group (ACRL-PEG-NGF and not NGF-PEG-NGF). This leaves acrylate groups free to later crosslink to an acrylate of another PEGda molecule. The volume was adjusted to 100 µL with PBS and syringe filtered inside the BSC. Figure 3.3 illustrates for the conjugation conditions.

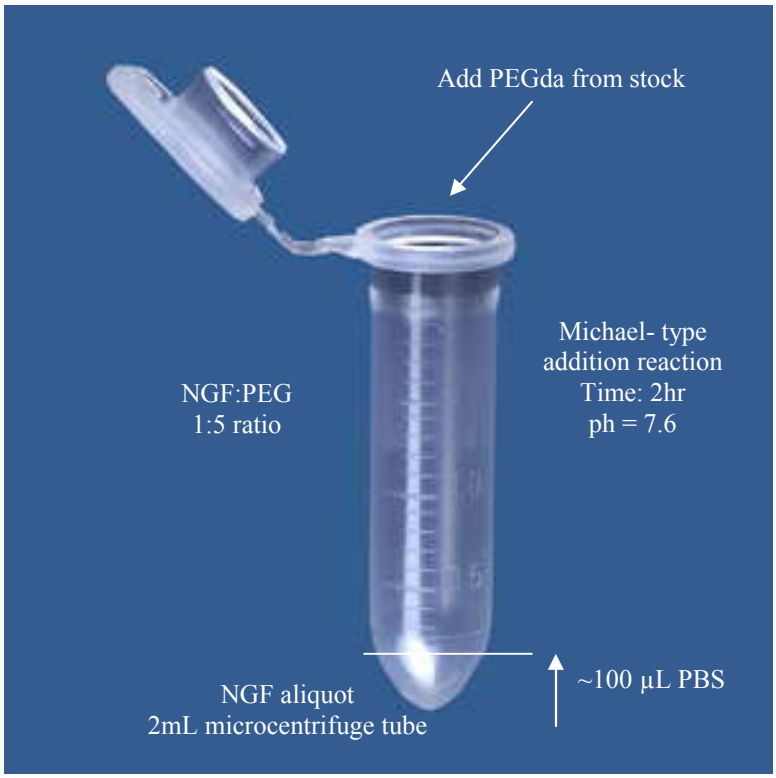


**Figure 3. 3. Michael-type addition reaction conditions**

Even though the exact percentage yield (% yield) is unknown, the initial amount of protein is still present either conjugated to PEG or unreacted (not linked to PEG, but remaining in solution). The only difference between the conjugation reaction between NGF and PEGda of 3.4kDa or 6kDa PEG, was that for the lower mw, the resulting ACRL-PEG3.4kDa-NGF was lyophilized and thus, turned into a powder, whereas the ACRL-PEG6kDa-NGF 100 µL were directly stored under -20 $^{o}$C until used.

### 3.1.1.6 Photopolymer Solutions Containing NGF

From the early prepared solution (20 wt% PEGda 3.4 kDa) a part was taken as calculated to add to the NGF aliquot vial, inside the BSC. As stated before, with the objective of not losing any NGF and having the same amount of protein from encapsulated or conjugated. The final solutions contained NGF (linked to PEG or entrapped) to produce hydrogel disks containing 500 ng to release per disk. The NGF aliquot vials containing then the photopolymer solution were wrapped with aluminum foil and used immediately. Figure 3.4 shows how the crosslinkable solutions were prepared for 20 wt% PEGda 3.4 kDa with NGF either conjugated or encapsulated.

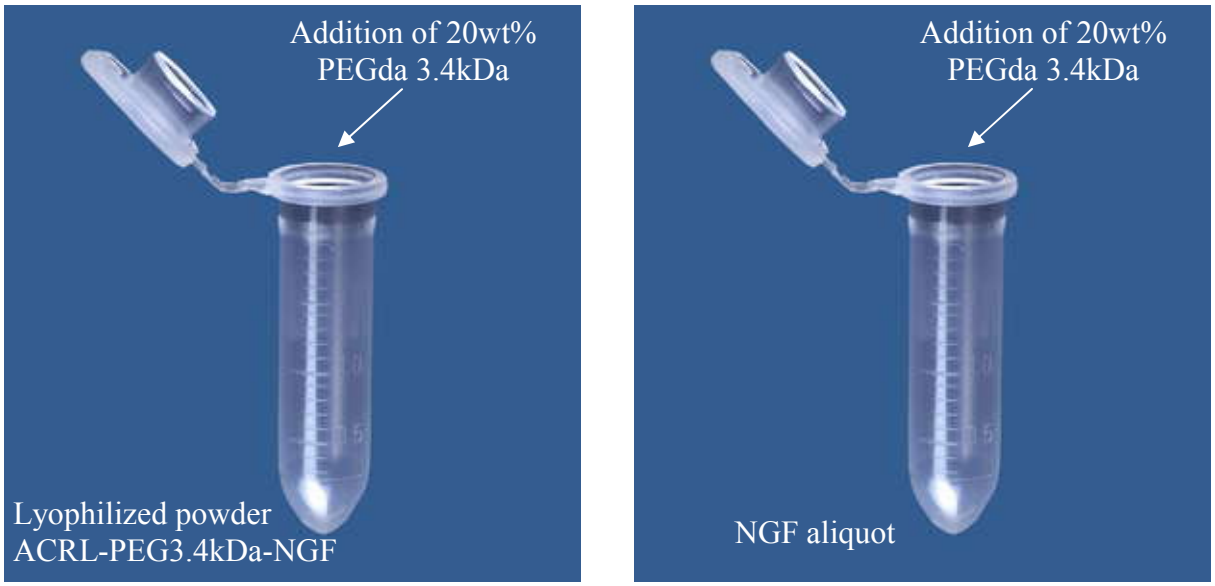


**Figure 3. 4. Left: Photopolymer solution containing NGF chemically bonded to PEG3.4kDa. Right: Photopolymer solution containing the protein free in solution**

The following image depicts the way in which 10% (w/v) PEGda 6 kDa solutions were obtained with the protein encapsulated or conjugated. Note that also for these solutions everything was calculated from the beginning as to maintain the same amount of NGF from start until the time of curing. For example, the conjugation reaction took place in a volume of 100µL.

It contained 40,000 ng NGF as the potential amount to be conjugated. Then, 0.1 g PEGda 6 kDa were added, 900 µL of PBS buffer and 10 µL of DMPA in NVP to the 100 µLPEG-NGF solution leading to a 10% (w/v) PEGda 6 kDa solution. The amount of PEG coming from the conjugation reaction was not taken into consideration within the 10% (w/v) PEGda concentration of solution. The previously described is shown in Figure 3.5 left. When preparing the solution of PEG 6 kDa with the protein encapsulated, a similar approach was followed. Again, an NGF aliquot was thawed and the other components were added. 980 µL PBS were added and other 20 µL came from the NGF solution aliquot. It is important to mention that solutions were mixed by pipetting up and down. A representative sketch of the components´ combination is found in Figure 3.5 right.

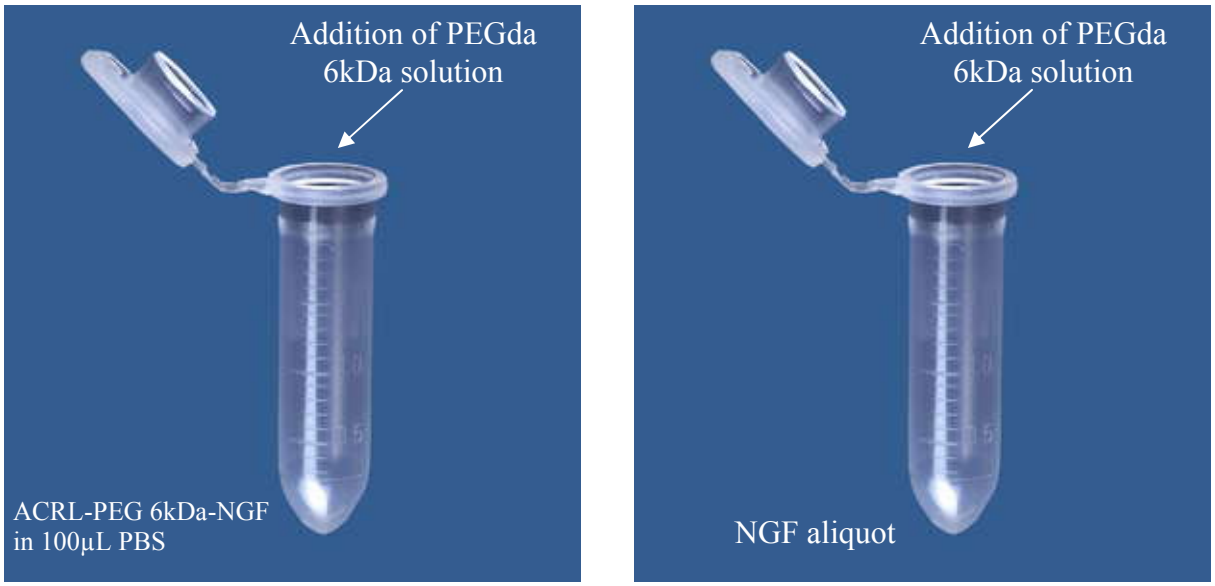


**Figure 3. 5. Addition of components to achieve a 10% (w/v) PEGda 6kDa containing NGF covalently linked (left) and free NGF in solution (right)**

#### 3.1.1.7 Stereolithography

The unit used to build the hydrogels presented here is a 3D Systems® stereolithography (SL) machine model 250/50. More detailed information about its function is given in Ch.1 in the stereolithography section. The SL machine´s inside and outside surroundings were wiped with 70% ethanol to get rid of dust as much as possible. It was turned on 30 min before starting to build allowing the SL machine laser to warm up. Previously, with the aid of SolidWorks™ and 3DLightyear™ (3D Systems®, Valencia, CA) softwares, an .stl file was created which contained the drawing of six cylinders. The drawing dimensions were smaller than the actual hydrogel desired size taking into account the dimensional swelling factor (DSF) [111]. By the DSF, we know that 20% PEG 3.4 kDa hydrogels increase their volume after constructed when left under an aqueous environment (specifically, PBS). The calculations were prepared so that each feature had 500 ng NGF to release whether swollen or shrunk. The .stl file previously uploaded to the system of the SL machine was opened to build six disks (one layer of the cylinders) per batch at the same time (An illustration for this can be found in Ch. 5, Figure 5.1). The elevator was fixed at the original position where the beam diameter is ~250μm [111] and stood static while constructing, since only one layer was built per batch. The laser power was measured before building with a power meter and compared its reading to the one given by the system. If there was variance, the apparatus parameters were edited as to show the reading that was given by the power meter. In addition, the laser position was also adjusted accordingly. The parameters to build were a critical exposure ($E_C$) of 12.00 and a penetration depth ($D_P$) of 2.82 based on [114]. The laser speed (LS) varied from 0.97 to 1.17 and the laser power (LP) oscillated from 21 mW to 23 mW.

The SL machine´s modifications for manufacture were those previously defined [111,112], where a small vat was used instead of a big container as can be observed in Figure 3.6.

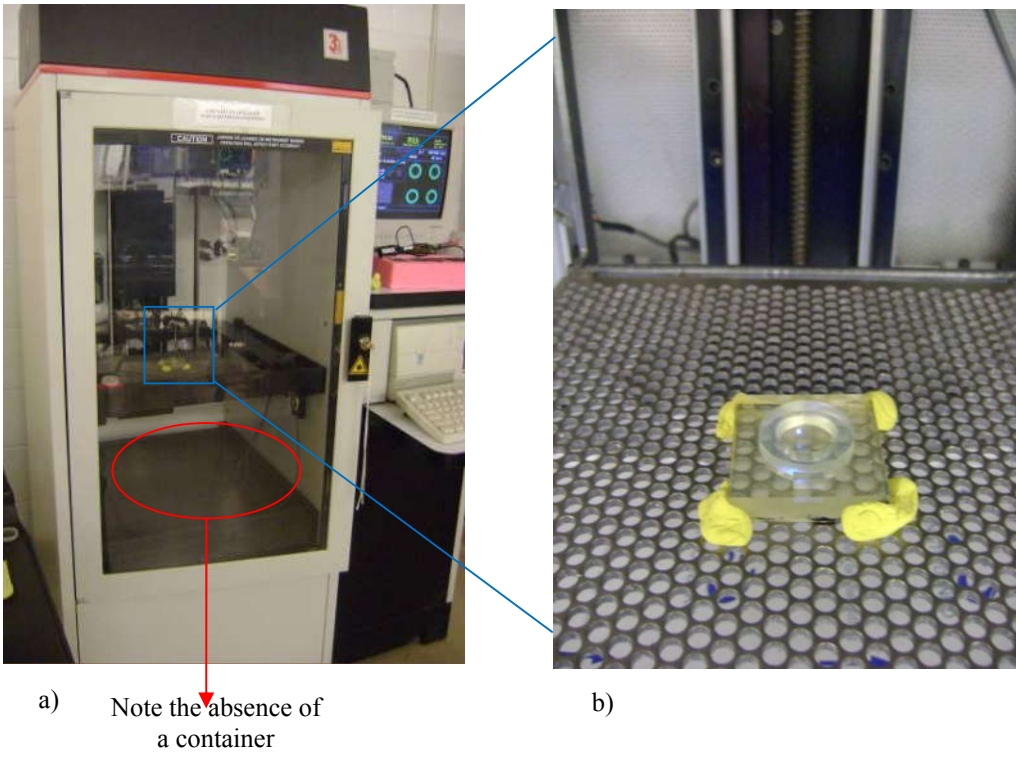


**Figure 3. 6. Modifications to the SL system. a) SL model without its original container, b) base adapted to elevator platform attached with clay**

To overcome some drawbacks, the mini-vat was also modified. One of the difficulties was that due to the fact that finished features are relatively small and tend to highly attach to bottom of the container where they are being constructed. It is too hard to remove them from the surface. Also, NGF is expensive and its availability is limited. For this reason, it was important to reduce the amount of solution required to build per layer. To overcome these problems two modifications were made:

1. The inner diameter of the container was reduced shown in Figure 3.7.
2. A transparency was pasted to the bottom of the container.

In this way, less solution was required to cure one layer and the hydrogel parts were removed easier and came out of higher quality (complete, not broken), as they were disturbed less with the spatula at the time of detaching them from the bottom of the mini-vat. To paste the transparency, a piece of transparency was cut of the size of the modified inner diameter. Then, a resin drop was distributed with the aid of an applicator and the transparency was placed on top. With a clean applicator the transparency was pressed to the bottom of the vat until no air was seen underneath. Next, a UV spot light (Green Spot™, UV Source, Inc.) was applied to cure the resin in between the surface of the vat and the transparency, which ultimately glued them. An image of the vat modifications is given in Figure 3.7. The yellowish color is because the picture was taken after crosslinking PEG 6 kDa where this vat was also used. The wavelength was longer and intensity of the laser was higher, overcuring the mini-vat and changing its color.

**Figure 3. 7. Vat on the right is the new modified. Note the reduction of the inner diameter to reduce the amount of solution required to crosslink one layer.**

The inner diameter of the new smaller container was measured with a caliper (Fig. 3.8) to be able to accurately calculate the amount of solution required to crosslink one layer of solution in this specific vat based on its dimensions.

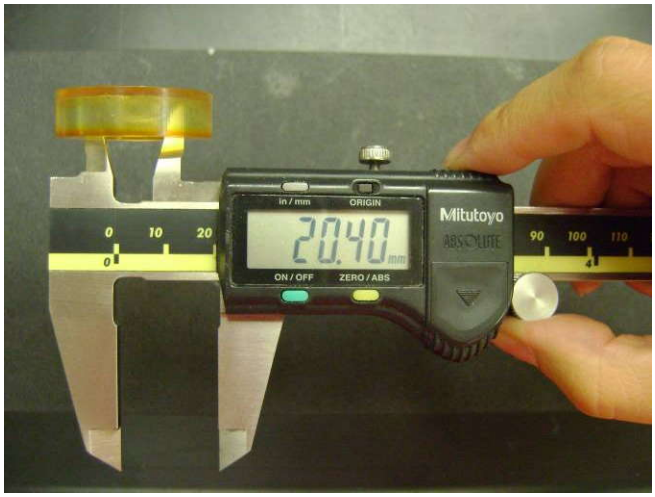


**Figure 3. 8. Inner diameter measurement of the new container of smaller inner diameter (20.4 mm).**

#### 3.1.1.7.1 Building in SLA

Six disks (number of samples (n) = 6) were built at the same time (per batch). After wiping with ethanol inside, outside and tools to be used, the base of the vat was leveled. A leveler was placed on top of the container over its base and the clay helped to set in place the base of the vat. The 24-well plate previously filled with 2mL of RPMI-640 per well was taken close to the building machine as well as a clean spatula. Control disks were built first. Controls consisted of the photopolymer solution only that without NGF. They were manufactured first to avoid contaminating them. 340µL were dispensed with a micropipette into the vat (Fig.3.9).

There was a need to evenly distribute the solution at the time of dispensing it with the aid of the pipette. This was done by touching (scanning) the container surface with the pipette tip as solution is coming out. The solution has preference for the walls of the container and an empty space at the center can be the result with the solution at the edges (meniscus) if not distributed.

**Figure 3. 9. Photopolymer solution being dispensed from a micripipette into the modified container.**

Then, the laser was commanded to pass once over the solution to crosslink one layer of the cylinders´ file (Fig.3.10), leading to the creation of six hydrogel disks.

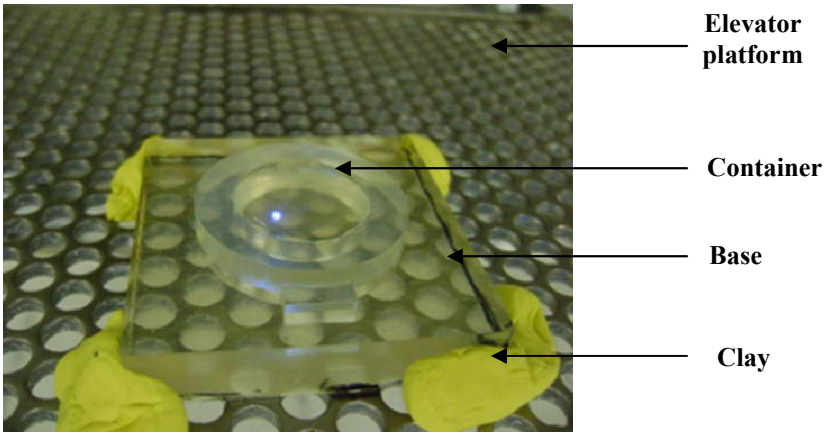


**Figure 3. 10. Laser beam (blue spot) passing over the photosensitive solution.**

First batches served to center the position of the vat and to make sure the laser was not hitting the walls of the container. Immediately after the disks were built, the vat was taken out of the chamber. The unreacted solution was retrieved with the pipette and sent back to its container. Taking reagent from a container and taking the unused back to the bottle is usually unaccepted. However, unreacted material in this case can be recycled at the moment (not stored to use another day). The disks were rinsed with ultrapure water three times to get rid the most of unreacted material at the surface of the hydrogels. The third time of rinsing, water was not discarded to avoid ejecting the disks at the time of removing them with the spatula. Hydrogels were individually transferred to wells of the 24-well plate (Fig. 3.11).

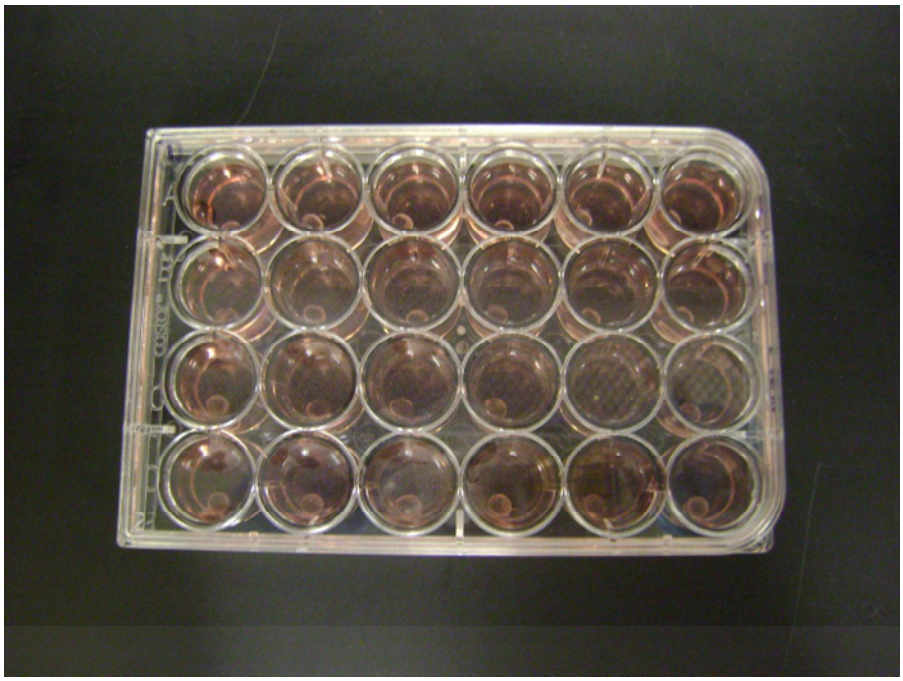

**Figure 3. 11. Hydrogels placed individually into wells of a 24-well plate in RPMI-1640. Note the size of the gels versus the volume of solution in which tNGF is being released.**

Just after constructing the control disks, photopolymer solution containing NGF free in solution was prepared. An amount from the leftover solution with which the controls were built was combined with NGF as early stated (Sec. 3.1.1.6, Fig. 3.4 right) just before manufacturing. PEG hydrogels containing the protein entrapped were created first followed by the ones containing chemically bonded NGF. Next, photocrosslinkable solution was mixed with ACRL-PEG-NGF (Fig. 3.4 left) and the same procedure as explained for controls took place to build disks containing the protein covalently linked.

The same procedure was repeated with a 30 wt% PEGda 3.4 kDa solution. Controls were created first followed by hydrogels containing NGF. The only difference is that from this concentration only hydrogels with the neurotrophin trapped within the polymeric mesh were created and not conjugated. This was to compare the release rate between solutions of the same molecular weight but different concentration (30 wt% PEG 3.4 kDa vs. 20 wt% PEG 3.4 kDa).

When all disks were fabricated, the 24-well plate containing them was taken back to the inside of the incubator at 5% CO2, 37 $^{o}$C and saturated moisture. Even though temperature readings were given digitally by the incubator, a thermometer was placed inside to confirm temperature conditions.

#### 3.1.1.8 PEG 6 kDa hydrogels manufacture

Due to the fact that we have not been able to gelate 10% PEGda 6 kDa solution under the stereolithography system, a different methodology was followed to create these hydrogels. The setup consisted on a OmniCure® spot UV lamp Series 2000 of long wavelength ($\lambda$ = 365nm). Since the lamp is flexible, it was set at a working distance of 15 cm (height above the photosensitive solution). A white sheet was placed at the bottom surface where the light would hit. On top of the sheet, the same vat utilized in the SL machine was placed. The white paper

served as an indicator to center the vat. In addition, it served to indicate the position of the vat and put it on the same spot every time. 400 μL of crosslinking solution were taken and dispensed evenly into the vat. The light was turned on with an automated fixed exposure time of 5 min. and cured a whole layer of solution. Figure 3.12 provides the setup utilized.

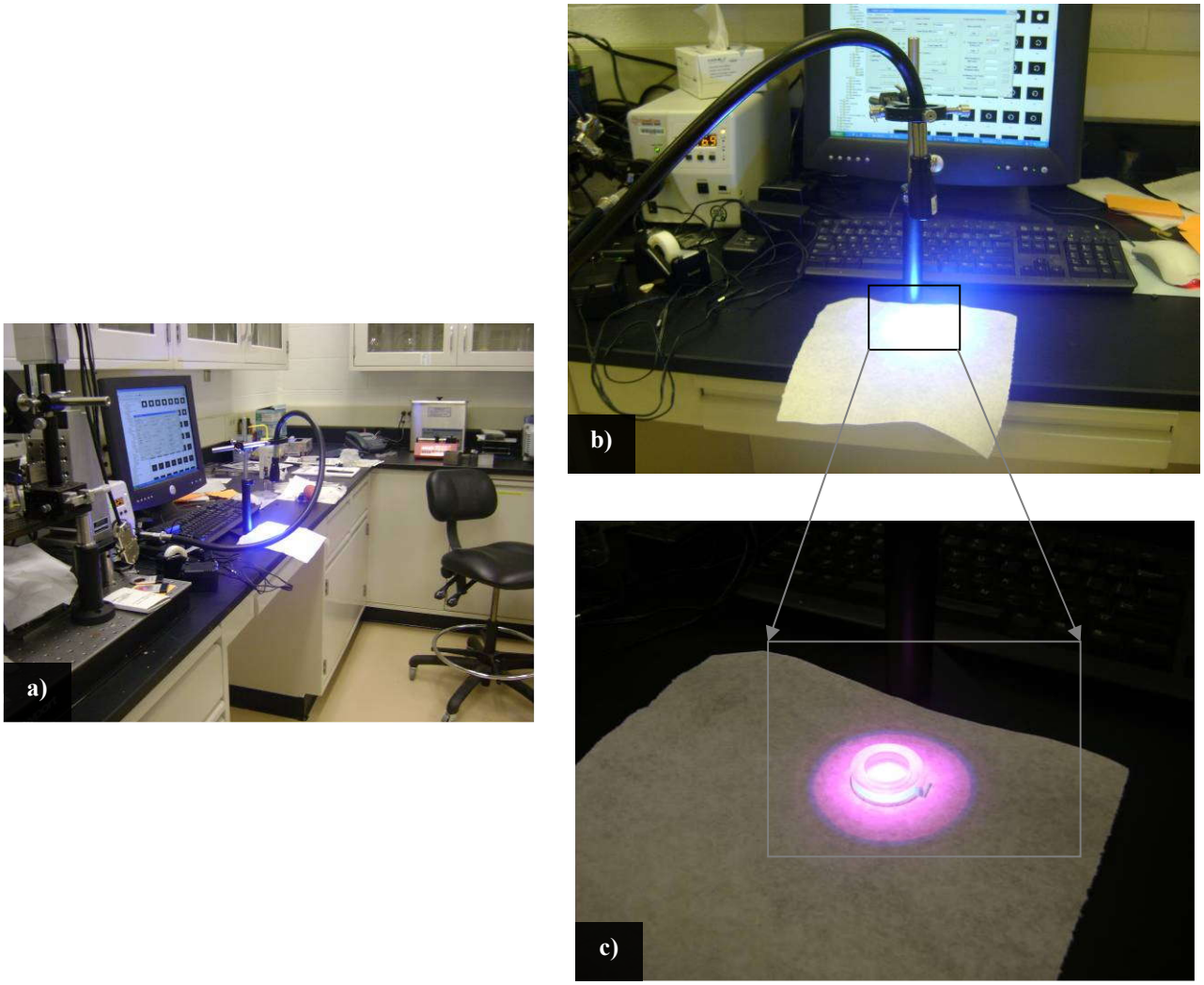


**Figure 3. 12. Sport light UV radiation setup. a) Side view, b)front view, c) close-up top view.**

To use as a mold to retrieve disks from the hydrogel layer, an Eppendorf™ pipette tip of 2-200µL was sanded from the outer diameter of its bigger opening (where the pipette fits) to have a circular knife-edge. Its inner diameter was measured with a caliper to confirm it had a size of 5mm (Fig. 3.13).

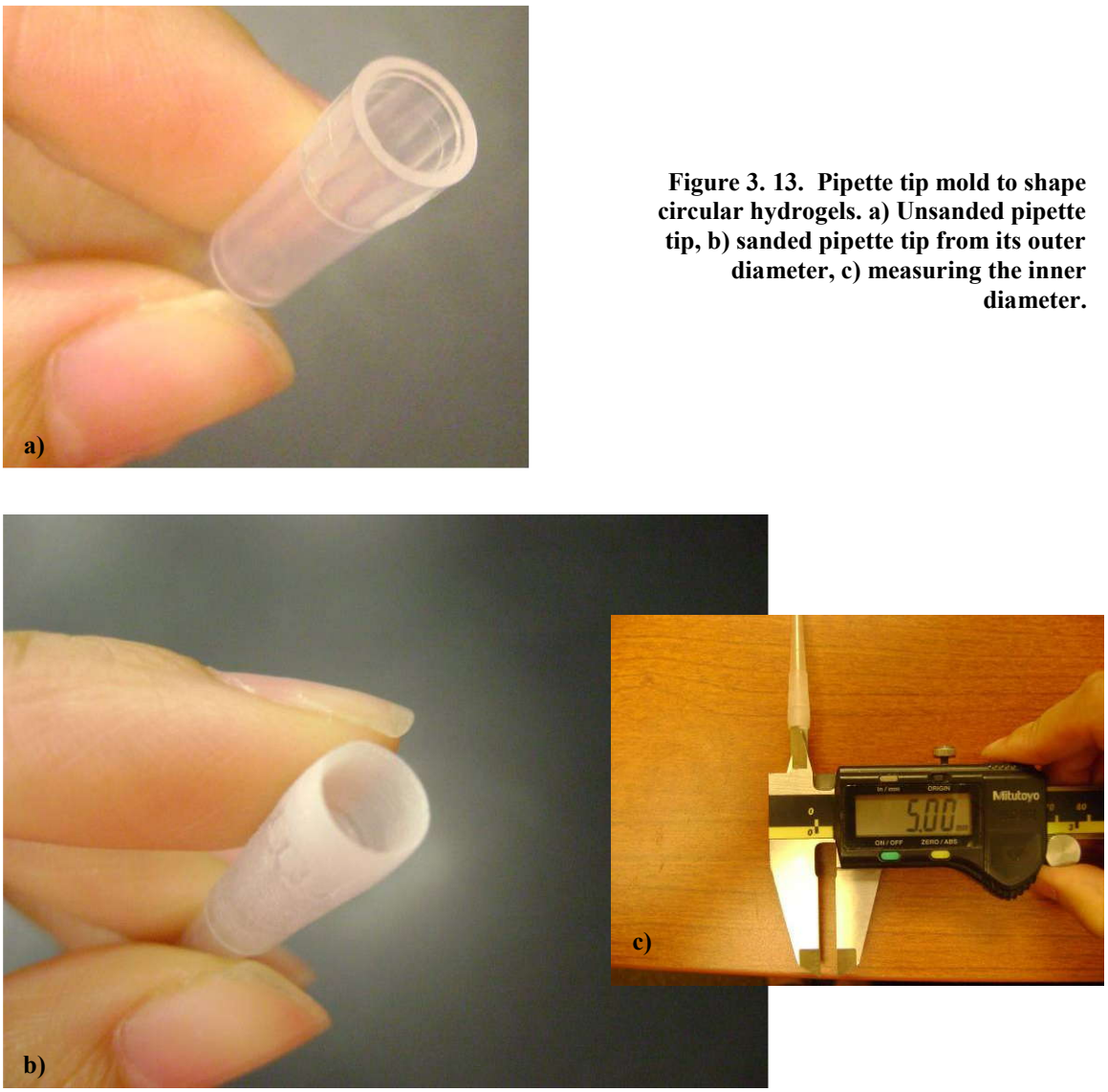


**Figure 3. 13. Pipette tip mold to shape circular hydrogels. a) Unsanded pipette tip, b) sanded pipette tip from its outer diameter, c) measuring the inner diameter.**

Similar to the process of building in SL, control disks were created first followed by disks containing the neurotrophin embedded and then having it chemically attached. Since a single layer was cured and not individual disks, the mandrel-like pipette tip was used to take them out of the mold. Taking a look at the layer cured (with or without the disks) it is noticeable that the PEGda 6 kDa solution also had affinity for the walls of the container. The area at the center is thin in comparison to the thicker perimeter (Fig.3.14b and c).


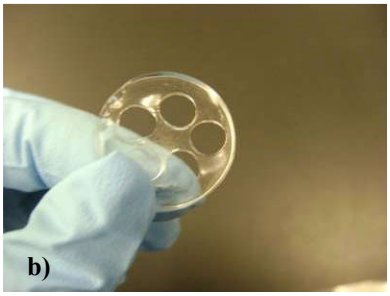


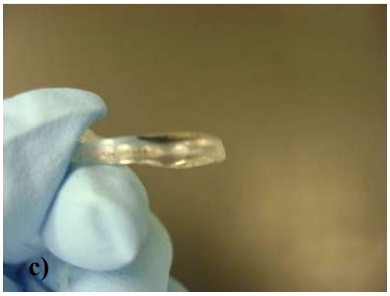


**Figure 3. 14. a) Hydrogel extrusion method, b) cured layer without the disks, thin at the center, c) cured layer thick from the perimeter.**

When taking away the excess material, disks were left attached to the bottom of the vat. Disks were rinsed three times and the procedure followed was similar to that described before when treating with PEG 3.4 kDa hydrogels. In the case of PEG 6 kDa disks, only 5 samples were created instead of 6 as with the SL process.

### 3.1.1.9 Lyophilized-Sterilized Hydrogels

In order to come closer to the real necessities and demands, a group of disks containing the protein entrapped went through the sterilization process to prove if they could withstand these conditions. The reason for this is that the market will require the sterilization of conduits for implantation and lyophilization for storage. Hydrogel disks of a 20 wt% PEGda 3.4 kDa solution were built. Two batches were built and rinsed: one for the control and the other were hydrogels with the protein embedded. Immediately after constructed, they were transferred with a spatula to 2 mL siliconized microcentrifuge tubes. The tubes had holes in the lid that were made with a 15 gauge needle. Tubes containing the disks were submerged right away into liquid nitrogen ($N_2(l)$) (Figure 3.15). Then, the microcentrifuge tubes were transferred to a FreeZone® lyophilizer (Labconco Corp., Kansas City, MO) to remove moisture from gels. After the freeze-drying process, disks were shipped to the University of Utah to receive hydrogen peroxide ($H_2O_2$) gas for sterilization and were received back to proceed with the releasing experiment. Once lyophilized and sterilized, hydrogels were taken as stated above individually into 2mL of RPMI-1640 to release their contents.

**Figure 3. 15. Left: Top view of microcentrifuge tubes inside liquid nitrogen. Tubes contain disk shaped hydrogels. Right: Hydorel disks taken out of the liquid nitrogen container. A red pen is included in the scenario to provide a sense of scale.**

### 3.1.1.10 Time Points

Control disks were left in solution from start to end of the experiments. Solutions holding the released protein from disks that diffused the physically trapped NGF were retrieved after 2, 4, 8, 12, 24, 48 hours and 1 week. Regarding hydrogels with the covalently linked NGF, solutions were recovered after 4, 8, 12, 24, 48 hours, 5 days and each subsequent 5 days until reaching 1 month. Each well was replenished with fresh medium every time after solution was taken out and the process was done inside the biosafety cabinet. Samples were stored in 2 mL siliconized microcentrifuge tubes at -20C until analyzed by enzyme-linked immunosorbent assay (ELISA) for NGF quantification or until used to prove for bioactivity by exposing pheochromocytoma (PC-12) cells to this medium.

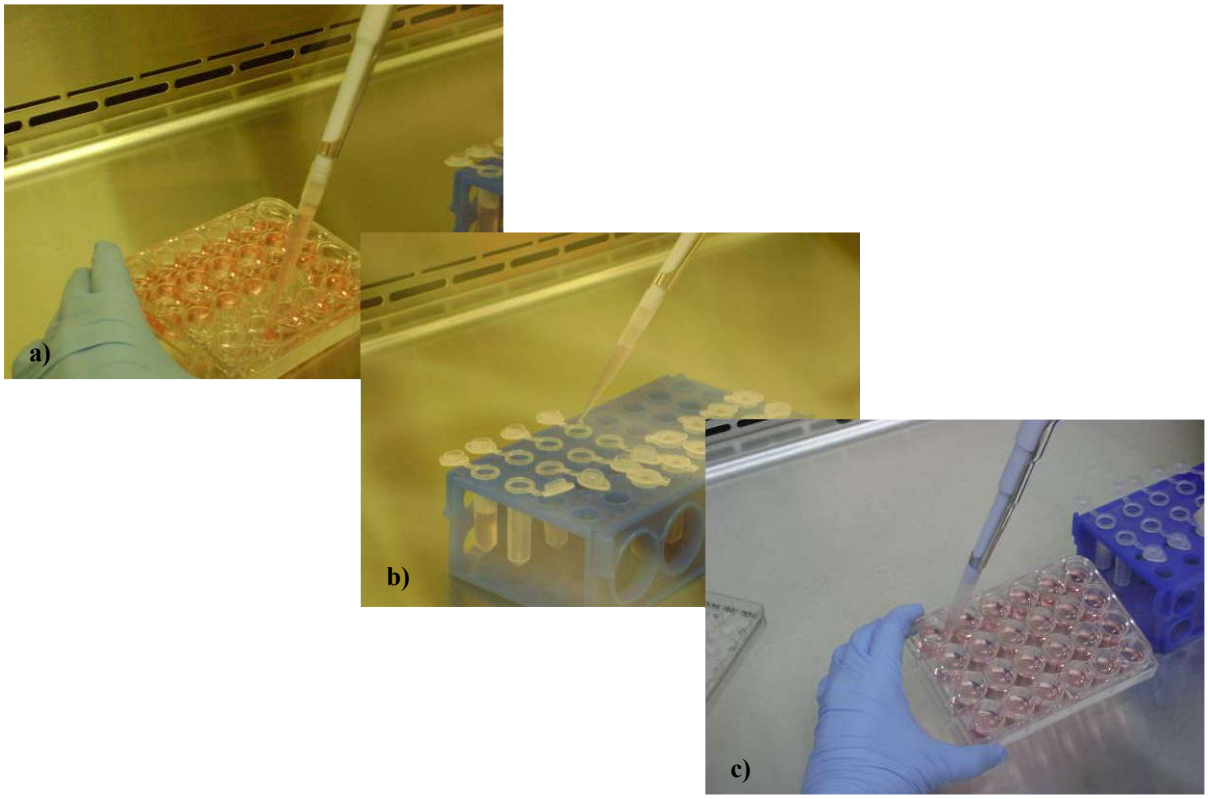


**Figure 3. 16. a) Retrieving supernatant, b)transferring to 2mL siliconized microcentrifuge tubes, c) Replenishing hydrogels in wells with RPMI-1640.**

When solutions were retrieved, care was taken to avoid scratching the hydrogels with the pipette tip. The surface of the of the 24-well plate was not touched and different pipette tips were used to avoid cross contamination. Moreover, before retrieving the supernatant, the solution was pipetted up and down at least three times to assure a homogeneous sample solution.

It was very important to keep track of the solutions. To know exactly which supernatant was from which disk, vials were labeled individually on top of their lids before taking them inside the freezer (Fig. 3.17). A marker was used to this end which ink withstands a wide range of temperatures and is hardly removed by common solvents (ethanol or acetone, for example). In addition, the case container was also labeled on the outside (both container and its lid) to identify it inside the freezer rapidly and easily.

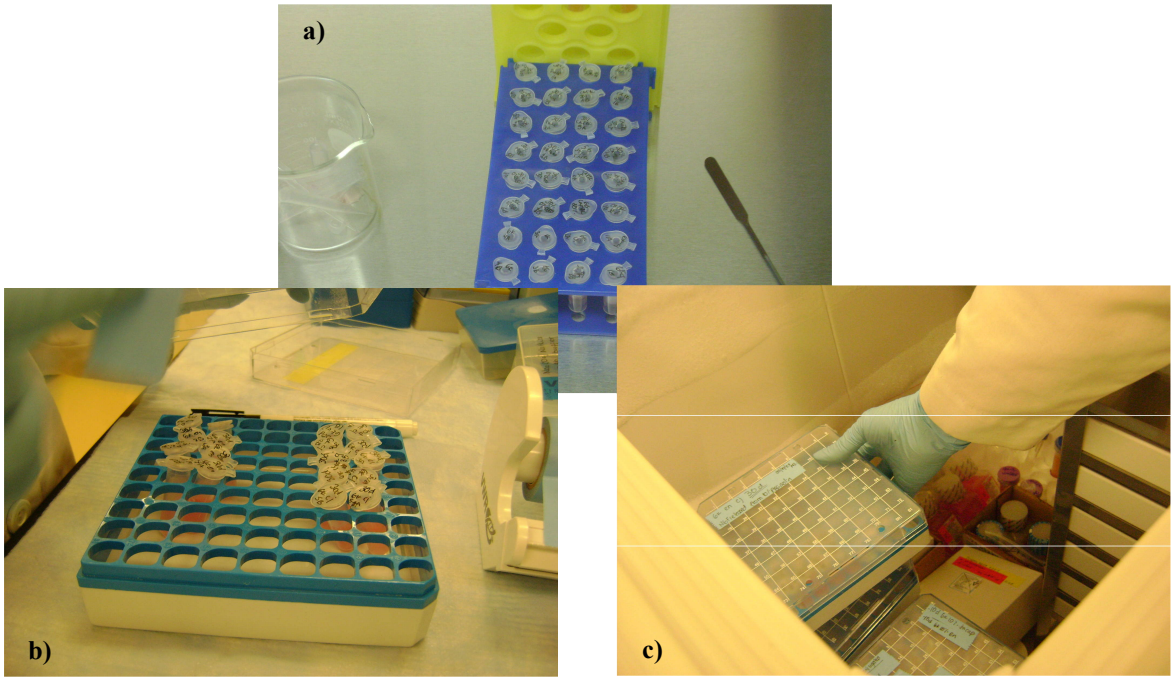


**Figure 3. 17. a) Individually labeled tubes still in rack, b) samples moved to a case after labeling and c) labeled case placed inside a -20°C freezer.**

Each time a time point solution was retrieved it was split into two tubes. From the same well, one sample went for ELISA analysis and another one for the PC-12 cell bioassay. With this, the same solution was used for ELISA and cell exposure. Figure 3.18 shows the split.

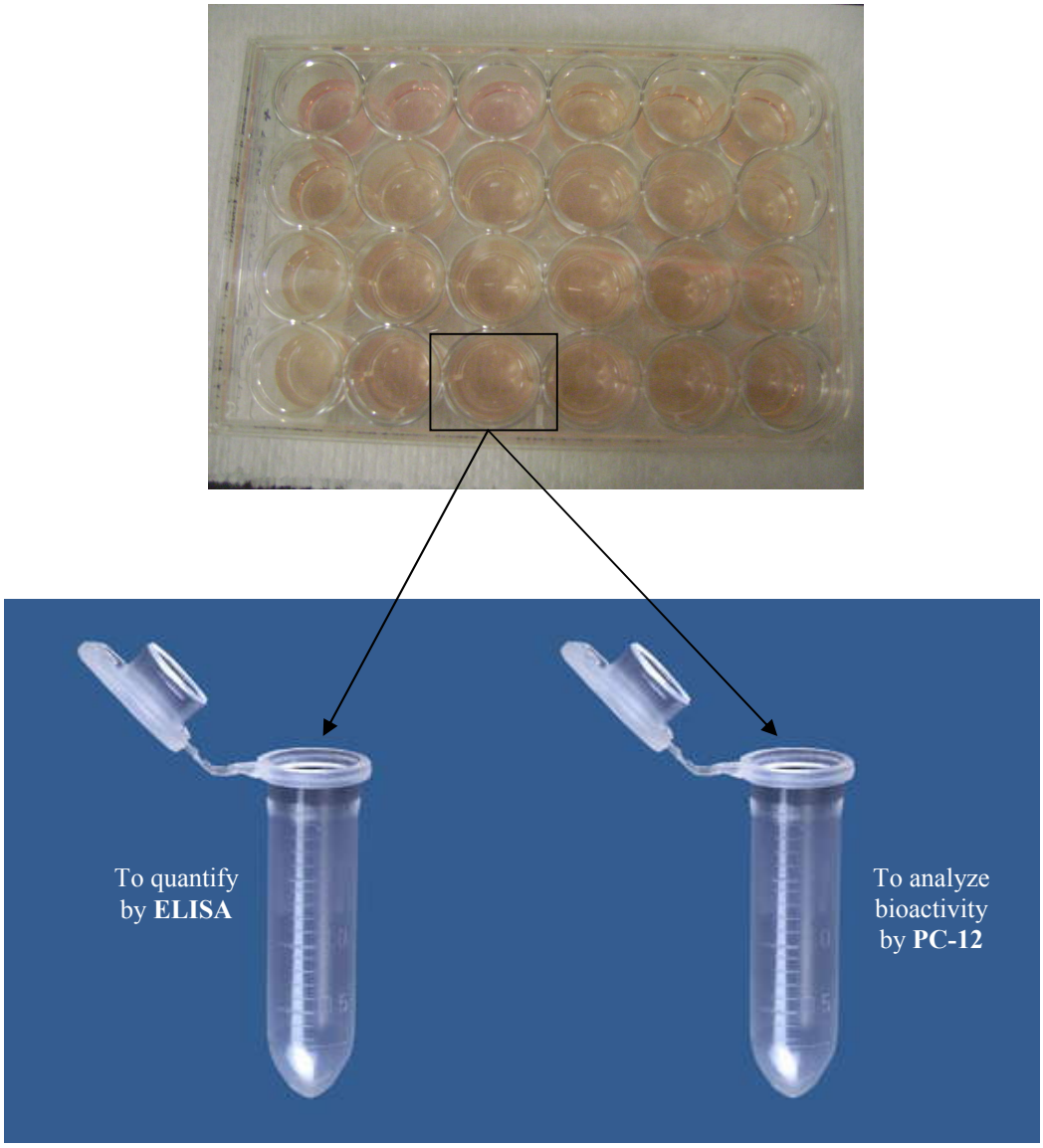


**Figure 3. 18. Split of retrieved supernatant.**

#### 3.1.1.11 ELISA

A sandwich enzyme-linked immunosorbent assay (ELISA, NGF $E_{max}$®, Promega Corp., Madison, WI) was performed on the samples to quantify the amount of protein released following the manufacturer instructions (Appendix 1). According to the instructions, buffers were prepared fresh the same day they were being used except for the washing buffer that was prepared once at the beginning of the analysis. To adjust the pH of solutions, the pH meter was calibrated in three points (4,7 and 10) with a resulting slope of 98.6. 96-wells ELISA nunc™ plates (Rochester, NY) were used for the assay. For every plate, a standard curve was prepared and only the linear portion of the curve was used to calculate the amount of NGF in the samples. Samples were diluted with the same buffer that was used for the standard dilutions. To know the dilution factor required for the samples, a plate was read with one sample of each time point and controls. Controls consisted of the supernatants of hydrogels without protein. Blanks consisted of the buffer that was used to perform the dilutions. Every time the plate was left settled it was covered with Parafilm®. Whenever the protocol indicated the need of shaking the plate, an orbital shaker was used and motion was set at 500rpm. At the end, the plate was read in a VersaMax™ microplate reader at $\lambda$ = 450nm within the first 30 min after adding 1.0 N HCl for stopping the reaction.

Every sample´s absorbance has to fit in between absorbance values of the linear portion of the standard curve. After reading the plate, one can get an idea of how concentrated the solutions are by looking at the plate´s color. For example, Fig.3.19 shows a plate with samples before stopping the reaction. The samples are still blue because HCl has not been added yet. Once HCl is added, color turns yellow in different intensities. For the plate shown, the last two columns contain the standard curve samples in serial dilutions from top to bottom.

The most concentrated samples of the standard curve are in the first row of the last two columns and the intense blue can be observed. From there down, the blue intensity decreases directly proportional to the concentration of NGF in the standard curve. All other wells contain different ranges of blue meaning different concentrations of the protein.

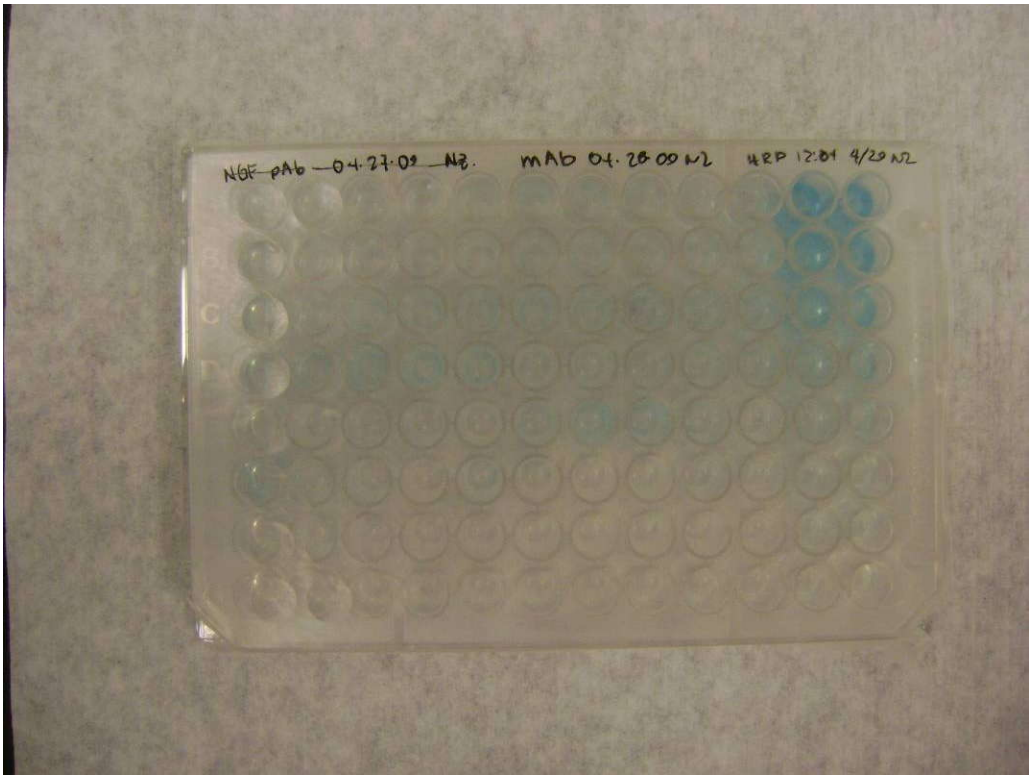


**Figure 3. 19. ELISA plate with samples and standard curve before the addition of 1.0 N HCl. Note how the samples concentration can be compared with those of the standard curve according to the color intensity. Standard curve is located at the two last columns in serial dilutions from top to bottom.**

### 3.1.1.11.1 Remarks About ELISA

- Buffers were prepared as stated in the protocol for accurate results.
- When adjusting the pH of buffers, NaOH or HCl were added drop by drop.

- When throwing contents in the sink, the plate was turned upside down fast to avoid cross contamination. It can be the case that the contents of a well invade an incorrect well if this is done slowly.
- Also, when flicking the plate over the counter (paper towels in between counter and plate) it was done fast for the same reason as stated above.
- ELISA reactions can be slowed down or sped up by decreasing or increasing the temperature, respectively. This is accomplished by placing the plate inside the refrigerator (4 $^{o}$C) or inside the incubator (37 $^{o}$C). Before adding the samples, coating and blocking processes can be made faster or slower. Advantage of this was taken when diluting the samples. While dilutions were taking place, the plate was taken inside the refrigerator if samples were not ready to follow the protocol. However, after addition of the sample times have to be respected and protocol´s procedure followed. For example, if the 2$^{nd}$ antibody is left incubating more than the specified time, it can lead to too much background and thus, a noisy signal as a result [115].
- When choosing the multichannel pipette between an 8 or 12 channels, the 8 multi-channels pipette was preferred since it is easier to handle.
- The plate reading has to take place no more than 30 min after stopping the reaction.

### 3.1.1.11.2 Quantified NGF Released

To change from absorbance values to concentration of protein in total NGF ng released data was organized in graphs. A linear equation given by the linear portion of the standard curve was used to perform the calculations (Fig. 3.20).

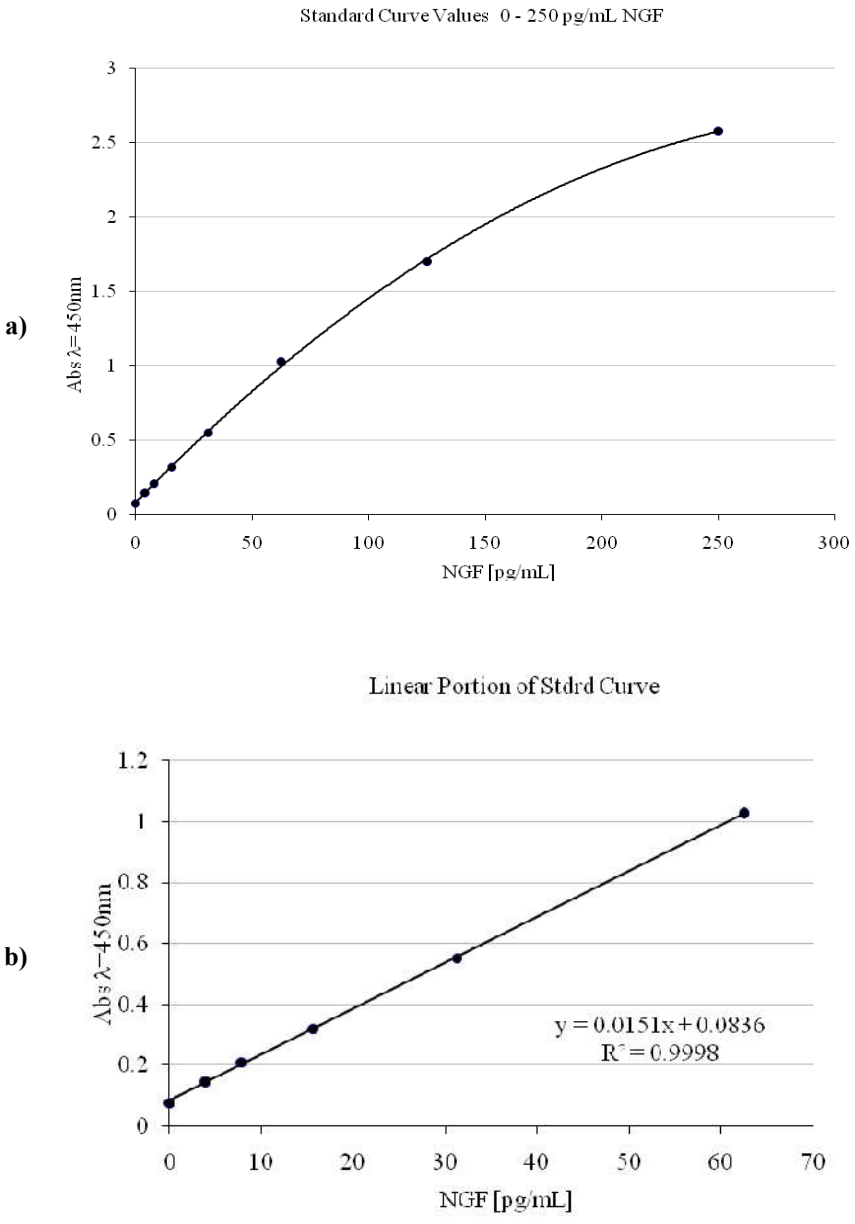


**Figure 3. 20. a) Example of standard (stdr) curve from one of the read plates and b) linear portion of stdr curve showing the r-value and linear equation of the graph.**

From the previous equation (Fig. 3.20b) the concentration can be calculated by solving for x.

$$y = 0.0151x + 0.0836$$

$$x = (y-0.0836)/0.0151$$

Where:

$y$ = absorbance and

$x$ = concentration of NGF in pg/mL

The resulting concentration (pg/mL) was multiplied by the dilution factor or the sample. It was then divided by a thousand to convert from pg to ng. Last, it was multiplied by 2 mL since it was the volume of the supernatant. Controls were not subtracted since they gave negative absorbance and concentration values. This gave finally the total amount of NGF ng present in 2 mL of medium. Table 3.3 illustrates the steps to calculate total NGF per sample.

**Table 3. 3. Calculations to know the total amount of NGF released per sample in a 2mL volume.**

| Sample Abs | NGF pg/mL (abs-0.0836)/0.0151) | x dil factor (NGF pg/mL) | NGF ng/mL (/1000) | Total ng of NGF (x 2mL) |
|---|---|---|---|---|
| 0.525 | 29.23 | 5261.7 | 5.26 | 10.52 |
| 0.543 | 30.42 | 5476.3 | 5.48 | 10.95 |
| 0.464 | 25.19 | 4534.6 | 4.53 | 9.1 |

However, results were reported as cumulative values. To convert to cumulative values, each hydrogel release values were tracked. The first time point value (ie. at 2 hrs) was reported as it is, total ng of NGF (released after 2 hrs). For the second time point (ie. at 4 hrs), its total ng NGF release values were added with the total ng of NGF of the previous time point (ie. total ng NGF after 4 hrs + total NGF released after 2 hrs). An average of the added values was calculated

and plotted. From this mean, a standard deviation was calculated. The standard error (SE) was also determined. Table 3.4 exemplifies for data management.

**Table 3. 4. Data management to acquire cumulative values. Numbers on top of columns refer to the amount of time in hours that the hydrogels were releasing NGF. Cum refers to the cumulative value which is the summation of the quantified amount of protein at that time point plus the previous time point value. Numbers in bold are the plotted mean. In this example n=5**

| | 2 | 4 | cum | 8 | cum | 12 | cum |
|---|---|---|---|---|---|---|---|
| Disk1 | 51.94 | 6.76 | 58.69 | 8.57 | 67.26 | 4.63 | 71.90 |
| Disk2 | 36.49 | 6.33 | 42.81 | 10.52 | 53.34 | 3.75 | 57.09 |
| Disk3 | 38.39 | 7.19 | 45.58 | 10.95 | 56.53 | 4.99 | 61.52 |
| Disk4 | 45.57 | 4.52 | 50.09 | 9.07 | 59.15 | 3.42 | 62.57 |
| Disk5 | 50.05 | 4.63 | 54.69 | 11.50 | 66.19 | 3.23 | 69.42 |
| AVERAGE | **44.49** | | **50.37** | | **60.49** | | **64.50** |
| STDEV | 6.87 | | 6.48 | | 6.06 | | 6.05 |
| STERR | 3.07 | | 2.90 | | 2.71 | | 2.70 |

### 3.1.1.12 PC-12 Bioassay

Pheochromocytoma cells were originally obtained from American Type Culture Collection (ATCC). However, before their use in this experiment, PC-12 cells were stored frozen in dulbecco's modified eagle medium (DMEM) plus 5% dimethyl sulfoxide (DMSO) for at least four years at -140 $^{o}$C. PC-12s were thawed in DMEM plus 10% fetal bovine serum (FBS). Immediately after thawing, cells were seeded on a T-25 culture flask. PC-12 cells were slowly adapted (Table 3.5) to RPMI-1640 medium because they were previously grown and frozen under DMEM.

As cells were growing and total fluid renewals (TFR) were performed the following solutions were given to the cells (Table 3.5):

**Table 3. 5. Solutions given to PC-12s to slowly change their medium from DMEM to RPMI-1640. Through the different fluid renewals, medium containing different concentrations of media types were varied until only RPMI-1640 was provided and no DMEM [116].**

| TFR | Day | DMEM (%) | RPMI-1640 (%) |
|---|---|---|---|
| 1 | 2 | 100 | 0 |
| 2 | 4 | 75 | 25 |
| 3 | 6 | 50 | 50 |
| 4 | 8 | 25 | 75 |
| 5 | 10 | 0 | 100 |

RPMI-1640 was supplemented with 10% heat inactivated horse serum (HoS), 5% fetal bovine serum (FBS), 1% glutamine-penicillin-streptomycin (GPS), 10 mM HEPES and 1 mM sodium pyruvate.

Cell culture procedures took place inside the BSC. Cells were passaged with trypsin-EDTA to a T-75 flask after reaching ~80% confluency. Still, the old T-25 flask containing leftover cells was kept as a culture backup. PC-12s were cultured and used at their exponential growing phase for the NGF bioactivity assay.

One day before using cells for the bioassay PC12s were pre-induced to extend neurites. RPMI-1640 medium was changed for RPMI-1640 supplemented with 20 ng/mL NGF. After one day, cells were counted, centrifuged (850 rpm x 5 min) and resuspended in media without NGF. They were then seeded on wells of a 24 well plate at 5000 cells/well. 24 hours were allowed to pass to let cells adhere to the surface of the wells. After that, their solution was changed for those released by the hydrogels. Negative controls were PC-12s with fresh RPMI-1640 and PC-

12s with supernatant of disks without NGF. Positive controls were 10 and 20 ng/mL that allowed for comparison with the released protein from PEG hydrogels. Analysis of neurite extension was performed under an inverted microscope (Leica DM IRB, Leica Microsystems, Germany). Images of cells were taken with a CCD camera (Retiga 2000R Fast 1394, QImaging Corp., Canada) adapted to the microscope at 20X magnification after 24, 48 and 72 hrs.

#### 3.1.1.13 Hydrogels´ Imaging

Pictures of the hydrogels were taken of their normal size and magnified. For the first images of hydrogels, a digital camera was employed and pictures of hydrated samples were acquired. For the magnified images dry samples were sputtered with gold for 30s and seen under a scanning electron microscope (SEM) (S-4800 UHR FE-SEM, Hitachi, Pleasanton, CA).

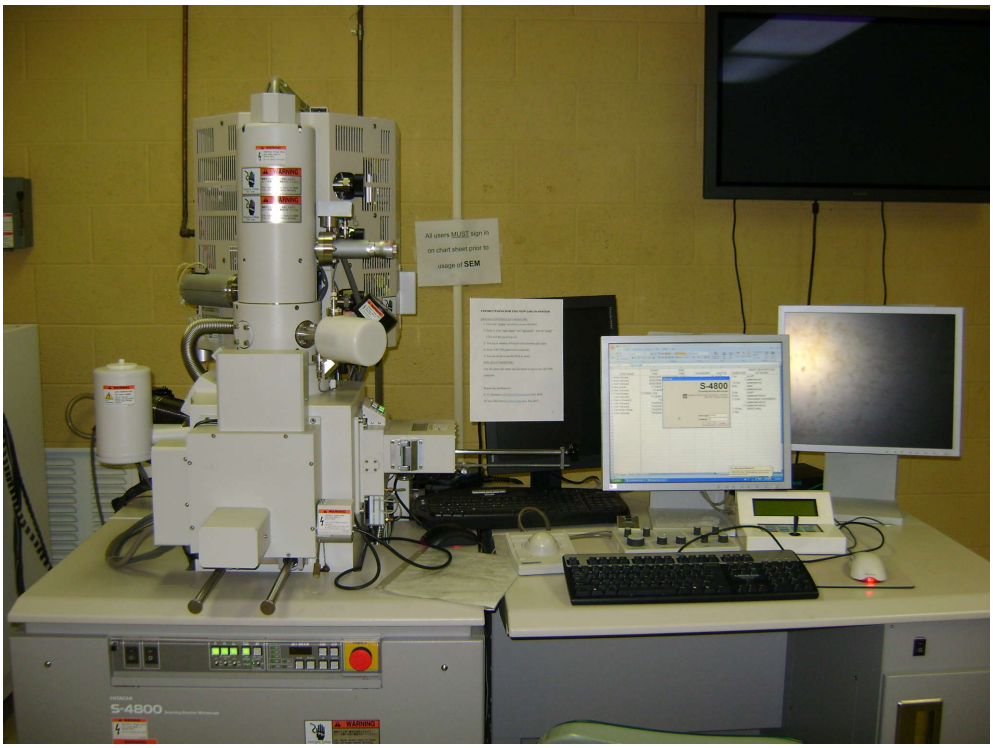


**Figure 3. 21. Scanning Electron Microscope used to take high magnification images of PEG hydrogels.**

### 3.1.2 PEG Hydrogels with Bioactive Domains

A 20 wt% PEGda 3.4 kDa was prepared. Four mL of HEPES buffer and 0.0251 g of Irgacure® (I-2959) were added to an amber bottle containing 1g PEGda 3.4 kDa. The solution was syringe filtered with a low protein retention 2 µm pore size membrane filter. The solution was split into 2 parts. One part consisted of 20 wt% PEGda 3.4 kDa solution and the other part was 1mL of solution to which 20 mg of ACRL-PEG-RGDS were added. ACRL-PEG-RGDS was previously synthesized by another member of our group who also drew the CAD-files that were used for this experiment [111]. The files consisted of a positive and negative image of the same drawing. (Fig. 3.22).

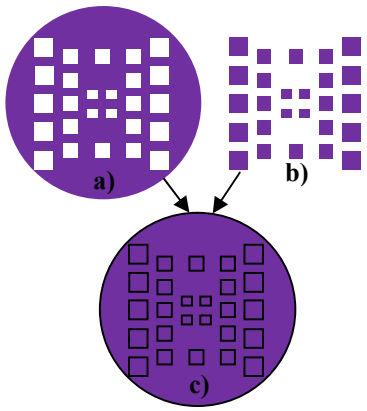


**Figure 3. 22. Spatially controlled multiple material manufacture. a) and b) are the designs provided created in SolidWorks® to ultimately produce c) the final desired hydrogel sketch. Purple sites resemble the areas where the laser passes scanning.**

#### 3.1.2.1 Building in SL

Overall, the same procedure took place as in the previous experiment (Section 3.1.1.7). However, regions within the hydrogels consisted of different files (Fig.3.22) and different materials. The working area was cleaned with 70% alcohol. SL parameters were a critical exposure of 12, penetration depth of 2.75, laser speed of 0.929 to 1.3 and a power oscillating between 22.35 and 27mW. The vat was accommodated with an air bubble leveler and the base was then stabilized with clay to be attached to the elevator platform. 360 µL of the PEG solution

that contained RGDS were pipetted into the container and the laser was commanded to draw the small squares file (Figure 3.22b) by passing twice over the same surface. The vat was taken out of the system and the unreacted solution was retrieved and placed back into the photopolymer vial of PEG+RGDS to reuse later. The mini-container was taken back inside the system to its base and 220 μL more of the same solution were added and again, the laser scanned twice the same surface. Now, the small squares were tightly attached to the bottom of the vial. One more time the leftover solution was pipetted and taken back to its corresponding vial. The small container was rinsed to get rid of the non-crosslinked material. Added water was disposed by tilting the container. The vat was then dried with a Kimwipe being careful of not damaging the small features by touching them. With the squares still in place, the container was taken again to its base inside the SL chamber. The file to use was now changed to cure around the squares only (Figure 3.22a). 360 μL of the plain PEG solution were added and the laser was sent once to cure the file sketch. 220 μL more were added and the laser cured one layer again. The uncured solution was retrieved and re-stocked. The vat was rinsed with ultrapure water and the finished part was removed with a spatula. Each disk after being created was transferred to a well of a 24-well plate containing PBS without flipping the disk.

#### 3.1.2.2 Bioactive PEG Analysis

Inside the biosafety cabinet a 24-well plate was filled with 1 mL of Dulbecco's Modified Eagle Medium (DMEM). Hydrogels that were previously in PBS were individually transferred to a well of the multi-well plate containing DMEM. Since the hydrogel disk fits loosely inside the well, a silicone ring was placed on top to secure it to the bottom of the well. The rings were acquired by cutting a silicone hose about 5 mm thick per slice. The rings were previously

autoclaved and their outer diameter fit tightly into the inside walls of a 24-well-plate´s well. The well-plate was left inside the incubator overnight at 37 $^{o}$C, 5% $CO_2$ and 90% humidity.

#### 3.1.2.2.1 HDFs Culture

Human dermal fibroblasts were originally obtained from Cambrex BioScience (Walkersville, MD). For this experiment, they were thawed from the biological sciences facilities where they were under -140 $^{o}$C. To start, they were placed into a T-25 flask and transferred to a T-75 once they reached approximately 80% confluency. They were cultured in DMEM supplemented with 10% FBS and 5% GPS. Conditions were 37 $^{o}$C, 5% $CO_2$ and 90% humidity inside the incubator.

#### 3.1.2.2.2 HDFs Seeding

After 24 hours of having the multi-well plate inside the incubator, it was taken inside the BSC. One day old medium was retrieved and disposed. Each well was filled with 1 mL of cell suspension at a concentration of 10,000 cells/mL in DMEM.

Under the inverted microscope, images of the hydrogels were taken at 50 and 100X after 24 and 48 hours. Controls consisted of wells with 1 mL cell suspension without the hydrogels and without the silicone rings.

### 3.1.2.3 PEG hydrogels´ Fabrication of Compound Materials

To confirm that the stereolithography machine is capable of constructing single parts of different materials, PEG hydrogels were built containing specific domains of a fluorescent dye that showed the place where a different material was present. The same procedure as in Section 3.1.2.1 was used. The differences were the solutions used and the files´ sketches. The crosslinkable PEG solution used was a 20 wt% poly(ethylene glycol) dimethacrylate which mw

was of 1 kDa (PEGDMA MW 1000, Polysciences, Inc., Warrington, PA). It was dissolved in HEPES buffer and it contained a final concentration of 0.5% Irgacure 2959. The solution was split in two. One part was kept original without additives and was used to build the area surrounding the small squares. The other part consisted of 1mL of the original solution plus 20mg dextran labeled with fluorescein isothiocyanate (FITC-dextran, Sigma-Aldrich, St. Louis, MO) with an excitation/emission of 490/520nm. PEGdma solution containing the fluorescent dye was used to construct the small squares. The .stl files used are shown in Figure 3.23.

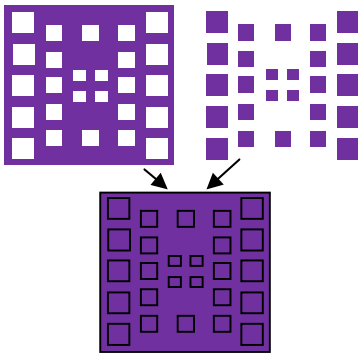

**Figure 3.23. Top images (negative and positive) that give rise to the bottom design when they are overlapped. Purple sites resemble the areas where the laser passes crosslinking the solution.**

Fabricated hydrogels were immersed in ultrapure water until observed under the microscope. Images were taken at 10X magnification with the CCD camnera now adapted to a Leica MZ16 microscope (Leica Microsystems, Germany).

### 3.1.3 $^{1}$H NMR

A proton nuclear magnetic resonance ($^{1}$H NMR) was performed to characterize PEGda 3.4 and 6 kDa with the aid of a Bruker 300 MHz spectrometer. The following procedure took place with guidance from chemists at the UTEP´s chemistry department [117, 118]. Sample preparation involved the dissolution of polymer in deuterated chloroform ($CDCl_3$). This solvent was chosen because the company from where PEG was obtained stated that PEG is readily

soluble in chloroform. Moreover, $CDCl_3$ has been reported in literature to be used with PEG compounds. Furthermore, chloroform has a chemical shift (δ) at 7.27 that does not interfere with our expected signals. For example, it is known that $\delta_{PEG}$ = 3.6ppm. If deuterated water ($D_2O$) were to be used it would have a chance to interfere with the quality of PEG $^1H$ NMR spectrum since $D_2O$ exhibits a peak at δ = 4.8 ppm. In addition, the solvent used had 1% tetramethylsilane (TMS or $(CH_3)_4Si$). This is a highly hindered molecule of δ = 0, used as an internal standard.

The number of repetitive units (n) of the PEGda chain was calculated from $^1H$ NMR. Ultimately, the molecular weight of the polymeric compounds was confirmed by this method. The molecular weight of the polymer equals the molecular weight of the monomer times the number of times it repeats (n).

$$\mathbf{mw_{PEG} = (mw_{UNIT})(n)}$$

The monomer repetitive unit is $-CH_2CH_2O-$ and its mw = 44g/mol. Therefore, the mw of PEG:

$$\mathbf{mw_{PEG} = 44n}$$

To calculate n, a ratio between the integrated area under the hydrogen (H) atoms´ signal corresponding to the repetitive units over the area of the H atoms´ peak at the end groups was estimated. Each signal has to be divided by the number of hydrogen atoms that lead to their appearance. The integrated area under each signal was calculated and given by the NMR spectrometer software.

$$n = \frac{\text{Area of the repetivite units signal}}{4} \div \frac{\text{Area of the repetivite units signal}}{\text{Number of hydrogens that account fot this end group signal}}$$

Figure 3.24 illustrates the chemical configuration of hydrogen atoms in the PEGda molecule. Each letter corresponds to a different signal in the $^{1}H$ NMR spectrum. Blue capital letter A indicates a single peak that will be present due to the repetition of four equivalent H atoms in the monomer. Small red letters a, b and c indicate the three types of hydrogen atoms from the vinyl groups that will make the three signals of the end groups to appear in the spectrum.

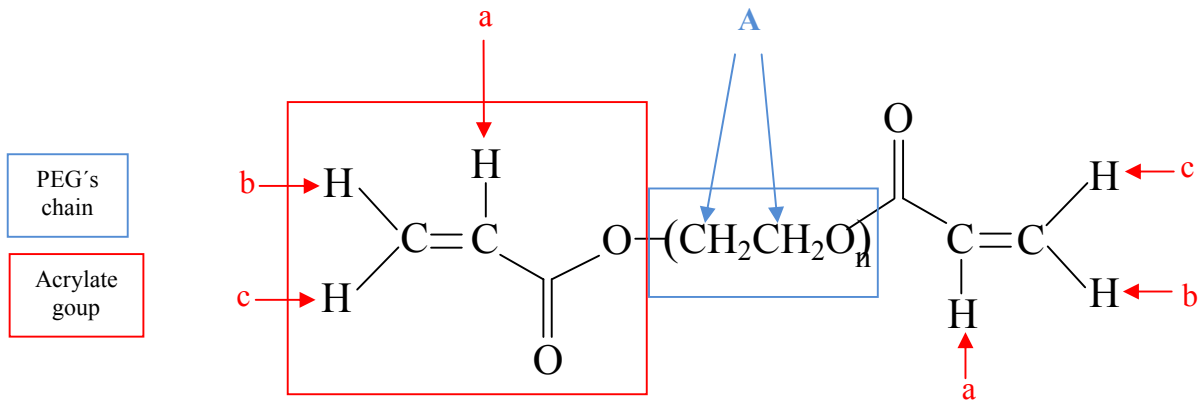


**Figure 3. 24. Poly(ethylene glycol) diacrylate molecular structure. A,a,b and c show the different H atoms´ chemical organization in PEGda.**

The number of repetitive units (n) was then calculated using the signal of the single hydrogen attached to the carbonyl atom (red small case letter a) as follows:

$$n = \frac{A}{4} \div \frac{a}{2}$$

Values for the integrated areas of **A** and **a** are given in the results section on the NMR spectrum for PEGda 3.4 and 6 kDa, respectively. Finally, the molecular weight of PEG (mwPEG) was calculated after solving for n and multiplying the n value times 44. Outcome is presented in the results section, Chapter 4.

*Chapter 4*

## 4.0 Results

This chapter presents the results of two projects. The first one is about the controlled release of growth factors from PEG hydrogels. The second one comprises the capabilities of stereolithography to produce parts comprised of different materials. This second experiment was done in collaboration with another tissue engineering researcher from our group. Additional results (images and tables) not presented here, are shown in the Appendix 2 and 3.

## 4.1 Nerve Growth Factor Release

The release of nerve growth factor (NGF) was examined from different poly(ethylene glycol) matrices. The solutions from which PEG hydrogels were made of consisted of different molecular weights (mw): 3.4 and 6 kiloDaltons (kDa) and varying poly(ethylene glycol) diacrylate (PEGda) concentrations: 20 and 30 wt% for PEG 3.4 kDa and 10% (w/v) for PEG 6 kDa. The main objective of prolonging the protein´s stance within the hydrogels while controlling its release was accomplished. Not only the different methods of protein inclusion affected the growth factor release, but also the properties of the gels influenced the yield of free NGF in solution. Points in the graphs represent the mean ± standard deviation (SD), and the number of sample replicates (n) is given for each set of data. Information is presented as the cumulative release, which is the amount of protein detected at a given time point plus the value of the previous time point analyzed. In addition, a biological assay was performed to test for NGF bioactivity. With the aid of the inverted microscope we were able to observe the morphological changes of pheocromocytoma (PC-12) cells in response to the NGF present in the supernatant of the samples, showing the protein's bioactivity. Hence, we were able to

demonstrate that the stereolithography technique is a viable method to create PEG hydrogels containing releasable bioactive nerve growth factor.

### 4.1.1 Hydrogels' Imaging

Swollen hydrogels from PEG 3.4 kDa were confirmed to be of 5 mm in diameter after measurements with a ruler took place (Fig. 4.1). However, 3.4kDa disks were thicker than the higher molecular weight 6kDa gels, due to the building process. Constructing the 6kDa disks took longer, giving time to the photopolymer to settle and move to the sides of the container where it has preference to be and photopolymer solution had more time to settle. Moreover, hydrogel disks did not have 1mm in height evenly. This can be noted by looking at the side view of disks over a glass slide (Fig.4.2.).

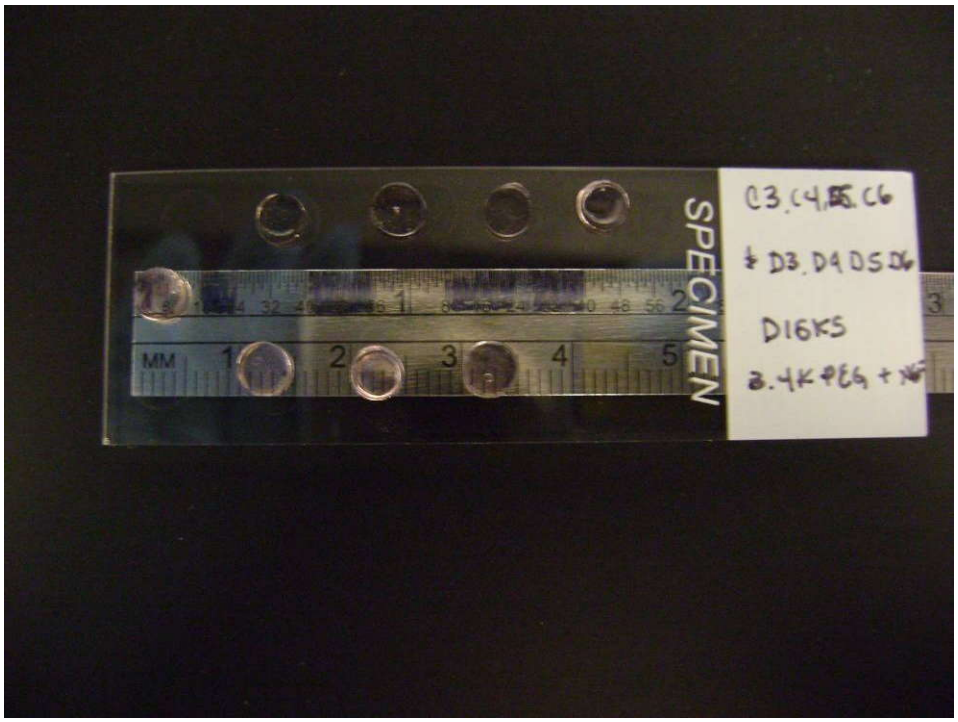


**Figure 4.1. Top view of swollen hydrogels. Diameter is confirmed to be of 0.5cm as predicted**

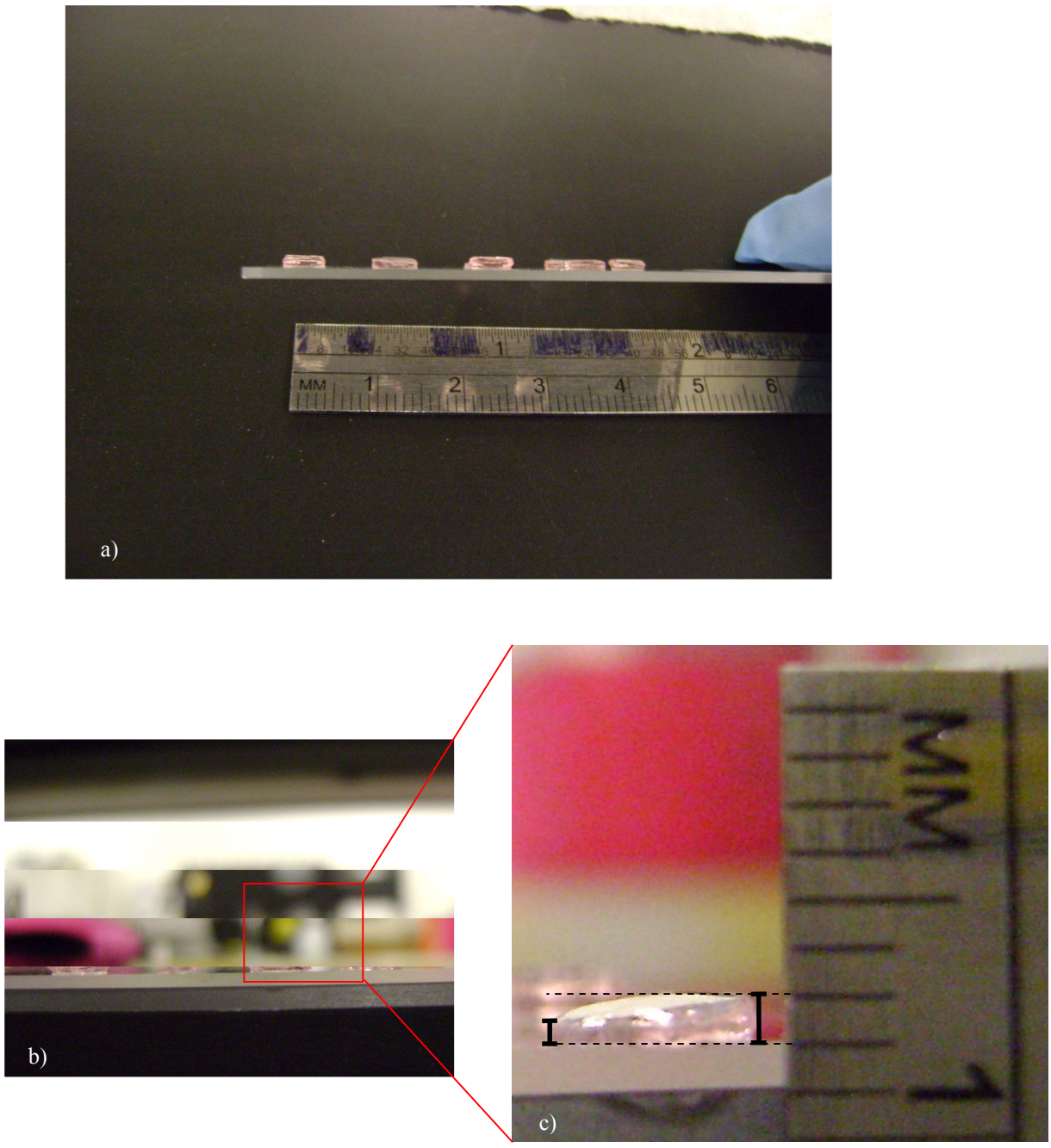


**Figure 4.2. Side view of swollen hydrogels over a glass slide. a) Disks on top of a glass slide placed at the edge to be able to measure their height, b) measure of the gel width and c) close up of the measurement. Note that one side of the gel is in fact 1mm thick, but that height is not even throughout the whole hydrogel diameter**

Higher magnified images were taken under the scanning electron microscope (SEM) to explore the physical conditions of the hydrogels. Pictures of gold sputtered dry samples and non sputtered samples were taken. Overall, the hydrogels shown are not deformed and their dimensions look even from the upper view. No significant differences were seen from gold coated samples and non gold sputtered.

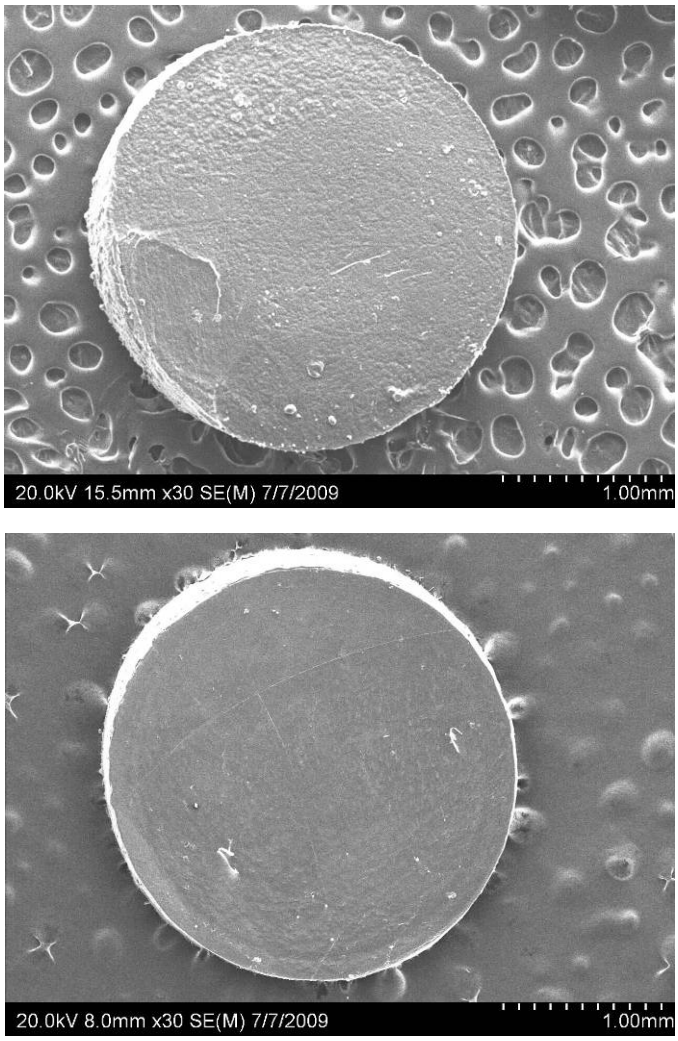


**Figure 4.3. Upper: Gold sputtered shrunk (dry) 10% (w/v) PEG 6kDa disk. Down: Non-coated dry gel made of 30 wt% PEG3.4kDa**

### 4.1.2 20 wt% PEG 3.4 kDa

The protein release from 20% PEG 3.4 kDa hydrogels was analyzed from three batches of disks of different conditions: with the protein encapsulated, conjugated and lyophilized-sterilized gels containing NGF physically entrapped. For all of the samples, a small amount of NGF was released when the experiments were stopped in comparison to the potential NGF available for diffusion. When the protein was encapsulated, 44±6.9 ng were present in the retrieved solution of the first time point. By the 2nd day most of the NGF quantified was out (74±6.4) and a total of 93±9 ng were released by the 7th. This was the highest amount of NGF diffused for this mw concentration as shown in Figure 4.4.

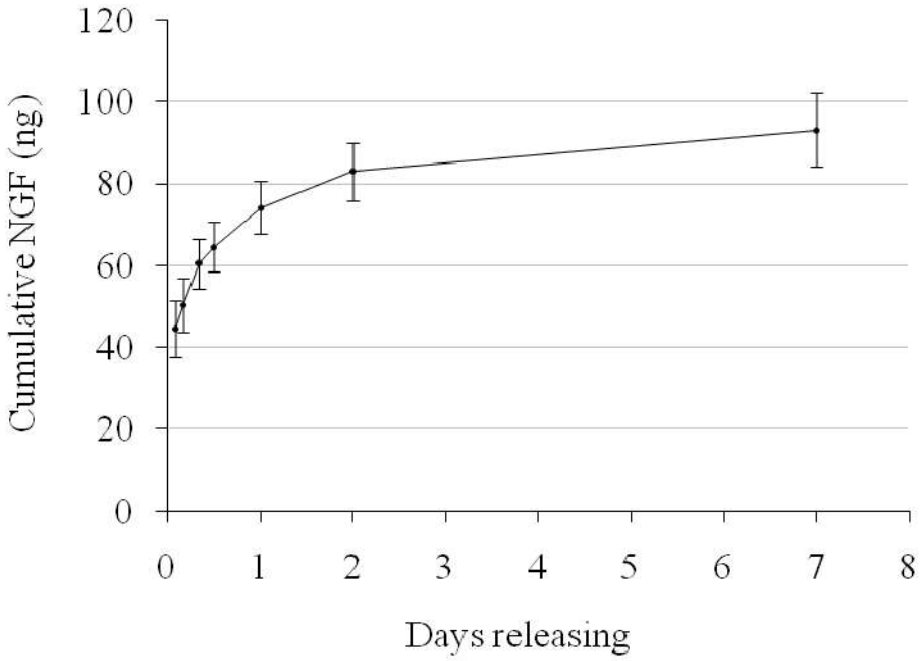


**Figure 4.4. Cumulative NGF release over a seven day period from 20% PEGda 3.4 kDa hydrogels containing the protein encapsulated (n = 5)**

By conjugating the neurotrophin to the polymer, its release decreased both in rate and amount. The release profile of the encapsulated protein was different from the conjugated

protein diffusion. The first diffusion time point recorded when NGF was physically trapped was after two hours, whereas it was 4hrs when chemically bonded NGF diffused out. These time points were different because expectations were a slower NGF release when it was chemically linked to PEG and a faster release when NGF was physically incorporated. When conjugated, only 7±1 ng were released at the first time point (4hrs). It is important to mention that besides the fact that the initial release was recorded after twice the time of the previous incorporation method, the amount quantified decreased significantly (7ng recorded at the first time point when conjugated, vs. 44ng when entrapped). Then, a burst was seen during the first two days and then the protein kept diffusing at a constant rate up to 20 days. Ten days later NGF release was still sustained (19.6±0.8 ng NGF total quantified after 30 days) as illustrated in Figure 4.5.

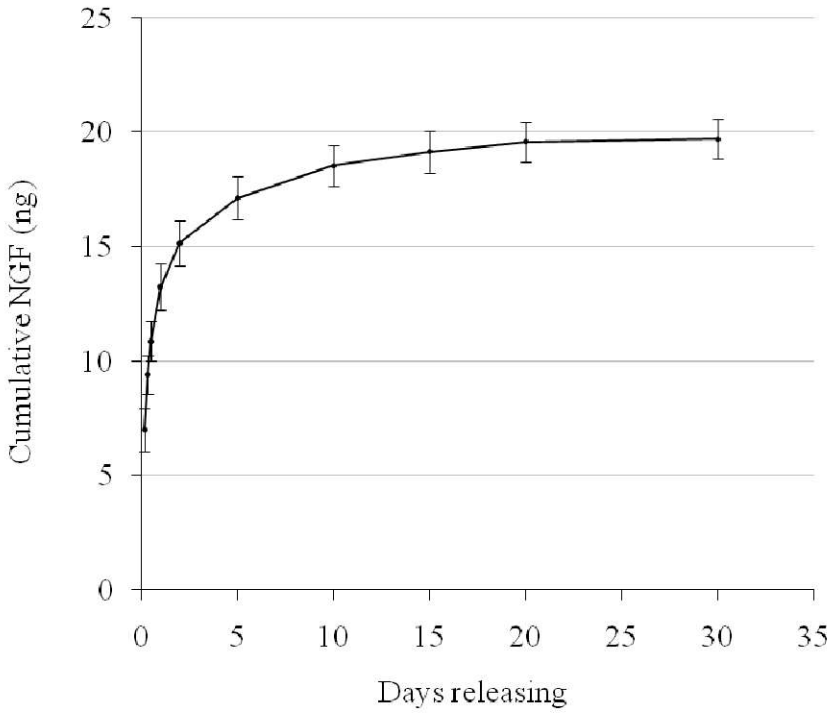


**Figure 4.5. Cumulative NGF release over a 30 days period from 20% PEGda 3.4 kDa hydrogels containing the protein conjugated (n ≥ 5)**

Knowing that the market conditions require a sterile product that can be stored, the experiment was repeated including the process of lyophilization and sterilization. Less than 10ng (7.11 ±0.7 ng NGf) were diffused after one week from sterile-lyophilized-reswollen disks. Surprisingly, even though NGF was encapsulated in dried-sterilized gels, less than when having the neurotrophin conjugated leached out, as it can be seen in Figure 4.6

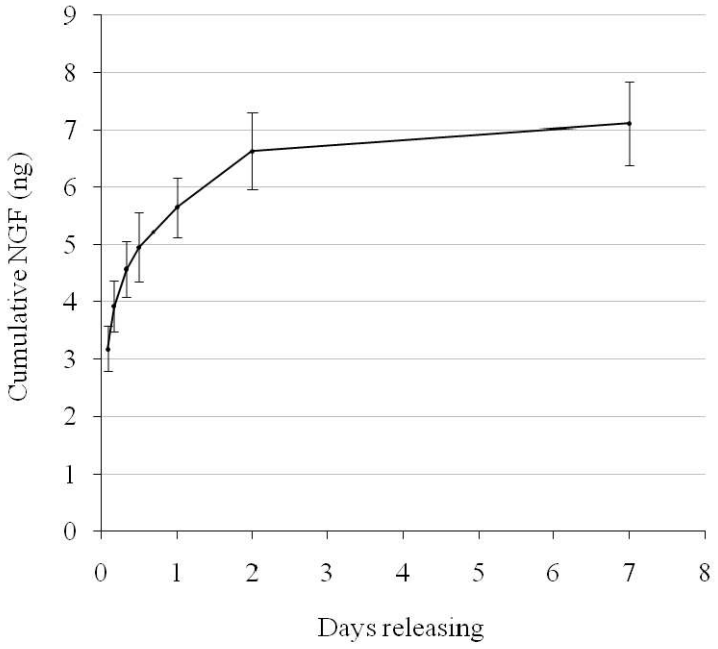


**Figure 4.6. NGF release over a 7 day period from 20% PEGda 3.4 kDa sterile hydrogels containing the protein encapsulated (n = 6)**

### 4.1.3 30 wt% PEG 3.4 kDa

To compare how the concentration of the polymer affects the release rate of the NGF, a 30% concentration of the same molecular weight was used as a matrix with the protein entrapped. Findings were that the higher the PEG's concentration, the fewer the amount and rate of NGF that was diffused. After 2hrs, only 25±4.7ng NGF went out. At the 7$^{th}$ day, only 46±4..3ng were diffused and a trend in the graph suggests that the protein would keep releasing.

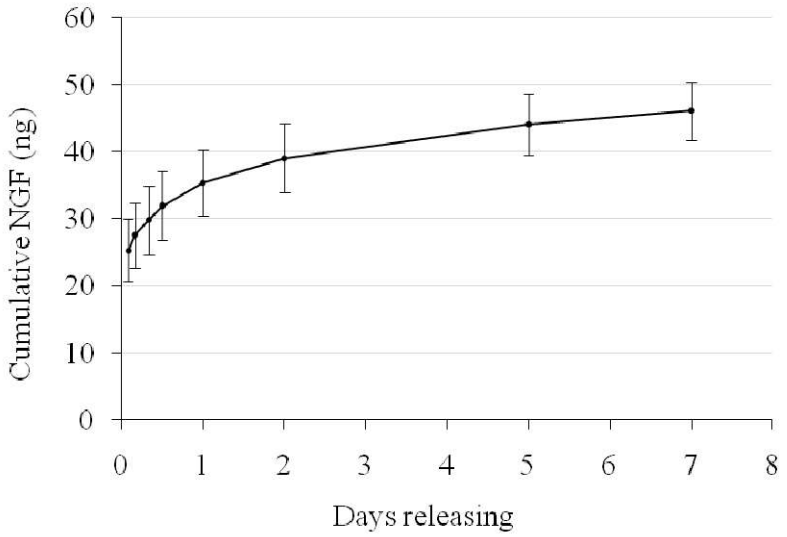


**Figure 4.7. Cumulative NGF release over a seven day period from 30% PEGda 3.4 kDa hydrogels containing the protein encapsulated (n = 5)**

The following graph summarizes the NGF release outcome from different methods of incorporation into PEG 3.4kDa hydrogels of 20 and 30 wt % (Figure 4.8).

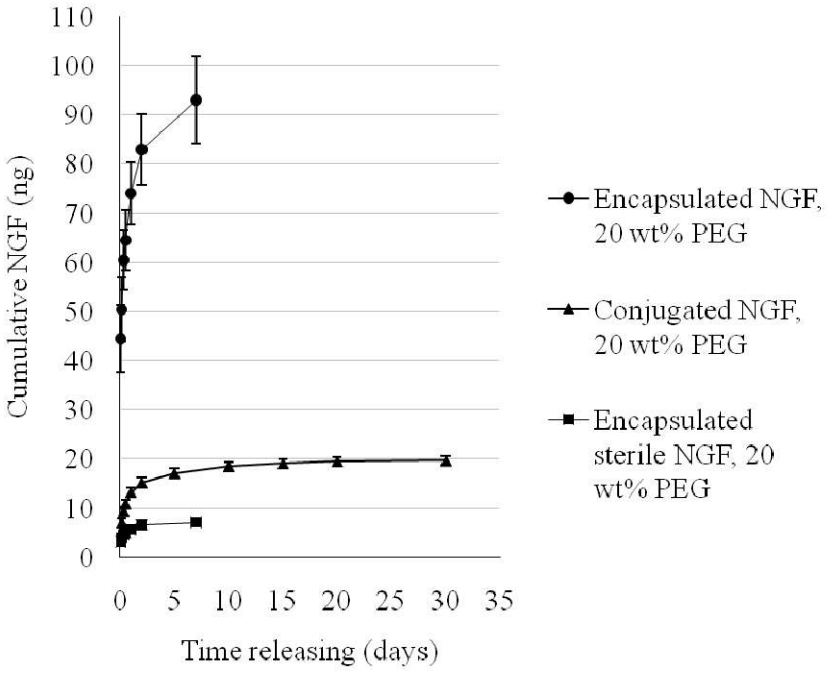


**Figure 4.8. NGF release from PEG 3.4 kDa hydrogels**

### 4.1.4 10% (w/v) PEG 6kDa

As it is commonly known, diffusion is affected both by the size of the molecule being released and the size of the matrix´s mesh. In this study, a higher PEGda mw of 6 kDa was used to build hydrogels for the same purpose as before with the PEG 3.4 kDa scaffolds. Noticeably more NGF was present in the withdrawn solutions from 6 kDa disks´ supernatants. According to the ELISA analysis, close to 300ng of the encapsulated NGF went out of their matrix. After the second day, a constant and slight amount but sustained release is seen thereafter. In contrast to the lower PEG mw 3.4 kDa gradual diffusion, the release profiles of NGF from PEG 6 kDa show an accentuated initial burst and a faster release during the first day (Fig. 4.9 and 4.10).

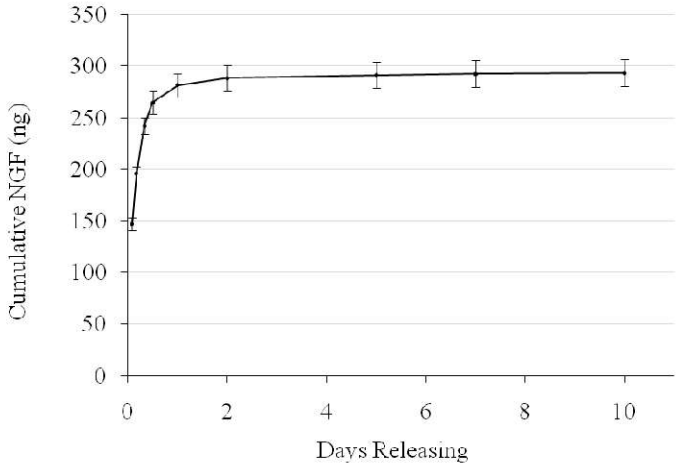


**Figure 4.9. Cumulative NGF release over a ten days period from 10% PEGda 6kDa gels containing the protein encapsulated (n = 4)**

When the neurotrophin was chemically bonded to the chains of the 6kDa polymer, less of it was released after 10 days in comparison to the diffusion of the physically entrapped protein. On the other hand, a slight increase in the amount of NGF in the supernatant over each time point is observable, reaching 253±47 ng at the $10^{th}$ day. In accordance to the predictions, chemically linked NGF initially diffused less than when it was only entrapped within the gel. An additional quantification was made at the $15^{th}$ day. Results reveal that a small amount of NGF

was still coming out of the hydrogels and it the results are illustrated in Figure 4.10. . Moreover, Fig. 4.11 sumarizes the NGF release encapsulated in comparisson to conjugated to 6kDa gels.

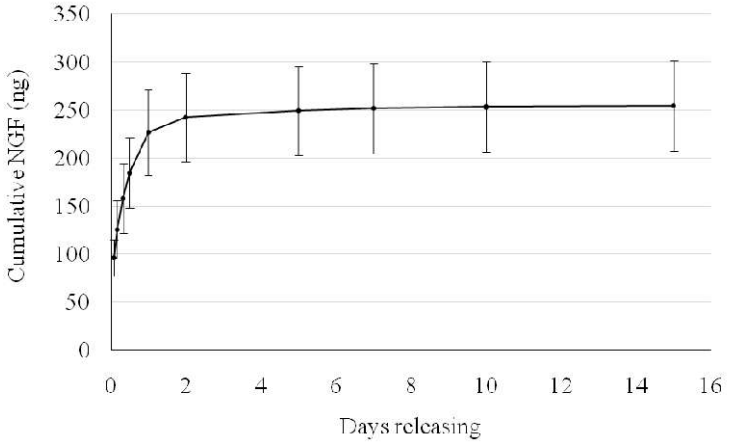


**Figure 4.11. Cumulative NGF release over a seven day period from 10% PEG 6 kDa hydrogels containing the protein conjugated (n = 5)**

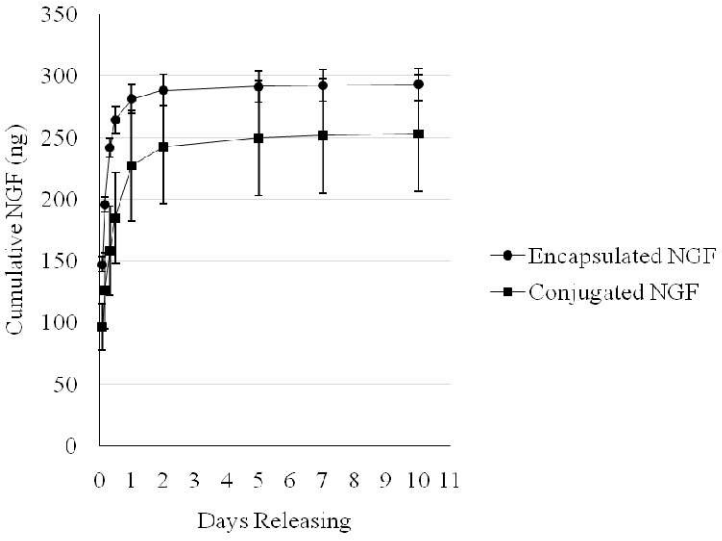


**Figure 4.10. NGF release from 10 % (w/v) PEG 6 kDa hydrogels**

### 4.1.5 NGF Bioactivity

Nerve growth factor was released from hydrogels into 2mL of RPMI-1640 medium. The amount released from the PEG gels was biologicaly significant (>5ng/mL [30]), except for the lyophilized-sterilized disks. As PC-12 cells mimic neuron cells by extending neurites when

induced by chemical cues, they were exposed to the supernatannts retrieved to test for NGF bioactivity, which promotes neurite growth. While some consider processes longer than one cell body diameter as neurites [102, 105, 107, 119,120], PC-12s´ extensions in this experiment are considered neurites when their length exceeds the double of the cell body diameter [9,39]. Besides the supernatants, cells were cultured with NGF 0, 10 and 20ng/mL as negative and positive controls, respectively. Findings indicate more bioactivity for the NGF released from the PEG 3.4 kDa disks than the 6 kDa gels, even though the higher mw hydrogels diffused more of the neurotrophin. Moreover, PEG 3.4 kDa supernatants exhibit similar bioactivity to the positive controls. Chosen pictures to present are after 48 hrs of exposure because cell density was still acceptable as to appreciate individual cell morphology. Images are from cells seeded in a 24-well plate at 5000 cells/well (Fig. 4.12).

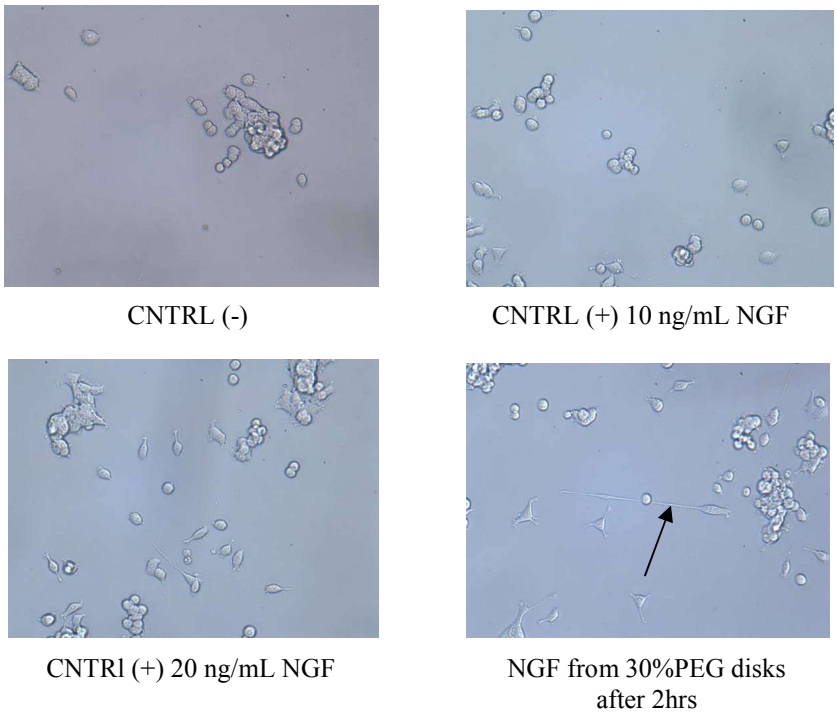


**Figure 4.12. Phase contrast images of PC-12 cells exposed to different NGF concentrations. Magnification is 20X**

## 4.2 PEG Bioactive Domains Incorporated by SL

Hydrogels containing bioactive domains and inert areas were fabricated by manipulating the manufacturing process. The inclusion of a fluorescent dye served to illustrate the regions patterned with a different material than the rest of the substrate. Even though the following figure is not a fluorescent image, the various materials comprising the substrate are clearly noticeable (Fig. 4.13).

**Figure 4.13. Overlapping the two computer sketches on the left built in SL with different materials lead to the manufacture of a single part made out of different components**

Preservation of bioactivity by those domains was shown. Human dermal fibroblasts (HDF) cells seeded on top of PEG hydrogels recognized the sites containing the cell adhesion signal RGDS and anchored to them. Images taken after 24 and 48 hours after seeding resulted unpleasant to sight (Fig. 4.14 upper image), even though they clearly represent cell adhesion distribution throughout the hydrogel. Pictures were too bright and of a shiny red. Therefore, using the software Nero PhotoSnap from Nero Premium 7 images were edited to improve their quality as follows. First, they were converted into white and black and some pictures were inverted (white became black and vice versa). Then, bright and contrast were adjusted. Bright was removed and contrast was added to each image. Following in Figure 4.14 are shown two

images, an original file and the same picture modified. Subsequent images are edited photographs (4.15a and 4.15c).

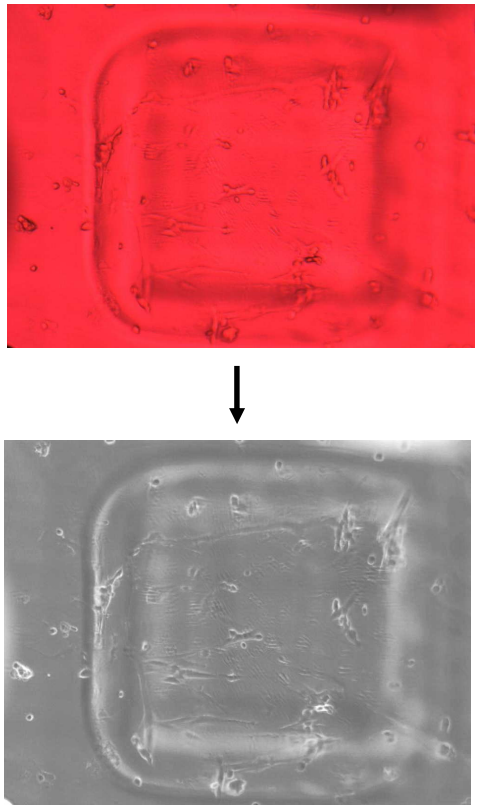

**Figure 4.14. Original image (up) and the same picture after edited (down)**

Morphology of the cells provides information about their behavior. Rounded cells are known to be detached from the surface, while elongated ones are identified to be anchored. Seeded HDFs exhibited a preference to attach at the indicated sites containing the oligomer sequence. Cells were found to be organized within the PEG bio-interactive domains. Bioactive domains correspond to the different sized squares pattern.

Figure 4.15 presents a PEG hydrogel previously customized with bioactive regions of the material PEG-RGDS. Black or white spots relatively big are air bubbles that were floating around in solution. A curved bright or obscure shadow is the silicone ring located at the top of

the disk-shaped hydrogels. The reason why spots resembling the same thing are sometimes bright and sometimes obscure is because the image was inverted in colors or not, respectively.

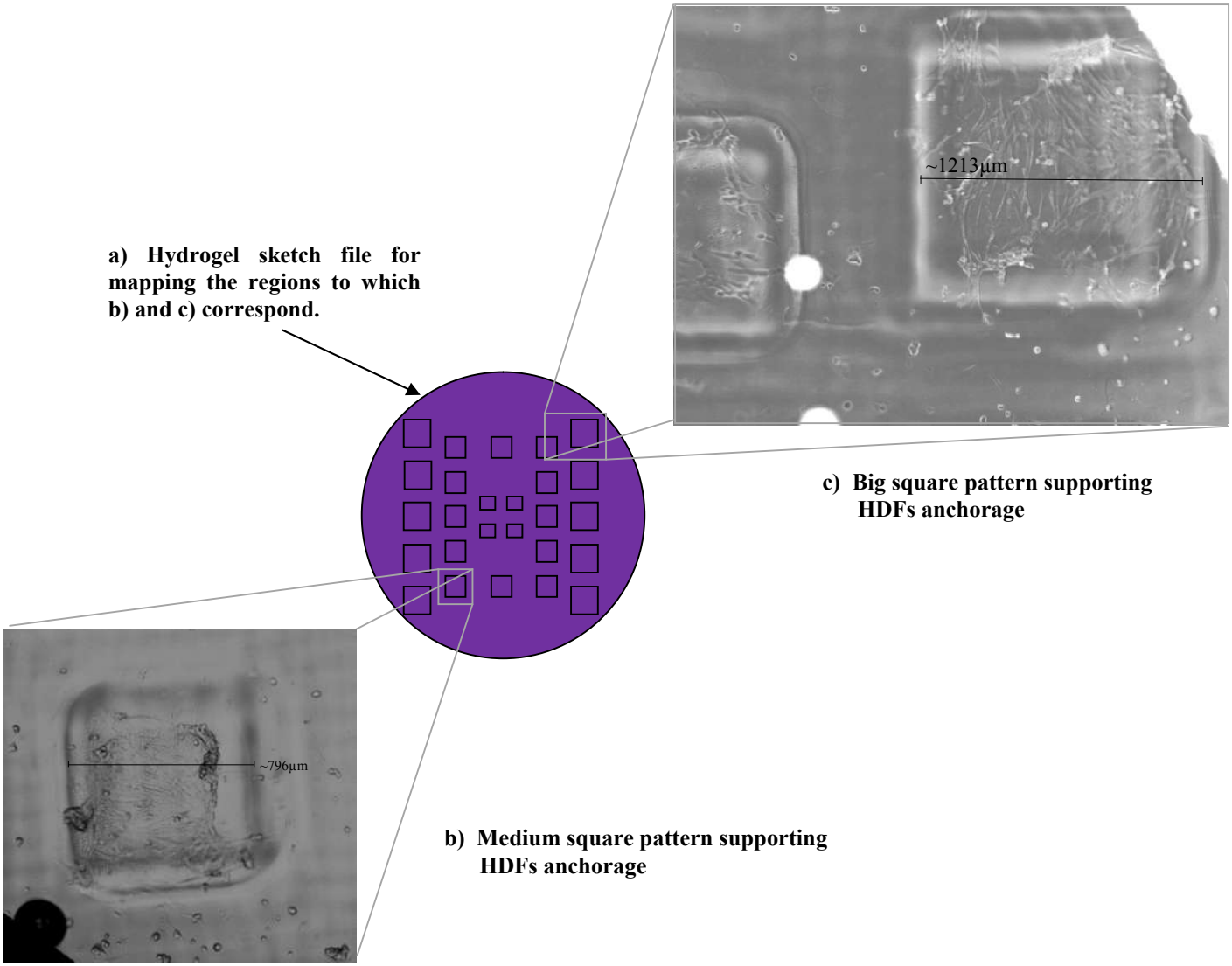


**Figure 4.15. Top view of HDFs seeded on top of a PEG disk-shaped multi-material hydrogel. Squares represent the bioactive PEG regions**

## 4.3 Proton Nuclear Magnetic Resonance

The integrated areas and chemical shifts for the two molecular weights of poly(ethylene glycol) diacrylate were given by the software of the 300 MHz NMR instrument. According with this, the number of repetitive units (n) and thus, molecular weights of the two different polymers were calculated. A more detailed explanation of how was this done is available in Section 3.3 of the materials and methods, Chapter 3. In addition to the original files (Fig. 4.16 and 4.18), amplified images of the bottom line are provided to appreciate better all the peaks and their split (Fig. 4.17 and 4.19). Spectrum modifications were done using Spin Works 2.5.4.

### 4.3.1 PEGda 3.4 kDa

$^1$H NMR (300 MHz, $CDCl_3$) δ = 1.25, 1.65, 3.65, 4.32, 5.85, 6.17, 6.42 (Fig. 4.16).

n = 2A/4a = (2)(812758)/(4)(5.02)

n = 78.085 repetitive monomers

$mw_{PEG}$ = (44g/mol)(n)

$mw_{PEG}$ = (44)(78)g/mol  1g/mol = 1 dalton (Da)

$mw_{PEG}$ = **3,436 g/mol** = 3.4kDa

### 4.3.2 PEGda 6 kDa

$^1$H NMR (300 MHz, $CDCl_3$) δ = 1.7, 2.05, 3.65, 4.32, 5.85, 6.15, 6.45 (Fig.4.18).

n = 2A/4a = 321.89(2)/(1.1954)(4)

n= 133 repetitive monomers

$mw_{PEG}$ = (44g/mol)(n)

$mw_{PEG}$ = (44)(133)g/mol  1g/mol = 1 dalton (Da)

$mw_{PEG}$ = **5,924 g/mol** = 6kDa

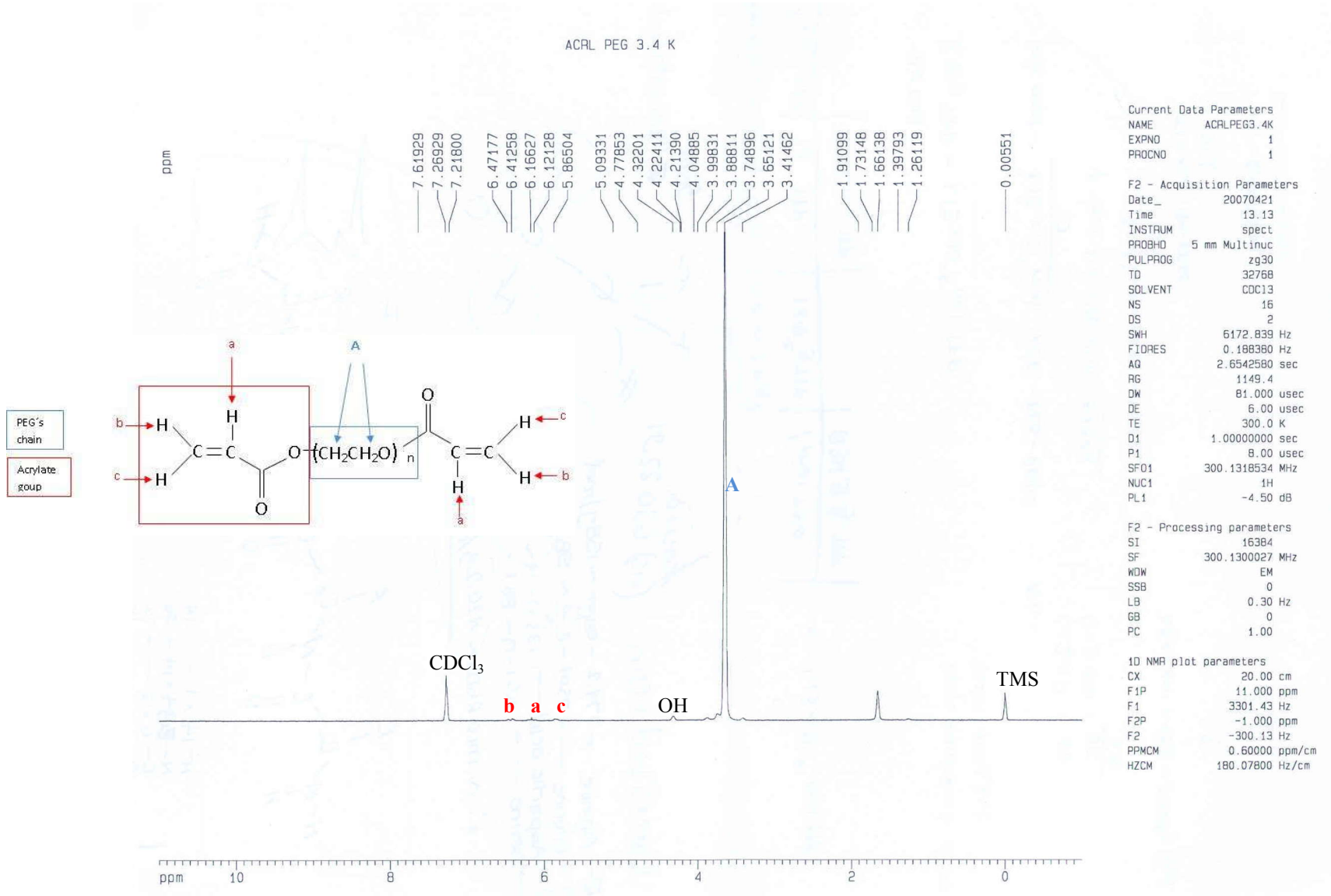


**Figure 4.16. Original $^{1}$H NMR spectrum for PEGda 3.4kDa showing the corresponding signal to specific hydrogen atoms**

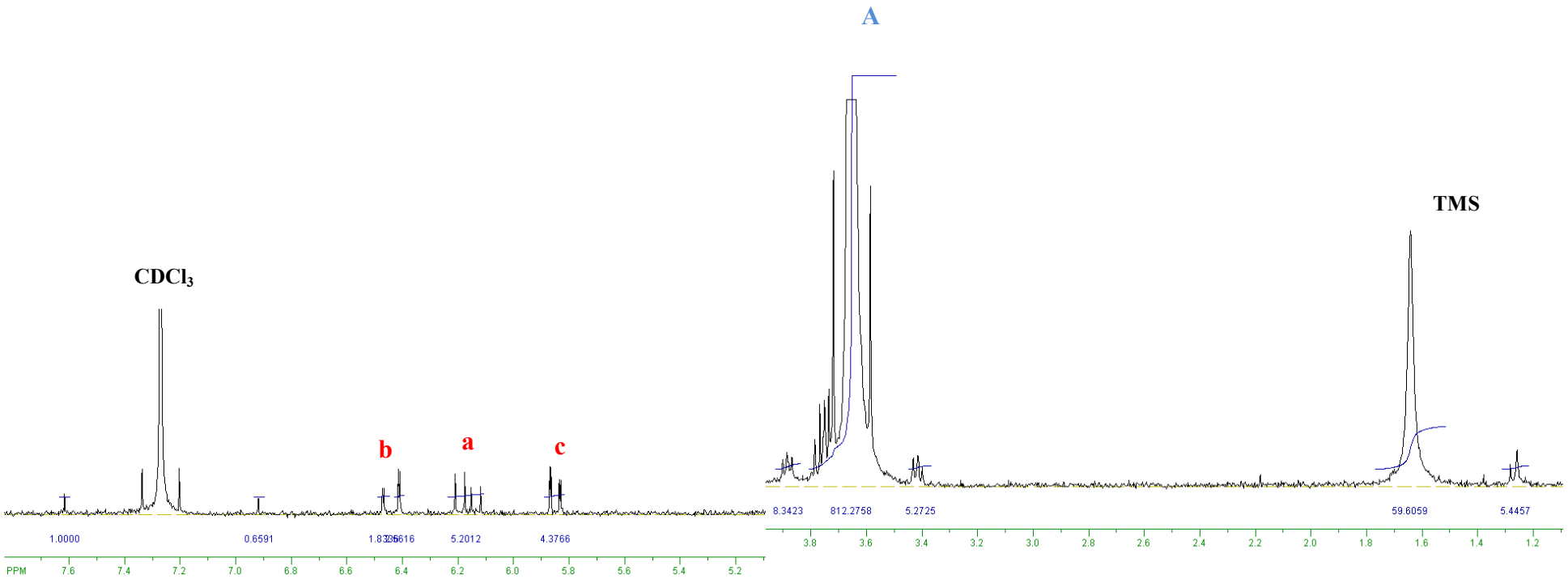


**Figure 4.17. $^{1}$H NMR closer view of PEG 3.4 kDa peaks´ split. Integrated areas are shown in blue below each signal. Chemical shifts are in green**

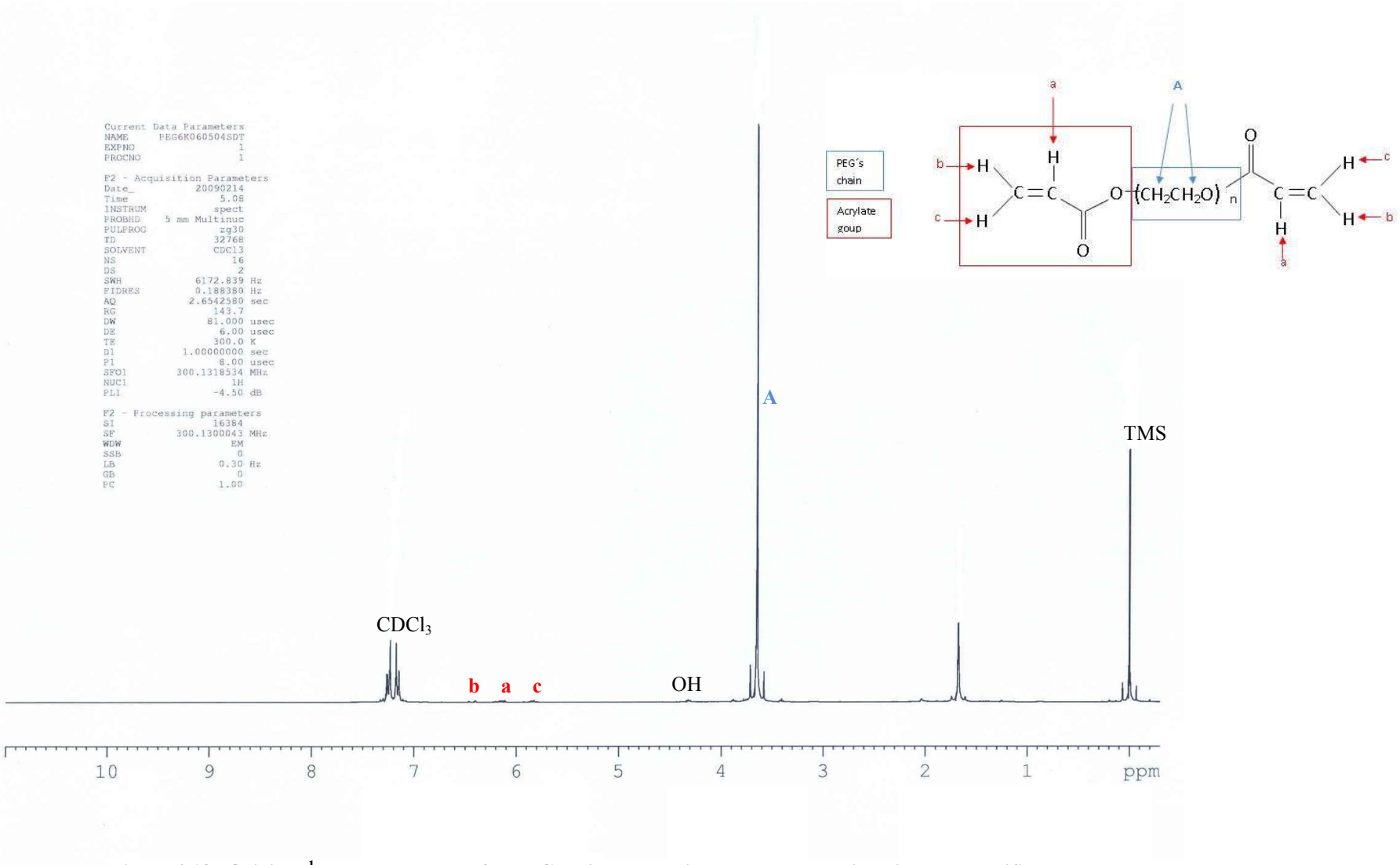


**Figure 4.18. Original $^{1}$H NMR spectrum for PEGda 6 kDa showing the corresponding signal to specific hydrogen atoms**

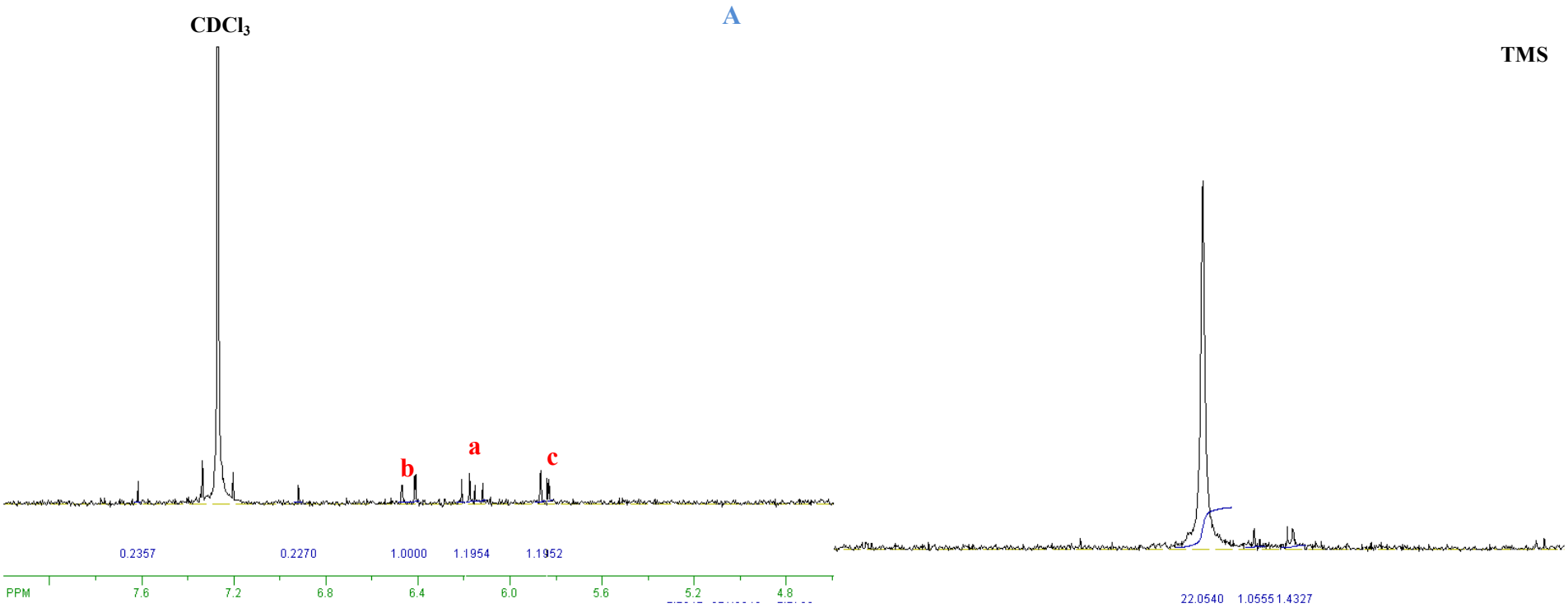


**Figure 4.19.** $^{1}$**H NMR closer view of PEG 6 kDa peaks´ split. Integrated areas are shown in blue below each signal. Chemical shifts are in green**

*Chapter 5*

## 5.1 Discussion

This section compares the present work with other relevant studies. Moreover, it tries to explain the outcome of the results and its significance.

## 5.1 NGF Release

Theoretically, each disk contents were intended to release 500ng of nerve growth factor. However, there was not a total control over the hydrogel disks' dimensions before building, for which the inclusion calculations may have varied. Still, a comparison between the protein encapsulated and conjugated was possible, since hydrogels built by either method contained the same quantity of the neurotrophin regardless if it was slightly less or slightly more than the 500ng predicted.

The reason why the inclusion of the protein was not as expected was due to the discrepancies between the ideal conditions and the real building parameters. Ideally, adding ~327µl of PEG photocrosslinkable solution to the thick walled SL vat would create features of 1 mm in height after the crosslinking process. Unfortunately, the solution has affinity for the walls of the container leaving an empty space at the center. The approach was then to add more volume of solution (340µL total). Even then, the parts built were thinner on the side closer to the center (less solution present there to crosslink) and thicker on the side closer to the vat's walls (where solution has a tendency to be) and it is illustrated in Fig. 4.2c. Nevertheless, a batch of disks was built at the same time equidistant from the center. Since hydrogel features made of 20% PEGda 3.4 kDa increase their size by 25% after swelling, disks were designed to be built by the laser .25 smaller than the desired 5mm in diameter. This is known as the dimensional

swelling factor defined as the desired swollen dimensions over the drawing design dimensions, established by another member of the reaserch group. According to this definition and knowing that the factor for the mentioned solution is 1.25, the formula was applied (sketch dimension = desired 5mm swollen/1.25) Calculations included 500 ng NGF per disk of 4mm in diameter to swell to a final 5mm diameter. As a result, even though they were not the ideally expected disks dimensions, they were all of identical size each containing the same amount of protein to release.

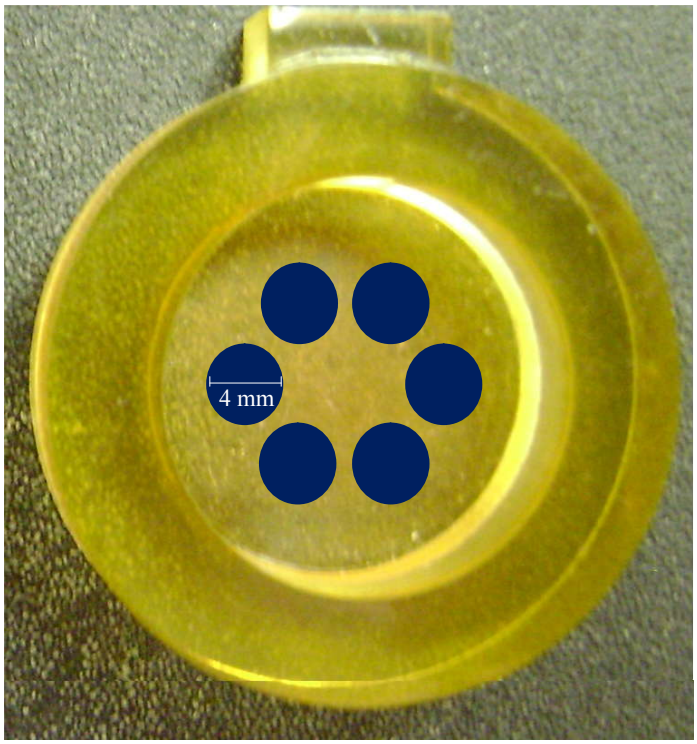


**Figure 5.1. Representation of the hydrogel disks´ distribution in the SL vat.**

Drug release profiles often show a high dose release over the first days of their diffusion commonly known as “initial burst”. In the case of NGF, special attention has to be given to reduce it, as high NGF levels can be an obstacle that may impede nerve regeneration [30, 121].

Moreover, this effect has to be diminished in order to have enough neurotrophin releasing throughout the desired time course accompanying the wound healing [30].

To counteract for the low retention of the drug by the material that embeds it, NGF was chemically linked (PEGylated) to PEG by a Michael-type addition reaction. In this way, NGF forms now part of the hydrogel material. The PEG-NGF bond can be dissociated by hydrolysis, leaving then NGF free to move. It was hypothesized that this method of protein inclusion would decrease its diffusion rate at the same time that it would lower the unwanted burst. Consistent to our predictions, PEGylating NGF did reduce its release in contrast to only trapping it within PEG. Unfortunately, ELISA revealed that the total amount of NGF conjugated that came out from 20% PEG 3.4 kDa gels after 30 days did not reach 20 ng. To our awareness, close to 100 ng was the maximum amount of NGF observed from PEG 3.4 kDa out of 500 ng theoretically incorporated. However, that took place only after one week and no assumptions can be made on how much could have been released after a longer time. For example, protein closer to the edges of the disk diffuse faster than the growth factor at the center. An explanation for this is that once one NGF diffuses leaves a space that might be taken by an inner protein. Again, this new NGF might leave a vacancy that might or might not be occupied by another [99]. In other words, at the beginning, NGF diffuses fast and as time goes through, the protein release rate decreases. For this reason, 7 days might not have been enough opportunity for NGF to find its way out. Another possible explanation why a small amount of NGF was detected is that it was maybe lost when rinsing the hydrogels immediately after manufacture. Also, the neurotrophin might have been denatured and not detected by ELISA. This assay permits the detection of the protein by its conformation and if NGF suffered any changes in its folding there is a risk of not being recognized. This is what could have happened to the protein released from the sterilized gels.

Hydrogen peroxide gas was used for hydrogels´ sterilization after the freeze-dry process, risking the structure of NGF. Consistent with this, the amount of NGF detected from the sterilized disks did not reach 10 ng.

Conjugating the protein to 10% PEG 6 kDa hydrogels did not prevent from losing most of the protein quantified by day 1. Either physically embedded or chemically linked to PEG 6 kDa , NGF released accounted for more than 250 ng from these matrices, considerably more than hydrogels made of a lower molecular weight, 3.4 kDa regardless of the polymer concentration.

Two variants might have had an effect over this higher diffusion rate and quantity from 10% PEG 6 kDa gels: the increase in molecular weight of the polymer from 3.4 kDa to 6 kDa and its lower concentration, 10%. This represents less crosslinkable groups. Longer chains translate in less crosslinkable end groups and lower polymer concentration stands for a less number of acrylate end groups. This leads to fewer interconnections and bigger holes within the polymeric mesh due to big spaces through which small molecules diffuse. As a relatively small unit of 26 kDa NGF easily leaves its carrier, 10% PEG 6 kDa. In contrast, it was found that this neurotrophin hardly left meshes made out from 20 or 30 wt% PEG 3.4 kDa. As it is commonly known, diffusion is affected both by the size of the molecule being released and the size of the matrix´s network [106].

At the same time, the mesh dimensions are dictated by the hydrogel's precursor solution. PEG from a wide range of molecular weights has previously been studied for the controlled release of drugs [106, 108-110, 122,123]. In comparison to other studies on the effect of PEG concentration in hydrogels [9], results presented here confirm that varying the PEGda concentration affect the properties of the hydrogels yielding to different release profiles for NGF. Findings were that the higher the PEG's concentration, the lesser the amount and rate of NGF

that was diffused. Even though at first the emphasis was on controlling NGF release by conjugation reactions and thus chemically retaining it, results revealed that this objective could be accomplished by adjusting the polymer's concentration and mw. The NGF initial burst release was directly proportional to the molecular weight or PEGda.

The amount of acrylate groups present in the different PEGda molecules confirms the hypothetical explanation on the relationship between mesh composition and diffusion rate. From one molecule of PEGda mw 3.4 kDa, acrylates account for 0.042 parts of it. On the other hand, PEG mw 6 kDa exhibits that only 0.024 of the molecule composition is from acrylates. This resembles the fact that there are more reactive groups for crosslinking in the lower PEG molecular weight. The higher the molecular weight, the less ACRL groups. Regarding the solutions of varying molecular weights and PEG concentrations, Table 5.1 summarizes the approximate molar amounts of end groups per solution used, assuming 100% acrylation. Note that the solution of highest concentration and lowest mw (30% PEGda 3.4 kDa) has the highest molar concentration of acrylates.

**Table 5. 1. Acylate molar concentration in the solutions involved for hydrogels fabrication that were used to test NGF release**

| PEG mw (kDa) | Sol´n $\%_{PEG}$ | ACRL [M] |
|---|---|---|
| 6 | 10 | 0.033 |
| 3.4 | 20 | 0.147 |
| 3.4 | 30 | 0.253 |

NGF diffusion from PEG hydrogels of 3.4 kDa PEGda precursor solution was constant and took place smoothly. Other carriers such as microspheres [99] and microtubules [100] have shown to effectively reatin drugs, proteins and release them at a desirable rate. However, they

might jeopardize the conduit stucture by making it vulnerable to defects. Furthermore, the use of organic solvents for drug vehicles formation might trigger proteins by denaturing them, thus, compromising their bioacitivity [106]. A positive issue in this study is the fact that NGF was directly incorporated into the nerve conduit hydogel. Even though the amount of protein released was less than the expected, our objective was met. We were able to decrease the rate and amount of protein diffusion while retaining it longer within its matrix by linking the nerve growth factor to the polymer with covalent bonds. Moreover, we have shown that the NGF diffusion behavior can be controlled by changing the molecular weight and concentration of PEGda.

## 5.2 NGF Bioactivity

Many studies have been done to identify the range of NGF concentration in the body [124-127]. Concentration is an important aspect to take into consideration when proposing methods for this cue release. Even though NGF is the most widely known of the neurotrophins [69], little and non reliable information is found regarding NGF levels in healthy people or individuals with a pathology. Literature supports this conclusion by presenting huge discrepancies in the quantity of NGF found in serum [128] or plasma [129] among different research studies or within the same study [69]. Based on this, it is hard to predict the NGF amount to provide in a nerve scaffold for further release. Yet, a research group suggests that >5ng/mL is presumably the NGF amount provided by the body [30]. Our release profile demonstrates, overall, higher NGF levels released. Even though higher amounts of the protein were washed out from 10% PEG 6 kDa hydrogels than from 20 or 30 wt% PEG 3.4 kDa gels, bioactivity was conserved only by NGF diffused from PEG 3.4 kDa disks. It is assumed that this might be due primarily to the process of photocrosslinking. NGF could be denatured when

exposed to UV light and bioactivity might be affected by the time NGF spent in solution. Different systems were used to gelate PEGda 3.4 kDa and PEGda 6 kDa. The creation of the 6 kDa disks involved a different photoinitiator and exposure to UV radiation (λ=365nm) for a longer time (5 min) and a closer working distance than PEG 3.4 kDa curing conditions. Even though producing sterile PEG hydrogels is still a limitation, it was shown that the stereolithography technique is a viable method to create PEG hydrogels containing bioactive nerve growth factor.

## 5.3 PEGda Characterizarion

Characterization of materials is a very important step in every study. Knowing the materials can give an explanation of the outcome results where they were employed. For the molecular examination of PEGda, proton NMR ($^1$H NMR) spectroscopy was used. $^1$H NMR has ben widely used to incursion into the structural parameters of hydrogels [130, 131]. Specifically, poly(ethylene glycol) has been tested by $^1$H NMR to confirm the modifications done to the polymer such as inclusion of functional groups [132]. NMR characterization is usually accompained by another method of analysis such as gel permeation chromatography [133, 134]. Although, for the purpose of relating more in depth with the differences between the low and high mw of PEG proton NMR gave us enough information. However, more advantage can be taken from this instrument since it involves a simple technique and it is usually not time consuming if the researcher is well related with the spectrometer.

*Chapter 6*

## 6.0 Conclusion

It was shown that the stereolithography technique allows for multiple material parts fabrication. Localized regions of PEG hydrogels patterned with the material containing a cell adhesion signal or not having it were evidenced. Regarding protein release from PEG gels, a decreased growth factor diffusion rate was achieved when protein was covalently bonded to poly(ethylene glycol). It was also demonstrated that a higher release is obtained when NFG is only embedded into its matrix. The protein release rate was shown to be directly proportional to the molecular weight of the polymer and indirectly proportional to the concentration of PEG.

Poly(ethylene glycol) diacrylate is a suitable material to build hydrogel scaffolds for peripheral nerve regeneration. The inclusion of biologically active moieties was possible with the aid of a rapid prototyping technique, stereolithography. Moreover, the sustained release of nerve growth factor was achieved over a period of 30 days from poly(ethylene glycol) hydrogels of 3.4 kDa molecular weight.

## 6.1 Future Work

The next step to improve the present work and give continuity would be to explore methods to obtain sterile hydrogels with retained bioactivity. In addition, advantage of the layer by layer manufacture process of SL can be taken by building scaffolds with nerve growth factor (NGF) gradients, since it is known that axons grow in the direction of low to high NGF concentration [135]. Furthermore, PEG molecular weights and concentrations could be varied within the same hydrogel to control localized incorporation and release of chemical cues.

## 6.2 Recommendations

To improve accuracy, a repetitive pipette is recommended to dispense solutions. This should be taken into account specially when filling multi-well plates to reduce variance due to the human error. The use of a repetitive pipette is also a less time consuming process. Regarding the conjugation reaction, it is important to find a method to be able to report the % yield of the reactions done. However, one should take into consideration the amount of sample needed for testing and the quantity that is available both for analysis and experimentation. In addition, the same sample that is analyzed is the one that should be used for the investigation.

Technical Bulletin

# NGF $E_{max}$® ImmunoAssay System

INSTRUCTIONS FOR USE OF PRODUCTS G7630 AND G7631.



Promega

# NGF $E_{max}$® ImmunoAssay System

All technical literature is available on the Internet at: www.promega.com/tbs/
Please visit the web site to verify that you are using the most current version of this Technical Bulletin. Please contact Promega Technical Services if you have questions on use of this system. E-mail: techserv@promega.com.



## I. Description

The NGF (Nerve Growth Factor) $E_{max}$® ImmunoAssay System is designed for the sensitive and specific detection of NGF in an antibody sandwich format (1) (Figure 1). In this format, flat-bottom 96-well plates are coated with Anti-NGF Polyclonal Antibody (pAb), which binds soluble NGF. The captured NGF is bound by a second specific monoclonal antibody (mAb). After washing, the amount of specifically bound mAb is detected using a species-specific antibody conjugated to horseradish peroxidase (HRP) as a tertiary reactant. The unbound conjugate is removed by washing, and following incubation with a chromogenic substrate, the color change is measured. The amount of NGF in the test solutions is proportional to the color generated in the oxidation-reduction reaction. Using this system, NGF in tissue culture supernatants or tissue extracts can be quantitated in the range of 3.9–250pg/ml.

**Promega Corporation** · 2800 Woods Hollow Road · Madison, WI 53711-5399 USA
Toll Free in USA 800-356-9526 · Phone 608-274-4330 · Fax 608-277-2516 · **www.promega.com**
Printed in USA. Part# TB226
Revised 3/07

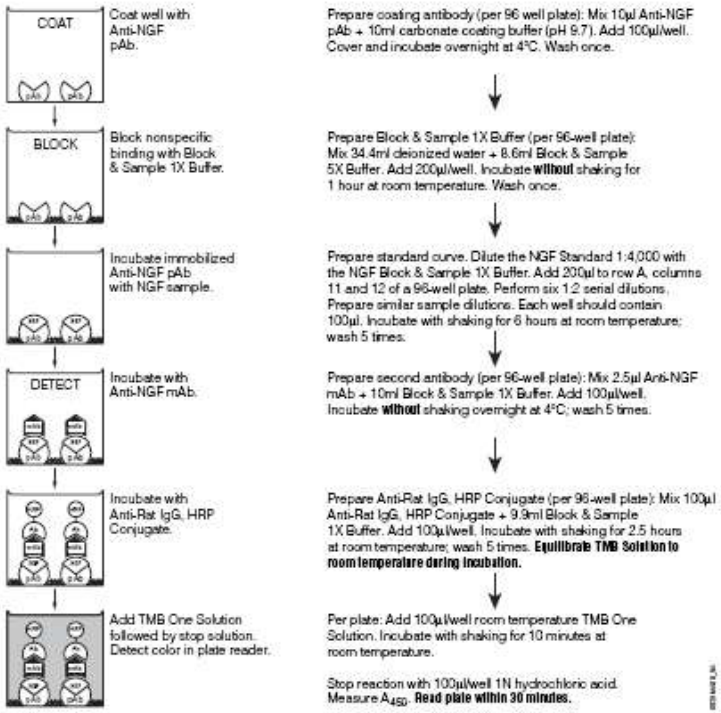


**Figure 1. Schematic representation of the NGF $E_{max}$® ImmunoAssay System.** For a detailed protocol, or when using this system for the first time, please read Sections III–VI carefully.

The NGF $E_{max}$® ImmunoAssay System offers several benefits:

- **Specificity:** Specific detection of NGF; typically less than 3% cross-reactivity with other neurotrophic factors at 10ng/ml.
- **Sensitivity:** Detects a minimum of 7.8pg/ml of NGF.
- **Flexibility:** Available in sizes for two or five 96-well ELISA plates; can configure plates as desired.
- **High Value:** Optimized reagents and protocol.







## II. Product Components and Storage Conditions

The NGF $E_{max}$® ImmunoAssay System is offered in two sizes, designed to accommodate two or five 96-well plates. Both systems contain the same reagents, except Cat.# G7631 contains more of each component.

| Product | Size | Cat.# |
|---|---|---|
| NGF $E_{max}$® ImmunoAssay System | 2 × 96 wells | G7630 |

Each system contains sufficient reagents for 160 sample determinations (plates not included) plus standard curves. Includes:

- 20µl Anti-NGF pAb
- 22ml Block and Sample 5X Buffer
- 20µl NGF Standard
- 10µg Anti-NGF mAb
- 200µl Anti-Rat IgG, HRP Conjugate
- 25ml TMB One Solution
- 1 Protocol

| Product | Size | Cat.# |
|---|---|---|
| NGF $E_{max}$® ImmunoAssay System | 5 × 96 wells | G7631 |

Each system contains sufficient reagents for 400 sample determinations (plates not included) plus standard curves. Includes:

- 50µl Anti-NGF pAb
- 54ml Block and Sample 5X Buffer
- 50µl NGF Standard
- 20µg Anti-NGF mAb
- 500µl Anti-Rat IgG, HRP Conjugate
- 2 × 25ml TMB One Solution
- 1 Protocol

**Storage Conditions:** When stored at –20°C in its original package, the product expires on the date listed on the product label. The product must not be used beyond this date. Once thawed and stored at 4°C, the product is stable for three months. Return each component to 4°C immediately after use. Avoid refreezing reagents. After dilution, use reagents the same day. Do not add any preservatives to these diluted solutions, as they may interfere with the assay.

## III. General Considerations

The NGF $E_{max}$® ImmunoAssay System has been tested using the following protocols. Plate coating requires an overnight incubation. Plates are blocked for one hour and samples are incubated for six hours the next day. Incubation with Anti-NGF mAb also is performed overnight. When transferring the NGF standard and the experimental samples to the plate, take care not to disturb or scratch the surface of the wells, as this may dislodge the coating antibodies and result in significant loss of signal. If unfamiliar with the technique, practice the pipetting procedures on a trial plate.

### Limitations of the Assay

- For research use only. Not for use in diagnostic procedures.
- Absorbance values beyond the range of the standard curve are not valid.
- For consistent results, dilute samples using the Block & Sample 1X Buffer.

## IV. Sample Preparation

The NGF $E_{max}$® ImmunoAssay System may be used to quantitate NGF in tissue culture supernatants or tissue extracts. The system uses an anti-rat IgG conjugate that may demonstrate cross-reactivity with samples containing mouse IgG or human IgG, resulting in increased absorbance readings. Avoid using samples containing high levels of IgG such as serum, plasma and spleen. Store experimental samples frozen at –20°C before use. Avoid multiple freeze-thaw cycles. Remove particulates from samples by centrifugation before use in the assay.

Avoid using samples containing high levels of IgG such as serum, plasma and spleen.

Acidification, and subsequent neutralization with base, has been shown to increase the amount of detectable NGF in extracts from a variety of tissues from several species (2–4). For NGF, the acidification may cause proteolysis of the 7S to the 2.5S form, the release of NGF from soluble receptors or both. Regardless, acid treatment can be performed in vitro, and it can increase the level of detectable factor. Increased NGF detection following acid treatment is a species- and tissue-specific phenomenon and can, in some instances, lead to a decrease in detection of NGF levels. Therefore, it is important to **test the acid treatment procedure for any given species and tissue to determine the benefit of pretreatment.**

**Note:** This assay is designed to measure free NGF. **To measure the amount of free mature NGF in your samples, proceed directly to the ELISA protocol in Section V.A without acid treatment.** To assay for total NGF, acid-treat and then neutralize the samples as described in the procedure below before proceeding with the ELISA protocol. **Do not attempt to acid-treat the NGF Standard.**





Promega

### Acid Treatment Procedure

This procedure acidifies samples diluted 1:5 in Dulbecco's PBS (DPBS) to approximately pH 2.6 and then neutralizes them to approximately pH 7.6. Depending on the amount of carrier protein in the samples, additional dilutions may or may not require the use of Block & Sample 1X Buffer to minimize loss of NGF.

For low protein matrices, we recommend direct acid treatment to a pH of 2.0–3.0 for 15–20 minutes. Following neutralization with NaOH, subsequent dilutions, if necessary, should be done with Block & Sample 1X Buffer before adding samples to the assay plate.

For all matrices, verify that the pH is 3.0 or lower using pH paper. In animal sera, the amount of 1N HCl required to lower the pH will vary depending upon the species. We suggest adding 110–125µl of 1N HCl per milliliter of undiluted serum or plasma and checking the pH before adding additional amounts of acid. Samples can be acid-treated in advance and stored at –20°C or –70°C.

**Materials to Be Supplied by the User**
(Solution compositions are provided in Section VIII.B.)

- DPBS
- 1N HCl, reagent grade
- 1N NaOH, reagent grade

**Caution:** HCl and NaOH are caustic. Avoid contact with skin or eyes.

1. Dilute the sample by adding 4 volumes of DPBS.
2. Add 1µl of 1N HCl for each 50µl of diluted sample. Verify that the pH is 3.0 or lower.
3. Mix and incubate for 15 minutes at room temperature.
4. Neutralize by adding 1µl of 1N NaOH per 50µl of sample. Check the pH to ensure that it is approximately 7.6.

Promega Corporation · 2800 Woods Hollow Road · Madison, WI 53711-5399 USA
Toll Free in USA 800-356-9526 · Phone 608-274-4330 · Fax 608-277-2516 · www.promega.com
Printed in USA. Part# TB226

## V. Protocol for NGF Quantitation

**Materials to Be Supplied by the User**
(Solution compositions are provided in Section VIII.B.)

- 96-well (flat bottom) ELISA plate
- carbonate coating buffer
- plate sealer
- TBST wash buffer
- 1N hydrochloric acid
- microplate reader capable of monitoring absorbance at 450nm
- pipettors capable of accurately delivering volumes of 1µl–1ml
- multichannel pipettor
- wash bottle or automated plate washer (DYNEX UltraWash Plus or equivalent)
- plate shaker (DYNEX Micro-Shaker® II or equivalent)
- 50ml (for better mixing) or 15ml polypropylene tubes for dilutions

**Note:** This assay has been tested using Nunc MaxiSorp™ plates (Nunc Cat.# 439454) and Microtiter®-Immunoassay Microplates (Immulon® 4; Thermo Labsystems Cat.# 3855). There are no observable differences in the performances of plates from these manufacturers. For best well-to-well accuracy, we recommend a high-quality, name-brand polystyrene ELISA plate.

### V.A. Plate Coating

1. In a 15ml or 50ml polypropylene tube, add exactly 10µl of the Anti-NGF pAb to 10ml of carbonate coating buffer to prepare enough reagent for each full 96-well plate. **Mix thoroughly**, but avoid creating excess bubbles. Use a multichannel pipettor to add 100µl to each well of a polystyrene ELISA plate.

   **Hint:** Keep the undiluted Anti-NGF pAb on ice when removed from 4°C storage.

2. Seal the wells with a plate sealer and incubate overnight at 4°C.

   **Note:** This assay has been optimized using the carbonate coating buffer prepared as described in Section VIII.B; other buffers may give poor results.





Promega

### V.B. Preparing Block & Sample 1X Buffer

Each 96-well plate requires approximately 43ml of Block & Sample 1X Buffer to be used on the second day. To prepare Block & Sample 1X Buffer, place 34.4ml of deionized water in a 50ml polypropylene tube. Aspirate 8.6ml of Block & Sample 5X Buffer with a sterile pipettor, being careful not to contaminate the stock solution, and add it to the water. Mix gently and completely by inversion prior to use.

### V.C. Blocking the Plate

1. Remove the coated plate from the refrigerator. Flick out the contents of the wells and slap the plate upside down three times on a paper towel to help clear the wells. Vigorously wash all wells with TBST wash buffer using an automated plate washer, wash bottle or multichannel pipettor. For manual washing, fill each well with TBST wash buffer, flick out the contents over a sink and slap the plate three times on a paper towel. Add 200µl of Block & Sample 1X Buffer to each well using a multichannel pipettor. Do not touch or scratch the surface of the wells where antibody is bound to the plate.

   **Note:** We strongly recommend the use of an automated plate washer for consistent results.

2. Incubate at room temperature for one hour **without** shaking.

**Promega Corporation** · 2800 Woods Hollow Road · Madison, WI 53711-5399 USA
Toll Free in USA 800-356-9526 · Phone 608-274-4330 · Fax 608-277-2516 · **www.promega.com**

### V.D. Preparing the NGF Standard Curve

The NGF Standard provided with this system will generate a linear standard curve from 3.9–250pg/ml. Use only values that are within the linear range to determine the NGF concentration of the test samples. The NGF Standard is supplied at a concentration of 1µg/ml. Accurately dilute the supplied NGF Standard 1:4,000 in Block & Sample 1X Buffer to achieve a concentration of 250pg/ml. For example, dilute 10µl of the NGF Standard into 790µl of Block & Sample 1X Buffer (1:80 dilution), then dilute 10µl of this into 490µl of the Block & Sample 1X Buffer for a final dilution of 1:4,000.

1. Following plate blocking, flick out the contents of the wells over a sink. Slap the plate three times upside down on a paper towel to remove residual liquid and wash once with TBST wash buffer as described in Section V.C, Step 1. Designate two columns of wells (16 wells) for the standard curve. To prepare the NGF standard curve within the assay plate, add 100µl/well of the Block & Sample 1X Buffer to wells in rows B through H in the two columns designated for the standard curve (Figure 2).
2. Add 200µl of the diluted NGF Standard (250pg/ml) to the first well in each column designated for the standard curve.
3. Immediately perform serial 1:2 dilutions (100µl/well) down the plate in the columns designated for the standard curve. In the last set of wells for the standard curve, do not add any NGF. The final concentrations (in duplicate) within the plate will be 0–250pg/ml (Figure 2).

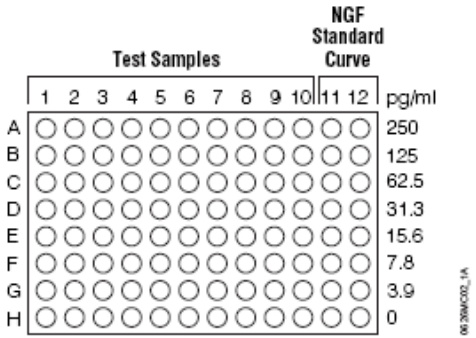


**Figure 2. Recommended ELISA plate format for standard curve and test samples.**







### V.E. Addition of Sample

We recommend starting with a 1:4 dilution of each test sample and preparing 1:2 serial dilutions per column in the ELISA plate. Alternatively, screen samples at a single concentration and subsequently reassay all positive samples not on the linear portion of the curve to determine the exact NGF concentration.

Where the sample carrier solution may contribute nonspecific sources of NGF (such as serum in culture media), we also recommend performing a series of negative control reactions containing the carrier solution alone.

1. After preparing the NGF Standard curve, add 100µl of the samples (acid-treated or untreated; whichever is appropriate for your system) to each of the remaining wells. (See Section IV for the acid treatment of samples.)

**Note:** Add samples as quickly as possible to minimize evaporation.

2. Seal the wells with a 96-well plate sealer and incubate the plate for six hours at room temperature with shaking (500 ± 100rpm).

   **Note:** Best results are obtained using a plate shaker. Alternatively, plates may be incubated at 37°C without shaking, although a slight loss in sensitivity of the assay may occur.
   **Do not** stack plates when incubating at 37°C.

3. Wash all wells five times with TBST wash buffer as in Section V.C, Step 1.

### V.F. Addition of Anti-NGF mAb

1. In a 15ml or 50ml polypropylene tube, add 2.5µl of the Anti-NGF mAb to 10ml of Block & Sample 1X Buffer (1:4,000 dilution) to prepare enough reagent for a full 96-well plate. **Mix thoroughly**, but avoid creating excess bubbles. Use a multichannel pipettor to add 100µl of the diluted Anti-NGF mAb to each well, being careful not to touch or scratch the bottom or sides of the wells.
2. Seal the wells with a plate sealer and incubate overnight at 4°C **without** shaking.
3. The next day, wash all wells five times with TBST wash buffer as described in Section V.C, Step 1.

### V.G. Addition of Anti-Rat IgG, HRP Conjugate

1. Prepare a fresh 10ml working solution of Block & Sample 1X Buffer by combining 8ml of deionized water and 2ml of Block & Sample 5X Buffer in a 15ml polypropylene tube. Again, use care not to contaminate the stock solution. Mix gently and completely by inversion prior to use.

   **Hint:** Keep the Anti-NGF mAb and Anti-Rat IgG, HRP Conjugate on ice when removed from 4°C storage.

2. In a 15ml or 50ml polypropylene tube, accurately add 100µl of the stock Anti-Rat IgG, HRP Conjugate to 9.9ml of Block & Sample 1X Buffer (1:100 dilution) to prepare enough reagent for a full 96-well plate. **Mix thoroughly** and avoid creating excess bubbles. Using a multichannel pipettor, add 100µl of the diluted Antibody Conjugate to each well, being careful not to disturb the bottom or sides of the wells.

3. Incubate for 2.5 hours at room temperature with shaking (500 ± 100rpm).

   **Note:** Best results are obtained using a plate shaker. Alternatively, plates may be incubated without shaking, although a slight loss in sensitivity of the assay may occur.

   **Hint:** During this incubation, equilibrate the TMB One Solution to room temperature.

4. Wash all wells five times with TBST wash buffer as described in Section V.C, Step 1.

### V.H. Color Development

1. Add 100µl of the room temperature TMB One Solution to each well using a multichannel pipet.

2. Incubate at room temperature with shaking for 10 minutes.

3. Stop the reaction by adding 100µl of 1N hydrochloric acid to the wells in the same order in which TMB One Solution was added in Step 1 above. Blue will change to yellow upon acidification. Take care to avoid creating bubbles.

   **Caution:** Take care to avoid contact of the TMB One Solution and 1N hydrochloric acid with skin and eyes.

4. Record the absorbance at 450nm on a plate reader within 30 minutes of stopping the reaction. See Figure 3 for a representative NGF standard curve.

   **Note:** The exterior bottom of the plate must be optically clean for accurate measurement. Wipe the exterior bottom with 70% ethanol if necessary.







### V.I. Representative Standard Curve

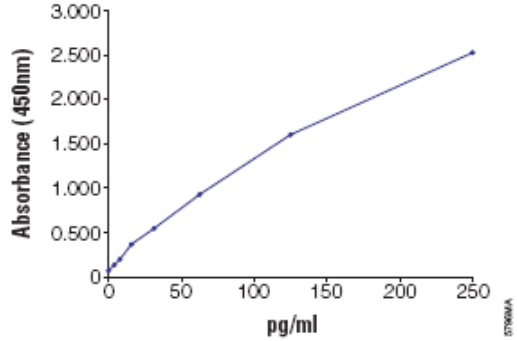


**Figure 3. Representative NGF standard curve obtained using the NGF $E_{max}^{®}$ ImmunoAssay System.**

## VI. Troubleshooting

For questions not addressed here, please contact your local Promega Branch Office or Distributor. Contact information available at: **www.promega.com**. E-mail: **techserv@promega.com**

| Symptoms | Causes and Comments |
|---|---|
| Sample absorbance is above range of standard curve | Sample too concentrated:<br>• Further dilute the sample.<br>• Assay multiple dilutions of each sample to ensure that at least one point will fall in the useful range of the standard curve. |
| Sample absorbance is below range of standard curve | Sample too dilute. Re-assay at a higher sample concentration. |
| High absorbance in all samples | NGF present in buffer or media. Perform negative control reactions containing carrier solution but no sample whenever NGF may be present in buffer or media. |
| | Color reaction too long. If absorbance exceeds dynamic range of plate reader, repeat assay with a shorter color development time, or use a plate reader with a greater dynamic range. |
| | Mouse, human or rat samples containing high levels of IgG were used. Avoid using samples containing high levels of IgG such as serum, plasma and spleen. See Section IV for more details. |

## VI. Troubleshooting (continued)

| Symptoms | Causes and Comments |
|---|---|
| Low absorbance in all samples | Color reaction too slow:<br>• Increase duration of color development reaction.<br>• Recheck the dilutions of each component of the assay. |
| Variability in replicate samples | Technique problems in performing the assay:<br>• Ensure that all wells are washed completely.<br>• Allow plate to warm to room temperature for 10–15 minutes before starting blocking procedure.<br>• Add stop solution to wells in the same order as TMB One Solution.<br>• Change pipette tips before adding each reagent.<br>• Perform additional replicates.<br>• Check calibration of the pipettor. |
| Low activity in NGF Standard | Improper storage. The standard is stable, if stored undiluted, for six months at –20°C and three months at 4°C. |

## VII. References


1. Hornbeck, P. (1994) In: *Current Protocols in Immunology*, Vol. 1, Coico, R. ed., John Wiley & Sons, Inc. Unit 2.1.
2. Zettler, C. *et al.* (1996) Detection of increased tissue concentrations of nerve growth factor with an improved extraction procedure. *J. Neurosci. Res.* **46**, 581–94.
3. *Acid Treatment of NGF Samples* (1996) *Neural Notes* **II**(3), 23.
4. Okragly, A.J. and Haak-Frendscho, M. (1997) An acid-treatment method for the enhanced detection of GDNF in biological samples. *Exp. Neurol.* **145**, 592–6.






Promega

## VIII. Appendix

### VIII.A. Performance Characteristics of the NGF $E_{max}$® ImmunoAssay System

#### Cross-Reactivity of the NGF $E_{max}$® ImmunoAssay System

The NGF $E_{max}$® ImmunoAssay System demonstrates very low cross-reactivity with structurally related growth factors Human Recombinant Brain Derived Neurotrophic Factor (rhBDNF), Neurotrophin-3 (rhNT-3) and Neurotrophin-4 (rhNT-4) at concentrations as high as 10ng/ml, as shown below.

| Neurotrophic Factor | Actual Concentration (ng/ml) | % Cross-Reactivity |
|---|---|---|
| BDNF | 10 | <0.078 |
| NT-3 | 10 | <0.078 |
| NT-4 | 10 | <0.078 |

To evaluate the specificity of this assay system, 10ng/ml of rhBDNF (Cat.# G1491), NT-3 (Cat.# G1501) and rhNT-4 were tested for binding using the protocols as described in Sections III–V. Results are expressed as the mean of triplicate determinations.

#### Intra-Assay Comparison

Acid-treated samples were diluted in Block & Sample 1X Buffer and assayed by one operator for a total of eight determinations each.

| | NGF | |
|---|---|---|
| | Sample 1 | Sample 2 |
| N | 8 | 8 |
| Mean (pg/ml) | 194 | 404 |
| SD (pg/ml) | 8 | 17 |
| CV (%) | 4.1 | 4.2 |

N=sample size, SD=standard deviation, CV=coefficient of variance

Promega Corporation · 2800 Woods Hollow Road · Madison, WI 53711-5399 USA
Toll Free in USA 800-356-9526 · Phone 608-274-4330 · Fax 608-277-2516 · www.promega.com

## VIII.B. Composition of Buffers and Solutions

### 1N hydrochloric acid

Add 82.7ml of concentrated hydrochloric acid to 917.3ml deionized water.

### carbonate coating buffer

| | |
|---|---|
| 0.025M | sodium bicarbonate |
| 0.025M | sodium carbonate |

Adjust pH to 9.7 using 1N HCl or 1N NaOH.

### lysis buffer

| | |
|---|---|
| 137mM | NaCl |
| 20mM | Tris HCl (pH 8.0) |
| 1% | NP40 |
| 10% | glycerol |
| 1mM | PMSF |
| 10µg/ml | aprotinin |
| 1µg/ml | leupeptin |
| 0.5mM | sodium vanadate |

### DPBS (per liter)

| | |
|---|---|
| 0.2g | KCl |
| 8.0g | NaCl |
| 0.2g | $KH_2PO_4$ |
| 1.15g | $Na_2HPO_4$ |
| 133mg | $CaCl_2 \cdot 2H_2O$ |
| 100mg | $MgCl_2 \cdot 6H_2O$ |

Add room temperature deionized water to a final volume of 1 liter to the KCl, NaCl, $KH_2PO_4$ and $Na_2HPO_4$. Adjust pH to 7.35 using 1N HCl or 1N NaOH, if necessary. Add the $MgCl_2 \cdot 6H_2O$, mix thoroughly, then add the $CaCl_2 \cdot 2H_2O$, and mix thoroughly.

### TBST wash buffer

| | |
|---|---|
| 20mM | Tris-HCl (pH 7.6) |
| 150mM | NaCl |
| 0.05% (v/v) | Tween® 20 |

## VIII.C. Related Products

### $E_{max}$® ImmunoAssay Systems

| Product | Size | Cat.# |
|---|---|---|
| NT-3 $E_{max}$® ImmunoAssay Systems | 2 × 96 wells | G7640 |
| | 5 × 96 wells | G7641 |
| GDNF $E_{max}$® ImmunoAssay Systems | 2 × 96 wells | G7620 |
| | 5 × 96 wells | G7621 |
| BDNF $E_{max}$® ImmunoAssay Systems | 2 × 96 wells | G7610 |
| | 5 × 96 wells | G7611 |
| $TGF\beta_1$ $E_{max}$® ImmunoAssay Systems | 2 × 96 wells | G7590 |
| | 5 × 96 wells | G7591 |
| $TGF\beta_2$ $E_{max}$® ImmunoAssay System | 5 × 96 wells | G7600 |







## VIII.C. Related Products (continued)

### Items Available Separately

| Product | Size | Cat.# |
|---|---|---|
| TMB One Solution* | 100ml | G7431 |
| Block & Sample 5X Buffer* | 54ml | G3311 |
| mNGF, 2.5S | 100µg | G5141 |
| | 10µg | G5142 |
| mNGF, 7S | 100µg | G5151 |
| Anti-NGF mAb | 100µg | G1131 |
| | 20µg | G1132 |
| Anti-Human NT-3 pAb | 200µg | G1651 |
| rhNT-3 | 5µg | G1501 |
| Anti-Human BDNF pAb | 200µg | G1641 |
| rhBDNF | 5µg | G1491 |
| Anti-Rat CNTF pAb | 200µg | G1631 |
| Anti-Pan Trk pAb | 200µg | G1581 |
| Anti-TrkB In pAb | 100µg | G1561 |
| Anti-Human p75 pAb | 200µg | G3231 |
| rhGDNF | 5µg | G2781 |
| Anti-Human GDNF pAb | 200µg | G2791 |
| Anti-βIII Tubulin mAb | 100µg | G7121 |
| Anti-GFAP pAb | 100µg | G5601 |

*For Laboratory Use.

### Primer Pairs and Amplification Reagents

| Product | Size | Cat.# |
|---|---|---|
| β-Actin Primer Pair | 20 reactions | G5740 |
| CNTF Primer Pair | 20 reactions | G5770 |
| TrkB Primer Pair | 20 reactions | G5790 |
| NT-3 Primer Pair | 20 reactions | G6801 |
| p75 Primer Pair | 20 reactions | G6861 |
| Access RT-PCR System* | 20 reactions | A1260 |
| AccessQuick™ RT-PCR System* | 20 reactions | A1701 |

*For Laboratory Use.

Promega



**Promega Corporation** · 2800 Woods Hollow Road · Madison, WI 53711-5399 USA
Toll Free in USA 800-356-9526 · Phone 608-274-4330 · Fax 608-277-2516 · **www.promega.com**

Part# TB226
Page 16

Printed in USA.
Revised 3/07

*Appendix 2*

Conjugated NGF Cumulative Release from 20 wt% PEG 3.4 kDa (units are ng if not specified)

| Time (days) | Disk1 | Disk2 | Disk3 | Disk4 | Disk5 | Disk6 | Average | stdev | sterr |
|---|---|---|---|---|---|---|---|---|---|
| **0.17** | 8.184 | 6.223 | 5.809 | 6.576 | 7.764 | 7.478 | **7.006** | 0.940 | 0.384 |
| **0.33** | 10.350 | 8.618 | 8.270 | 9.226 | 10.073 | 9.913 | **9.408** | 0.841 | 0.343 |
| **0.50** | 12.067 | 10.170 | 9.770 | 10.632 | 11.502 | 11.098 | **10.873** | 0.853 | 0.348 |
| **1** | 14.694 | 12.620 | 12.146 | 12.875 | 13.893 | | **13.246** | 1.031 | 0.461 |
| **2** | 16.658 | 14.760 | 14.215 | 14.532 | 15.657 | | **15.164** | 0.992 | 0.444 |
| **5** | 18.485 | 16.747 | 16.688 | 16.100 | 17.587 | | **17.121** | 0.928 | 0.415 |
| **10** | 19.684 | 17.915 | 18.313 | 17.552 | 19.222 | | **18.537** | 0.893 | 0.400 |
| **15** | 20.357 | 18.483 | 19.028 | 18.118 | 19.769 | | **19.151** | 0.917 | 0.410 |
| **20** | 20.773 | 18.882 | 19.472 | 18.645 | 20.095 | | **19.574** | 0.875 | 0.391 |
| **30** | 20.873 | 19.000 | 19.607 | 18.763 | 20.206 | | **19.689** | 0.867 | 0.388 |

Encapsulated NGF Cumulative Release from 20 wt% PEG 3.4 kDa (units are ng if not specified)

| Time (days) | Disk1 | Disk2 | Disk3 | Disk4 | Disk5 | Average | stdev | sterr |
|---|---|---|---|---|---|---|---|---|
| **0.08** | 51.935 | 36.486 | 38.394 | 45.570 | 50.052 | **44.487** | 6.869 | 3.072 |
| **0.17** | 58.692 | 42.814 | 45.579 | 50.085 | 54.687 | **50.371** | 6.481 | 2.898 |
| **0.33** | 67.260 | 53.337 | 56.532 | 59.154 | 66.188 | **60.494** | 6.060 | 2.710 |
| **0.50** | 71.895 | 57.090 | 61.524 | 62.573 | 69.416 | **64.500** | 6.048 | 2.705 |
| **1** | 82.442 | 66.230 | 73.883 | 70.117 | 77.984 | **74.131** | 6.374 | 2.851 |
| **2** | 90.915 | 73.011 | 82.404 | 79.877 | 88.627 | **82.967** | 7.145 | 3.195 |
| **7** | 99.150 | 84.321 | 93.452 | 83.963 | 104.395 | **93.056** | 9.012 | 4.030 |

Encapsulated NGF Cumulative Release from 20 wt% PEG 3.4 kDa
Freeze-dried Sterilized Hydrogels (units are ng if not specified)

| Time (days) | Disk1 | Disk2 | Disk3 | Disk4 | Disk5 | Disk6 | Average | stdev | sterr |
|---|---|---|---|---|---|---|---|---|---|
| **0.08** | 3.099 | 3.516 | 2.897 | 3.796 | 2.873 | 2.921 | **3.184** | 0.385 | 0.157 |
| **0.17** | 3.913 | 4.288 | 3.520 | 4.609 | 3.663 | 3.532 | **3.921** | 0.444 | 0.181 |
| **0.33** | 4.601 | 4.935 | 4.375 | 5.345 | 4.149 | 4.054 | **4.576** | 0.493 | 0.201 |
| **0.50** | 4.962 | 5.355 | 4.843 | 5.903 | 4.361 | 4.337 | **4.960** | 0.601 | 0.245 |
| **1** | 5.698 | 5.925 | 5.454 | 6.520 | 5.258 | 5.091 | **5.658** | 0.517 | 0.211 |
| **2** | 6.862 | 6.981 | 6.446 | 7.646 | 5.970 | 5.907 | **6.635** | 0.663 | 0.271 |
| **7** | 7.416 | 7.413 | 6.990 | 8.204 | 6.298 | 6.351 | **7.112** | 0.725 | 0.296 |

Encapsulated NGF Cumulative Release from 30 wt% PEG 3.4 kDa (units are ng if not specified)

| Time (days) | Disk1 | Disk2 | Disk3 | Disk4 | Disk5 | Average | stdev | sterr |
|---|---|---|---|---|---|---|---|---|
| **0.08** | 32.542 | 24.926 | 26.542 | 20.772 | 21.695 | **25.295** | 4.680 | 2.093 |
| **0.17** | 35.012 | 27.289 | 28.874 | 22.628 | 23.997 | **27.560** | 4.857 | 2.172 |
| **0.33** | 37.468 | 29.868 | 31.098 | 24.437 | 25.929 | **29.760** | 5.104 | 2.283 |
| **0.50** | 39.738 | 32.323 | 33.262 | 26.308 | 28.154 | **31.957** | 5.215 | 2.332 |
| **1** | 42.763 | 35.363 | 36.978 | 30.255 | 31.686 | **35.409** | 4.924 | 2.202 |
| **2** | 46.834 | 39.111 | 40.265 | 33.818 | 35.295 | **39.065** | 5.088 | 2.275 |
| **5** | 50.782 | 44.120 | 45.858 | 39.274 | 40.197 | **44.046** | 4.643 | 2.077 |
| **7** | 52.329 | 46.206 | 47.929 | 41.714 | 42.345 | **46.105** | 4.345 | 1.943 |

Encapsulated NGF Cumulative Release from 10%(w/v) PEG 6kDa (units are ng if not specified)

| Time (days) | Disk1 | Disk2 | Disk3 | Disk4 | Average | stdev | sterr |
|---|---|---|---|---|---|---|---|
| **0.08** | 139.272 | 153.192 | 149.832 | 145.032 | **146.832** | 6.051 | 3.025 |
| **0.17** | 190.2 | 204.12 | 192.12 | 196.44 | **195.72** | 6.178 | 3.089 |
| **0.33** | 230.568 | 248.648 | 245.288 | 242.888 | **241.848** | 7.882 | 3.941 |
| **0.50** | 249.176 | 269.816 | 273.496 | 265.176 | **264.416** | 10.715 | 5.358 |
| **1** | 264.104 | 285.416 | 290.664 | 284.744 | **281.232** | 11.721 | 5.861 |
| **2** | 269.752 | 291.224 | 295.992 | 296.312 | **288.32** | 12.595 | 6.298 |
| **5** | 272.397 | 293.805 | 298.973 | 300.093 | **291.3168** | 12.907 | 6.454 |
| **7** | 273.218 | 294.706 | 300.066 | 301.202 | **292.2976** | 13.032 | 6.516 |
| **10** | 273.99 | 295.542 | 300.982 | 302.038 | **293.1384** | 13.079 | 6.539 |

Conjugated NGF Cumulative Release from 10%(w/v) PEG 6kDa (units are ng if not specified)

| Time (days) | Disk1 | Disk2 | Disk3 | Disk4 | Disk5 | Average | stdev | sterr |
|---|---|---|---|---|---|---|---|---|
| **0.08** | 120.078 | 104.525 | 99.047 | 87.569 | 69.830 | **96.210** | 18.825 | 8.419 |
| **0.17** | 157.245 | 149.947 | 126.296 | 115.392 | 79.672 | **125.710** | 30.855 | 13.799 |
| **0.33** | 197.807 | 184.382 | 159.636 | 142.296 | 105.811 | **157.986** | 36.241 | 16.207 |
| **0.50** | 223.559 | 208.694 | 179.868 | 182.688 | 127.139 | **184.390** | 36.830 | 16.471 |
| **1** | 274.967 | 254.502 | 210.796 | 236.656 | 159.187 | **227.222** | 44.753 | 20.014 |
| **2** | 288.935 | 272.630 | 223.004 | 253.184 | 172.835 | **242.118** | 45.855 | 20.507 |
| **5** | 297.244 | 279.978 | 229.088 | 261.349 | 179.736 | **249.479** | 46.455 | 20.776 |
| **7** | 299.408 | 282.143 | 230.837 | 263.850 | 181.357 | **251.519** | 46.727 | 20.897 |
| **10** | 301.397 | 283.924 | 232.234 | 265.935 | 182.642 | **253.226** | 47.030 | 21.032 |
| **15** | 302.634 | 285.337 | 233.471 | 267.716 | 183.894 | **254.610** | 47.090 | 21.059 |

*Appendix 3*

PC-12 exposed to hydrogels´ supernatants containing the released NGF. Scale bar = 100µm.

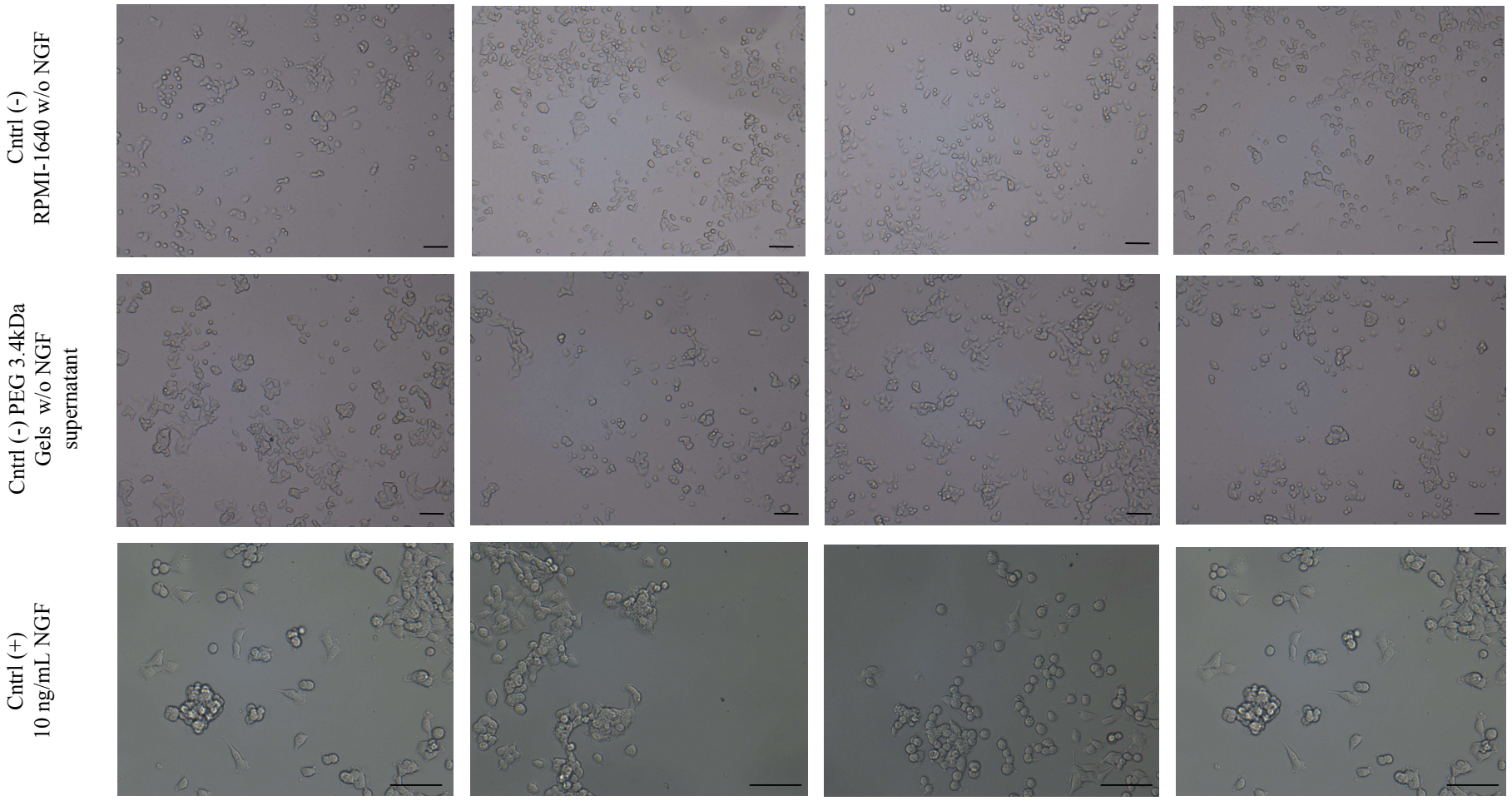

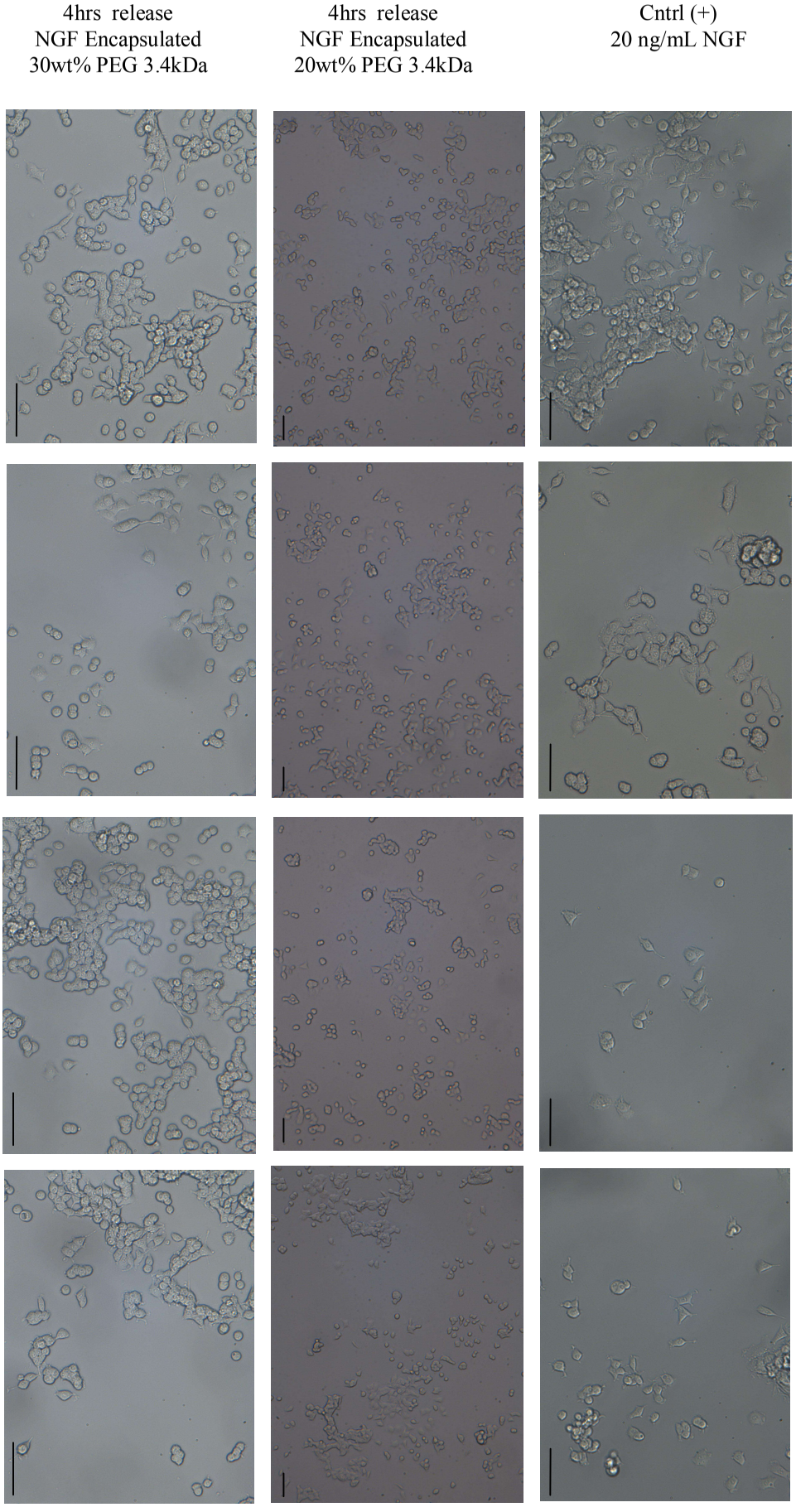
4hrs release
NGF Encapsulated
30wt% PEG 3.4kDa
4hrs release
NGF Encapsulated
20wt% PEG 3.4kDa
Cntrl (+)
20 ng/mL NGF

*Appendix 4*

**PEG : NGF Calculations**

*Encapsulated NGF*

**PEGda 3.4 kDa**
Considering the dimensional swelling factor (DSF), original file dimensions d=4mm
Each disk has to contain 500ng NGF to release.

First, calculate the amount of solution required to create one disk.
(dimensions before swelling r = 2mm, h = 1mm):

$V = \pi r^2 h$
$V = \pi(2mm)^2(1mm)$
$V = \frac{12.57mm^3}{} \left| \frac{1cm^3}{10^3\ mm^3} \right| \frac{1mL}{1cm^3} = 0.01257\ mL$
This means, each disk is made with 0.01257mL of solution

Second, calculate the number of disks that 1mL of solution can make:
Theoretically, each mL can make up to: 1mL/0.01257mL = 79.58 disks.

Third, calculate the amount of NGF required for 1mL of solution to contain 500 ng NGF per each 0.01257 mL (500ng NGF per disk):
500ng x 79.58 = 39,790ng ~ 40,000 ng
This means, **40,000 ng NGF** are required **in each mL of a 20% PEG sol'n**

- NGF was dissolved in RPMI-1640 media 100μg in 100 μL = [1,000,000 ng/mL]
- 20 wt% PEGda 3.4 kDa sol'n was prepared in PBS (pH=7.4) and 0.5% I-2959

$C_1V_1 = C_2V_2$

| | |
|---|---|
| $C_1 = 1{,}000{,}000$ ng/mL | Conc. of the NGF aliquot |
| $C_2 = 40{,}000$ ng/mL | Desired final conc. |
| $V_2 = 1$mL | Final volume |
| $V_1 = ?$ | mL of NGF sol'n required |

$V_1 = \frac{(40{,}000\ ng/mL)\ (1mL)}{1{,}000{,}000\ ng/mL} = 0.04\ mL \left| \frac{1\mu L}{1 \times 10^{-3}\ mL} \right. = \mathbf{40\ \mu L}$

- Therefore, every 40μL contains 40,000ng of NGF
- 40μL of NGF sol'n were added to 1mL of a 20 % photocrosslinkable PEG sol'n.
- Disks were built immediately. Hydrogells swell to final dimensions of 5mm in diameter, containing 500 ng to release.

*Encapsulated NGF*

**PEGda 6 kDa**

Dimensional swelling factor not considered. From a cured PEG layer, disks are stamped out with dimensions of: d = 5 mm h = 1mm, each disk containing 500ng NGF to release:

Volume of a hydrogel disk:

$V = \pi r^2 h$
$V = \pi(2.5mm)^2(1mm)$
$V = 19.63495\ mm^3 \sim 20\ mm^3$

$$V = \frac{19.64mm^3}{} \left| \frac{1cm^3}{10^3\ mm^3} \right| \frac{1mL}{1cm^3} = 0.01964\ mL = 19.64\mu L$$

There has to be 500ng per each 19.64 μL of solution (500ng NGF per disk):

Theoretically, each mL can make up to: 1.0 mL/0.01964 mL = 51 disks.
500ng x 51 = **25.47 ng** = 25.47 μL NGF sol'n.

- 100μg NGF dissolved in 100 μL RPMI-1640 + 1% BSA [1,000,000 ng/mL]
- ~ 25.47 μL NGF sol'n per mL of a 6kDa PEGda sol'n
- 10% (w/v) PEGda 6kDa sol'n was prepared in PBS (pH=7.4) and DMPA/NVP

$$C_1V_1 = C_2V_2$$

| | |
|---|---|
| $C_1 = 1{,}000{,}000$ ng/mL | Conc. of the NGF aliquot |
| $C_2 = 25{,}465$ng/mL | Desired final conc. |
| $V_2 = 1.0$ mL | Final volume |
| $V_1 = ?$ | mL of NGF sol'n required |

$$V_1 = \frac{(25{,}465\ ng/mL)\ (1.0\ mL)}{1{,}000{,}000\ ng/mL} = 0.02546\ mL \left| \frac{1\mu L}{1 \times 10^{-3}\ mL} \right. = \mathbf{25.47\ \mu L}$$

- Therefore, every 25.47 μL contains 25,465 ng of NGF
- 25.5 μL of NGF sol'n added to 1.0 mL of a 10 % photocrosslinkable PEG sol'n.

Crosslinking a 10% 6kDa PEGda layer of 1mm thick, volume required?
Container d = 20.4mm

$V = \pi\ r^2\ h$
$V = \pi\ (10.2mm)^2\ (1mm)$
$V = 326.85mm^3$

$$V = \frac{326.85mm^3}{} \left| \frac{1\ cm^3}{10^3\ mm^3} \right| \frac{1mL}{1cm^3} = 0.326.85\ mL = \mathbf{326.85\ \mu L}$$

*Conjugated NGF* (as determined 1:5 NGF to PEG ratio)

**PEGda 3.4 kDa**

1 mol PEG = 3400 Da  Dalton = g/mol
1 mol NGF = 26000 Da

Starting with the same 500ng NGF per 0.01257 mL PEG sol'n
Having to add the equal amount of 40,000 ng per mL of PEG sol'n

Taking 40,000ng NGF as the unit ratio

1 NGF : 5 PEG
40,000 ng NGF = 1

$$\frac{40{,}000\ \text{ng}}{} \left| \frac{1\text{g}}{1\text{x}10^{9}\text{ng}} \right| \frac{1\ \text{mol}}{26{,}000\ \text{g}} = 1.54 \times 10^{-9}\text{mol}$$

$(1.54 \times 10^{-9}\text{mol})\ (5) = 7.69 \times 10^{-9}$ mol PEG

$$\frac{7.69 \times 10^{-9}\ \text{mol PEG}}{} \left| \frac{3400\text{g}}{1\ \text{mol}} \right. = 2.62 \times 10^{-5}\ \text{g PEG}$$

**40,000 ng NGF : $2.62 \times 10^{-5}$ g PEG**

A stock solution of PEGda was prepared as follows:

0.004 4g PEG in 2 mL of PBS buffer previously prepared (pH = 8.55)
= [0.0022 g/mL] of PEG in PBS
The solution was syringe filtered.

$$C_1V_1 = C_2V_2$$

$$V_1 = \frac{(2.62 \times 10^{-5}\ \text{g/mL})\ (1\text{mL})}{0.0022\ \text{g/mL}} = 0.0119\text{mL}$$

$V_1 = 12\ \mu\text{L}$

An aliquot of 40μL of NGF (containing 40,000 ng of the protein) was thawed.
12 μL of the PEG were added to the NGF aliquot.

In addition, ~ 2mL of PBS (pH = 8.5) were also filtered and 48 μL of this buffer were added to the PEG-NGF to have a final vol of 100μL and control over the pH to be basic, since NGF was diluted in RPMI-1640 with a pH of 7.4.

The reaction was allowed to take place inside a 2mL siliconized vial covered with aluminum foil incubated at room temperature for two hours.

*Conjugated NGF* (as determined 1:5 NGF to PEG ratio)

**PEG 6 kDa**

1 mol PEG = 6000 Da  Dalton = g/mol
1 mol NGF = 26000 Da

Starting with the same 500ng NGF per 0.01964 mL PEG sol'n
Having to add the equal amount of 25,465 ng per 1.0 mL of PEG sol'n

Taking 25,465 ng NGF as the unit ratio

1 NGF : 5 PEG
1 NGF = 25,465 ng

$$\frac{25{,}465 \text{ ng}}{1 \times 10^{9} \text{ ng}} \left| \frac{1 \text{ g}}{26{,}000 \text{ g}} \right| \frac{1 \text{ mol}}{} = 9.79 \times 10^{-10} \text{ mol NGF}$$

$(9.79 \times 10^{-10} \text{mol})\ (5) = 4.897 \times 10^{-9}$ mol PEG

$$\frac{4.897 \times 10^{-9} \text{ mol PEG}}{} \left| \frac{6000 \text{g}}{1 \text{ mol}} \right. = 2.94 \times 10^{-5} \text{ g PEG}$$

**25,465 ng NGF : $2.94 \times 10^{-5}$ g PEG**

A stock solution of PEGda 6kDa was prepared as follows:

0.001g PEG in 2.0 mL of PBS (pH = 7.43)
= [0.0005 g/mL] of PEG in PBS
The PEG in PBS solution was syringe filtered.

$$C_1V_1 = C_2V_2$$

$C_1 = 0.0005$ g/mL
$C_2 = 2.94 \times 10^{-5}$ g/mL
$V_2 = 1$ mL

$$V_1 = \frac{(2.94 \times 10^{-5} \text{ g/mL})\ (1\text{mL})}{0.0005 \text{ g/mL}} = 0.0588 \text{ mL}$$

$V_1 = 58.8$ µL

- 25.5 µL NGF sol'n mixed with 58.8 µL PEG stock sol'n
- 15.7 µL added of a syringe filtered PBS buffer (pH = 7.4)
- Allow to react inside a 2mL siliconized vial covered with aluminum foil at RT for 2 hrs

*References*


[1] Huang Y-C, Huang Y-Y. Biomaterials and Strategies for Nerve Regeneration Artif Organs 2006;30:514-22.

[2] Vacanti CA. History of tissue engineering and a glimpse into its future. Tissue Eng 2006;12:1137-42.

[3] Huang Y-C, Huang Y-Y. Tissue Engineering for Nerve Repair. Biomed Eng Appl Basis Comm 2006;18:100-10.

[4] Raivich G, Kreutzberg GW. Nerve growth factor and regeneration of peripheral nervous system. Clinical Neurology and Neurosurgery 1993;95:S84-S88.

[5] Ide C. Peripheral nerve regeneration. Neuroscience Research 1996;25:101-21.

[6] Ignatiadis IA, Tsiampa VA, Yiannakopoulus CK, Xeinis SF, Papalois AE, Xenakis TH, Beirs AE, Soucacos PN. A new technique of autogenous conduits for bridging short nerve defects. An experimental study in the rabbit. Acta Neurochir Suppl. 2007;100:73-76.

[7] Hudson T.W., Evans G.R., Schmidt C.E. Engineering strategies for peripheral nerve repair. Clin Plast Surg. (1999) 26:617-628.

[8] Piotrowicz A, Shoichet MS. Nerve guidance conduits as drug delivery vehicles. Biomaterials 2006;27:2018-27.

[9] Gunn JW, Turner SD, Mann BK. Adhesive and mechanical properties of hydrogels influence neurite extension. J Biomed Mater Res 2005;72:91-7.

[10] Liu VA, Bathia SN. Three dimensional photopatterning of hydrogels containing living cells. Biomedical microdevices 2002;4:257-266.

[11] Yang S, Leong KF, Du Z, Chua CK. The design of scaffolds for use in tissue engineering. Part II. Rapid prototyping techniques. Tissue Engineering 2002;8:1-11.

[12] Lysaght MJ, Reyes J. The Growth of Tissue Engineering. Tissue Engineering 2001;7:485-493

[13] Langer R, Vacanti, JP. Tissue Engineering, Science 1993;260:920-26.

[14] NIH definition http://www.tissue-engineering.net/index.php?seite=whatiste

[15] Cortesini R. Stem cells, tissue engineering and organogenesis in transplantation. Transplant Immunology 2005;15:81–89.

[16] Xie E, Hua Y, Chen X, Bai X, Li D, Ren L, Zhang Z. *In vivo* bone regeneration using a novel porous bioactive composite. Applied Surface Science 2008;255:545–47.

[17] Youngmee Jung, Min Sung Park, Jin Woo Lee, Young Ha Kim, Sang-Heon Kim, Soo Hyun Kim. Cartilage regeneration with highly-elastic three-dimensional scaffolds prepared from biodegradable poly($_L$-lactide-co-ε-caprolactone). Biomaterials 2008;29:4630–36.

[18] Fuchs JR, Pomerantseva I, Ochoa ER, Vacanti JP, Fauza DO. Fetal tissue engineering: *in vitro* analysis of muscle constructs. Journal of Pediatric Surgery 2003;38:1348-53

[19] Ting Feng, Yuanwei Chen, Guoqi Shi, Xixun Yu , Changxiu Wan. A collagen based vitro model of angiogenesis designed for tissue-engineering material. Applied Surface Science 2008;255:312–14.

[20] Weiss DJ. Review. Stem cells and cell therapies for cystic fibrosis and other lung diseases. Pulmonary Pharmacology & Therapeutics 2008;21:588-94.

[21] Rosines E, Schmidt HJ, Nigam SK. The effect of hyaluronic acid size and concentration on branching morphogenesis and tubule differentiation in developing kidney culture systems: Potential applications to engineering of renal tissues. Biomaterials 2007;28:4806–17.

[22] Bozkurt A, Deumens R, Beckmann C, Damink LO, Schügner F, Heschel I, Sellhaus B, Weis J, Jahnen-Dechent W, Brook GA, Pallua N. In vitro cell alignment obtained with a Schwann cell enriched microstructured nerve guide with longitudinal guidance channels. Biomaterials 2009;30:169–79.

[23] Nervous system. Encyclopedia Britanica Online. Retrieved on Apr. 16 2009 from http://www.britannica.com/EBchecked/topic/409665/nervous-system

[24] http://www.dmacc.edu/instructors/rbwollaston/Chapter_8_Nervous_System.htm

[25] Medline Plus Medical Encyclopedia Myelin and nerve structure http://www.nlm.nih.gov/medlineplus/ency/imagepages/9682.htm

[26] Retrieved from the world wide web on February 2009. http://kvhs.nbed.nb.ca/gallant/biology/neuron_structure.html

[27] Human Anatomy TAJ Books International LLP, 2006.

[28] Bähr M, Bonhoeffer F. Perspectives on axonal regeneration in the mammalian CNS. Trends Neurosci. 1994;17:473-79.

[29] Bellamkonda RV. Leading Opinion. Peripheral nerve regeneration: An opinion on channels, scaffolds and anisotropy Biomaterials.2006;27:3515–3518.

[30] Yu X, Bellamkonda RV. Tissue-engineered scaffolds are effective alternatives to autografts for bridging peripheral nerve gaps. Tissue Engineering 2003;9:421-430.

[31] Tang JB. Vein conduits with interposition of nerve tissue for peripheral nerve defects. J Reconstr Microsurg 1995;11:21–6.

[32] Fansa H, Keilhoff G, Wolf G, Schneider W, Gold BG. Tissue engineering of peripheral nerves: a comparison of venous and acellular muscle grafts with cultured Schwann cells. Plast Reconstr Surg 2001;107:495–6.

[33] Retrieved on April 2009 from the world wide web: http://www.integra-ls.com/products/?product=88

[34] Bertleff MJOE, Meek MF, Nicolai J-PA. A prospective clinical evaluation of biodegradable neurolac nerve guides for sensory nerve repair in the hand. The Journal of Hand Surgery 2005;30:513-518.

[35] Neuralac nerve guide. Retrieved from the world wide web: http://www.polyganics.com/index.php?id=18.

[36] http://www.mlamed.com/images/ascension_neurolac.jpg

[37] Stamatialis DF, Papenburg BJ, Gironés M, Saiful S, Bettahalli SNM, Schmitmeirer S, Wessling M. Medical applications of membranes: Drug delivery, artificial organs and tissue engineering. Journal of Membrane Science 2008;308:1-34.

[38] Ichihara S, Inada Y, Nakamura T. Artificial nerve tubes and their application for repair of peripheral nerve injury: an update of current concepts. Injury, Int. J. Care Injured 2008;3954:S29-S39.

[39] Pfister LA, Alther E, Papaloïzos M, Merkle HP, Gander B. Controlled nerve growth factor release from multi-ply alginate/chitosan-based nerve conduits. European Journal of Pharmaceutics and Biopharmaceutics 2008;69:563–572.

[40] Rosner BI, Siegel RA, Tranquillo RT. Rational design of contact guiding, neurotrophic matrices for peripheral nerve regeneration. Annals of Biomedical Engineering 2003;31:1383-1401.

[41] Radulescu D, Dhar S, Young CM, Taylor DW, Trost H-J, Hayes DJ, Evans GR. Tissue engineering scaffolds for nerve regeneration manufactured by ink-jet technology. Materials Science and Engineeting C 2007;27:534-539.

[42] Iwan Zein, Dietmar W. Hutmacher, Kim Cheng Tan, Swee Hin Teoh. Fused deposition modeling of novel scaffold architectures for tissue engineering applications. Biomaterials 2002;23:1169–1185.

[43] Naing MW, Chua CK, Leong KF, Wang Y. Fabrication of customized scaffolds using computer-aided design and rapid prototyping techniques. Rapid Prototyping Journal 2005;11:249–259.

[44] Shoufeng Yang, Kah-Fai Leong, Zhaohui Du, Chee-Kai Chua. Review. The design of scaffolds for use in tissue engineering. Part I. Traditional factors. Tissue Engineering 2001;7:679-689.

[45] Shoufeng Yang, Kah-Fai Leong, Zhaohui Du, Chee-Kai Chua. Review. The design of scaffolds for use in tissue engineering. Part II. Rapid prototyping techniques. Tissue Engineering 2002;8:1-11.

[46] Alves NM, Bártolo PJ. Integrated computational tools for virtual and physical automatic construction. Automation in Construction 2006;15:257–271.

[47] Dimitrov D., van Wijck W., Schreve K., de Beer N..Investigating the achievable accuracy of three dimensional printing. Rapid Prototyping Journal 2006;12:42–52.

[48] Rüdiger Landers,Ute Hübner, Rainer Schmelzeisen,Rolf Mülhaupt. Rapid prototyping of scaffolds derived from thermoreversible hydrogels and tailored for applications in tissue engineering. Biomaterials 2002;23:4437–4447.

[49] Jia Ping Li, Joost R. de Wijn, Clemens A. Van Blitterswijk, Klaas de Groot. Porous $Ti_6Al_4V$ scaffold directly fabricating by rapid prototyping: Preparation and in vitro experiment. Biomaterials 2006; 27:1223–1235.

[50] Barry JJA, EvseevAV, Markov MA, Upton CE, Scotchford CA, Popov VK, Howdle SM. *In vitro* study of hydroxyapatite-based photocurable polymer composites prepared by laser stereolithography and supercritical fluid extraction. Acta Biomaterialia 2008;4:1603–1610.

[51] Melchels FPW, Feijen J, Grijpma DW. A poly(D,L-lactide) resin for the preparation of tissue engineering scaffolds by stereolithography. Biomaterials 2009;30:3801–3809.

[52] Chen H, Zhang Z, Brook MA, Sheardown H. Protein repellant silicone surfaces by covalent immobilization of poly(ethylene oxide). Biomaterials 2005;26:2391-2399.

[53] Yong Doo Park, Nicola Tirelli, Jeffrey A. Hubbel. Photopolymerized hyaluronic acid-based hydrogels and interpenetrating networks. Biomaterials 2003;24:893-900.

[54] West JL, Hubbell JA. Polymeric biomaterials with degradation sites for proteases involved in cell migration. Macromolecules 1999;32:241-244.

[55] Saito H, Hoffman AS. Delivery of Doxorubicin from biodegradable PEG hydrogels having Schiff base linkages. Journal of Bioactive and Compatible Polymers 2007;22:589-601.

[56] Sawhney AS, Pathak CP, Hubbell JA. Bioerodible hydrogel based on photopolymerized poly(ethylene glycol)-co-poly(α-hydroxy acid) diacrylate macromers. Macromolecules 1993;26:581-87.

[57] Kim S-H, Ha JH, Jung YJ, Cho C-S. Drug release from bioerodible hydrogels composed of poly-ε-caprolactone/poly(ethylene glycol) macromer semiinterpenetrating polymer networks. Arch Pharm Res 1995;18:18-21.

[58] Metters AT, Anseth KS, Bowman CN. Fundamental studies of a novel, biodegradable PEG-*b*-PLA hydrogel. Polymer 2000;41:3993-4004.

[59] Jeong B, Kibbey MR, Birnbaum JC, Won Y-Y, Gutowska A. Thermogelling biodegradable polymers with hydrophilic backbones: PEG-*g*-PLGA. Macromolecules 2000;33:8317-8322.

[60] Mann BK, Schmedlen RH, West JL. Tethered-TGF-β increases extracellular matrix production of vascular smooth muscle cells. Biomaterials 2001;22:439-444.

[61] Hahn MS, Taite LJ, Moon JJ, Rowald MC, Ruffino KA, West JL. Photolithographic patterning of polyethylene glycol hydrogels. Biomaterials 2006;27:2519-2524.

[62] Mann BK, Gobin AS, Tsai AT, Schmedlen RH, West JL. Smooth muscle cell growth in photopolymerized hydrogels with cell adhesive and proteolitically degradable domains: synthetic ECM analogs for tissue engineering. Biomaterials 2001;22:3045-51.

[63] Mahoney MJ, Anseth KS. Three-dimensional growth and function of neural tissue in degradable polyethylene glycol hydrogels. Biomaterials 2006;27:2265-2274.

[64] Retrieved from the world wide web: http://pslc.ws/macrogcss/acrylate.html

[65] Bencherif SA, Srinivasan A, Sheehan JA, Walker LM, Gayathri C, Gil R, Hollinger JO, Matyjaszewski K, Washburn NR. End-group effects on the properties of PEG-co-PGA hydrogels. Acta Biomaterialia 2009;5:1872-1883

[66] Laysan bio. Retrieved on Nov 2007 from www.laysanbio.com/

[67] Weining Bian, Nenad Bursac. Engineered skeletal muscle tissue networks with controllable architecture. Biomaterials 2009;30:1401–1412.

[68] Veronese FM, Pasut G. PEGylation,successful approach to drug delivery. DDT 2005;10:1451-1458.

[69] Vollhardt KPC, Schore NE. Organic Chemistry Structure and function. W.H. Freeman and Company, New York.

[70] Spectral Database for Organic Compounds SDBS. Retrieved on Nov. 2007 from http://riodb01.ibase.aist.go.jp/sdbs/cgi-bin/cre_index.cgi?lang=eng

[71] Lang UE, Gallinat J, Danker-Hopfe H, Bajbouj M, Hellweg R. Nerve growth factor serum concentrations in healthy human volunteers: physiological variance and stability. Neuroscience Letters 2003;344:13-16.

[72] Kerkhoff H, Jennekens FGI. Peripheral nerve lesions: the neuropharmacological outlook. Clinical Neurology and Neurosurgery 1993;95:S103-S108.

[73] Shao N, Wang H, Zhou T, Liu C. 7S Nerve growth factor has different biological activity from 2.5S nerve growth factor in vitro. Brain Research 1993;609:338-340.

[74] Moore JB, Mobley WC, Shooter EM. Proteolitic modification of the β nerve growth factor protein. Biochemistry 1974;13:833-840.

[75] Levi-Montalcini R, Hamburger V. Selective growth stimulating effects of mouse sarcoma on the sensory and sympathetic nervous system of the chick embryo. J Exp Zool 1951;116:321-361.

[76] Angeletti P, Calissano P, Chen JS, Levi-Montalcini R. Multiple molecular forms of the nerve growth factor. Biochim Biophys Acta 1967;147:180-182.

[77] Levi-Montalcini R, Caramia F, Luse SA, Angeletti PU. *In-vitro* effects of the nerve growth factor on the fine structure of the sensory nerve cells. Brain Research 1968;8:347-362.

[78] Derby A, Engleman VW, Frierdich GE, Neises G, Rapp SR, Roufa DG. Nerve growth factor facilitates regeneration across nerve gaps: Morphological and behavioral studies in rat sciatic nerve. Experimental Neurology 1993;119:176-191.

[79] Khor E, Lim LY. Implantable applications of chitin and chitosan. Biomaterials 2003;24:2339-2349.

[80] Madihally SV, Matthew HWT. Porous chitosan scaffolds for tissue engineering. Biomaterials 1999;20:1133-1142.

[81] Bruggeman JP, de Bruin B-J, Bettinger CJ, Langer R. Biodegradable poly(polyol sebacate) polymers. Biomaterials 2008;29:4726–4735.

[82] Mano JF, Sousa RA, Boesel LF, Neves NM, Reis RL. Bioinert, biodegradable and injectable polymeric matrix composites for hard tissue replacement: state of the art and recent developments. Composites Science and Technology 2004;64:789–817.

[83] Cao X, Shoichet MS. Delivering neuroactive molecules from biodegradable microspheres for application in central nervous system disorders. Biomaterials 1999;20:329-339.

[84] Pierucci A, Rezende de Duek EA, Rodrigues de Oliveira AL. Peripheral Nerve Regeneration through Biodegradable Conduits Prepared Using Solvent Evaporation. Tissue Engineering 2008;14:595-606.

[85] Capes JS, Andoh Y, Cameron RE. Fabrication of polymeric scaffolds with a controlled distribution of pores. Journal of Materials Science: Materials in Medicine 2005;16:1069–1075.

[86] Charles-Harris M, Navarro M, Engel E, Aparicio C, Ginebra MP, Planell JA. Surface characterization of completely degradable composite scaffolds. Journal of Materials Science: Materials in Medicine 2005;16:1125–1130.

[87] Schmidt CE, Shastri VR, Vacanti JP, and Langer R. Stimulation of neurite outgrowth using an electrically conducting polymer Applied Biological Sciences 1997;94:8948–8953.

[88] Mahoney MJ, Chen RR., Tan J, Saltzman WM. The influence of microchannels on neurite growth and architecture. Biomaterials 2005;26:771–778.

[89] Ghasemi-Mobarakeh L. *et al*. Electrospun poly(ε-caprolactone)/gelatin nanofibrous scaffolds for nerve tissue engineering. Biomaterials 2008;29:4532-4539.

[90] Grafahrend D, Julia Lleixa Calve, Salber J, Dalton PD, Moeller M, Klee D. Biofunctionalized poly(ethylene glycol)-block-poly(ε-caprolactone) nanofibers for tissue engineering. J Mater Sci: Mater Med 2008;19:1479–1484.

[91] Tabesh H, Amoabediny Gh, Nik, NS, Heydari M, Yosefifard M., Siadat SOR, Mottaghy K. The role of biodegradable engineered scaffolds seeded with schwann cells for spinal cord regeneration. Neurochemistry International 2009;54: 73-83.

[92] Heumann R, Korsching S, Bandtlow C, Thoenen H. Changes of nerve growth factor synthesis in non neuronal cells in response to sciatic nerve transection. J Cell Biol 1987;104:1623-1631.

[93] Fu SY, Gordon T. The cellular and molecular basis of peripheral nerve regeneration. Mol Neurobiol 1997;14:67-116.

[94] McConnel MP, Dhar, Naran S, Nguyen T, Bradshaw RA, Evans GRD. *In vivo* induction and delivery of nerve growth factor using HEK-293 cells. Tissue Engineering 2004;1492-1501

[95] Danielsson P, Dahlin L, Povlsen B. Tubulization increases axonal outgrowth of rat sciatic nerve after crush injury. Experimental Neurology 1996;139:238-243.

[96] Singh M, Berkland C, and Detamore MS. Strategies and Applications for Incorporating Physical and Chemical Signal Gradients in Tissue Engineering. Tissue Engineering 2008;14:341-366

[97] Bajpai AK, Shukla SK, Bhanu S, Kankane S. Responsive polymers in controlled drug delivery. Progress in Polymer Science 2008;33:1088–1118.

[98] Chan BP, Chan OCM, So K-F. Effects of photochemical crosslinking on the microstructure of collagen and a feasibility study on controlled protein release. Acta Biomaterialia 2008;4:1627-1636.

[99] Holland TA, Tabata Y, Mikos AG. Dual growth factor delivery from degradable oligo(poly(ethylene glycol) fumarate) hydrogel scaffolds for cartilage tissue engineering. Journal of Controlled Release 2005;101:111-125.

[100] Uebersax L, Mattotti M, Papaloïzos M, Merkle HP, Gander B, Meinel L. Silk fibroin matrices for the controlled release of nerve growth factor (NGF). Biomaterials 2007;28:4449-4460.

[101] Jean-Manuel Péan, Marie-Claire Venier-Julienne, Franck Boury, Philippe Menei, Benoit Denizot, Jean-Pierre Benoit. NGF release from poly(D,L-lactide-co-glycolide) microspheres, effect of some formulation parameters on encapsulated NGF stability. Journal of Controlled Release 1998;56:175-187.

[102] Meilander NJ, Yu X, Ziats NP, Bellamkonda RV. Lipid based microtubular drug delivery vehicles. Journal of Controlled Release 2001;71:141-152.

[103] Sakiyama-Elbert SE, Hubbell JA. Controlled release of nerve growth factor from a heparin-containing fibrin-based cell ingrowth matrix. Journal of Controlled Release 2000;69:149-158.

[104] Wood MD, Sakiyama-Elbert SE. Release rate controls biological activity of nerve growth factor released from fibrin matrices containing affinity-based delivery systems. Journal of Biomedical Materials Research 2008;84:300-312.

[105] Bhang SH, Lee T-J, Lim JM, Lim JS, Han AM, Choi CY, Kwon YHK, Kim B-S. The effect of the controlled release of nerve growth factor from collagen gel on the efficiency of neural cell culture. Biomaterials 2009;30:126-132.

[106] Yu LMY, Wosnick JH, Shoichet MS. Miniaturized system of neurotrophin patterning for guided regeneration. Journal of Neruroscience Methods 2008;171:253-263.

[107] Kapur TA, Shoichet MS. Chemically-bound nerve growth factor for neural tissue engineering applications. J Biomater Sci Polymer Edn 2003;14:383-394.

[108] Mellot MB, Searcy K, PishkoMV. Release of protein from highly cross-linked hydrogels of poly(ethylene glycol) diacrylate fabricated by UV polymerization. Biomaterials 2001;22:929-941.

[109] Sahu A, Bora U, Kasoju N, Goswami P. Synthesis of a novel biodegradable and self-assembling methoxy poly(ethylene glycol)-palmitate nanocarrier for curcumin delivery to cancer cells. Acta Biomaterialia 2008;4:1752-1761.

[110] Scott RA, Peppas NA, Highly crosslinked, PEG-containing copolymer for sustained solute delivery. Biomaterials 1999;20:1371-80.

[111] Arcaute K, Zuverza N, Mann BK, Wicker RB. Multi-material stereolithography: spatially-controlled bioactive poly(ethylene glycol) scaffolds for tissue engineering. Proceedings of the 18th Annual Solid Freeform Fabrication Symposium, University of Texas a Austin, August 2007.

[112] Arcaute K, Mann BK, Wicker RB. Stereolithography of three-dimensional bioactive poly(ethylene glycol) constructs with encapsulated cells. Annals of Biomedical Engineering 2006;34:1429–1441

[113] Pignatti PF, Baker ME, Shooter EM. Solution properties of beta nerve growth factor protein and some of its derivatives. J Neurochem 1975;25:155-9

[114] Arcaute K, Ochoa L, Mann BK, Wicker RB. Stereolithography of PEG hydrogel multi-lumen nerve regeneration conduits. ASME IMECE2005-81436 American Society of Mechanical Engineers International Mechanical Engineering Congress at Orlando, Florida, November, 2005.

[115] Garza Kristine, PhD. Associate Professor, Dept. of Biological Sciences and Border Biomedical Research at the University of Texas at El Paso. Personal communication.

[116] Almodovar Gladys, Research Engineering Science Associate IV, Biological Sciences at the University of Texas at El Paso. Personal Communication

[117] Salvador James, PhD. Associate Professor, Dept. Chemistry at the University of Texas at El Paso. Personal Communication

[118] Chavez David, PhD. Candidate, Dept. Chemistry at the University of Texas at El Paso. Personal Communication.

[119] You-Ming Fan, Chi-Pui Pang, Alan R. Harvey, Qi Cui. Marked effect of RhoA-specific shRNA-producing plasmids on neurite growth in PC12 cells. Neuroscience Letters 2008;440:170-175.

[120] Cao X, Shoichet MS. Defining the concentration gradient of nerve growth factor for guided neurite outgrowth. Neuroscience 2001;103:831-840.

[121] Barras FM, Pasche P, Bouche N, AEbischer P, Zurn AD. Glial cell line-derived neurotrophic factor released by synthetic guidance channels promotes facial nerve regeneration in the rat. J Neurosci Res 2002;70:746-55.

[122] Lu S, Anseth KS. Release behavior of high molecular weight solutes from poly(ethylene glycol)-based degradable networks. Macromolecules 2000;33:2509-15.

[123] West JL, Hubbell JA. Photopolymerized hydrogel materials for drug delivery applications. Reactive Polym 1995;25:139-47.

[124] Suda K, Barde YA, Thoenen H. Nerve growth factor in mouse and rat serum: correlation between bioassay and radioimmunoassay determinations. Proc Natl Acad Sci 1978;75: 4042–4046.

[125] Serrano T, Lorigados LC, Armenteros S, Nerve growth factor levels in human sera. NeuroReport 1996;8:179-181.

[126] Lorigados L, Söderstrom S, Ebendal T. Two-site enzyme immunoassay for β-NGF applied to human patient sera. J Neurosci Res 1992;32:329–339.

[127] Zhang S, Zettler C, Cupler EJ, Hurtado P, Wong K, Rush RA. Neurotrophin 4/5 immunoassay: identification of sources of errors for the quantification of neurotrophins. J Neurosci Methods 2000;99:119–127.

[128] Martocchia A, Sigala , Proietti A, D'Urso R, Spano PF, Missale C, Falasch P. Sex-related variations in serum nerve growth factor concentration in humans. Neuropeptides 2002;36:391–395.

[129] Bersani G, Iannitelli A, Maselli P, Pancheri P, Aloe L, Angelucci F, Alleva E. Low nerve growth factor plasma levels in schizophrenic patients: a preliminary study. Schizophrenia Res 1999;37:197–203.

[130] Baier Leach J, Bivens KA, Patrick CW, Schmidt C.Photocrosslinked Hyaluronic acid hydrogels: Natural, biodegradable tissue engineering scaffolds. Biotechnol Bioeng 2003;82:578-589

[131] Burdick JA, Chung C, Jia X, Randolph MA, Langer R. Controlled degradation and mechanical behavior of photopolymerized hyaluronic acid networks. Biomacromolecules 2005;6:386-391.

[132] Gobin A, West J. Val-Ala-Pro-Gly. An elastin derived non-integrin ligand: cell adhesion and specificity. Proceedings of the Second Joint EMBS/BMES Conference. Houston, TX, October 2002.

[133] Kwon IK, Matsuda T. Photopolymerized microarchitectural constructs prepared by microstereolithography (μSL) using liquid acrylate-end-capped trymethylane carbonate-based prepolymers. Biomaterials 2005;26:1675-1684.

[134] Piao L, Dai Z, Deng M, Chen X, Jing X.Synthesis and characterization of PCL/PEG/PCL triblock copolymers by using calcium catalyst. Polymer 2003;44:2025-2031.

[135] Cao X, Shoichet MS. Investigating the synergistic effect of combined neurotrophic factor concentration gradients to guide axonal growth. Neuroscience 2003;122:381-389.

## *Curriculum Vita*

Nubia Zuverza-Mena was born in Cd. Juarez, Chihuahua, Mexico on September 11, 1983. With her parents support, Luis F. Zuverza-Meza and Patricia Mena-Sierra, she received a high quality education. Up to her teenage years, extracurricular activities included ballet, painting classes along with outdoor activities such as excursions, camping and hiking. While in high school, she and friends of different team groups received two significant awards. The first one was for coming up with a shower system that avoids cold water to flow while waiting for the hot water to come out. In the second one, the team won the first place for their business plan. The plan was about recycling a by-product material of a "maquiladora" which byproducts comprise a mountain. A sudden field change took place while transitioning from high school to college. Ms. Zuverza got an associate degree in medical urgencies from the Red Cross in Cd. Juarez, where she volunteered as a paramedic. Due to the fact that the city she lives on is known for actively having life threatening situations, she and her colleagues were continuously active. Later on, the University of Texas at El Paso gave her the opportunity to participate in an internship at Orlando FL where she lived on Spring 2003. Nubia had to pay for her studies conducting interviews, working as a peer leader at the university and as a waitress during the weekends. In 2004, Zuverza started her research career at the chemistry department conducting phytoremediation studies. That experience gave her the chance to participate in national conferences. Before getting her BS in Chemistry on Dec. 2006, she moved to Arizona as a summer intern of a copper open-pit mine´s analytical lab. By the age of 23, she was accepted into the Metallurgy and Materials Engineering MS program at UTEP. There, Nubia explored a new research area: tissue engineering at the WM. Keck Center for 3D Innovation. The present thesis shows the results obtained from that experience.